AD-A256 728

AFIT/GE/ENG/92M-02

DTIC
ELECTE
OCT 2 8 1992
S
c
D

COMPARATIVE ANALYSIS OF GUIDANCE ALGORITHMS

FOR THE HYPER VELOCITY MISSILE AND AFTI/F-16

THESIS

Edward G. Rice, B.S.E.E.
Captain, USAF

AFIT/GE/ENG/92M-02

92-28333

92 10 27 121

AFIT/GE/ENG/92M-02

COMPARATIVE ANALYSIS OF GUIDANCE ALGORITHMS

FOR THE HYPER VELOCITY MISSILE AND AFTI/F-16

THESIS

Presented to the Faculty of the School of Engineering

of the Air Force Institute of Technology

Air University

In Partial Fullfilment of the

Requirements of the Degree of

Master of Science in Electrical Engineering

Edward G. Rice, B.S.E.E.

Captain, USAF

12 Nov, 1991

Approved for public release; distribution unlimited

Preface

This project has provided me with endless intrigue. In considering the problem of guiding a hyper-velocity missile from a moving platform to a moving target, a common perception said it was just another Kalman Filter design challenge. I began with lofty intentions of running a full up extended Kalman filter simulation but I became enthralled with the limited work available on the physical limitations of basic guidance algorithms. This became the emphasis of this project. The best filter scheme cannot overcome a guidance algorithms physical limitation. Only with an understanding of these limitations can one effectively integrate a guidance scheme with a Kalman filter. This effort is an exploration of these physical limits for four common guidance algorithms proposed for the HVM. My most untimely PCS to Griffiss AFB, and away
from the AFIT resources, forced the construction of an Extended Kalman Filter and the full error sensitivity analysis to be a recommended future effort. For the investigation and documentation I completed I thank my loving wife, who has kept my perspectives straight and my nose to the grind wheel. I also thank my God and Savior, who has told me "Whatsoever ye do, do all to the glory of God" [I Corinthians 10:31]

Table of Contents

List of Figures

List of Tables

List of Significant Symbols and Abbreviations

ABSTRACT

This analysis is an examination of four guidance algorithms proposed to guide a hyper-velocity missile (HVM) from a launch aircraft to a ground target. A technically risky flight demonstration program of the HVM on an AFTI/F-16 has been proposed. The four algorithms are the Line of Sight (LOS) (Often called the Beam Rider), the Line of Sight Plus (LOS+), the Pursuit, and the Proportional guidance algorithms. A simulation of the HVM is used to determine the no-noise capability of the algorithms within the HVM weapon system. The algorithms are each developed to exploit the launch aircraft's sensors to track the target and the missile, with only turn commands being sent to the missile. Each algorithm is tested in several scenarios, including one where a FLIR is the only tracker used. A comparative analysis of the four algorithms is then accomplished. The analysis shows that the LOS (Beam rider) algorithm is the best suited algorithm for the air to ground guidance of the HVM. The proportional guidance algorithm is an excellent contender but it exhibits a strong dependence on range and range rate measurements from the launch aircraft, i.e. an accurate radar must be used. The results of this analysis are preliminary since a missile tracking error analysis has not been accomplished to date. In the absence of FLIR tracking errors and system noise the LOS guidance algorithm can effectively guide a HVM to a direct hit on a moving ground target.

COMPARATIVE ANALYSIS OF GUIDANCE ALGORITHMS
FOR THE HYPER-VELOCITY MISSILE AND AFTI/F-16

I. Introduction

1.1 Background

The flight demonstration program of the Hyper-velocity Missile (HVM) using the AFTI/F-16 as the launch platform has been proposed and its technical risk is currently assessed as high [1]. Some major areas of concern in this weapon integration process are Forward Looking Infrared (FLIR) tracking difficulties, computational loading of the aircraft fire control computer, the HVM performance effects, and the uncertainties of missile update communications. The HVM is designed to be a low cost, light weight air to ground weapon. To achieve this, it is built with a minimal guidance capability and no target seeker. Consequently, the HVM relies on the launch platform to guide it into the target. The launch aircraft is required to (1) track the moving target, (2) track the flying missile, (3) compute a new guidance solution, and (4) communicate this solution to the airborne missile. This situation is made technically risky by the fact that the HVM flies so fast that it has only 2 to 4 seconds of flight time, and the very small missile has to be tracked with a FLIR that may not see well through the missile's rocket plume, or through atmospheric conditions.

The complete magnitude of these technical problems is not fully understood. Efforts have to be initiated to eliminate or greatly reduce these technical risk areas before the AFTI/F-16 and HVM integration proceeds. A first step towards reducing risk is the development of a weapon system model or simulation and the exploration of system sensitivities in these problem areas.

1.2 Problem Statement

With several uncertainties in the HVM weapon system concept an initial exploration of guidance schemes and algorithms is required to define sensor and missile requirements. The effects of removing the target tracker from the missile and of tracking the missile and the target from a stand-off flying platform are not fully understood or tested. The guidance requirements for a HVM which accepts only steering commands with minimal on-board processing need better definition. These guidance algorithms will require extreme accuracy, and an efficiency that will not expend the missiles limited control resources. The purpose of this research project is to develop and build a simple weapon system model, and perform preliminary sensitivity analysis of the proposed guidance algorithms.

1.3 Project Scope

This project includes the construction of a weapon system simulation and the analysis of four HVM guidance techniques against launch geometry effects and against range and range rate requirements. The guidance techniques explored are the line of sight (LOS) guidance, the modified line of sight (LOS+) guidance, the pursuit guidance and the proportional guidance algorithms. This selection encompasses the current guidance schemes in use today. This project models only one missile in flight, and sensor and system noise is not modeled since only the geometry effects are studied. The exploration of the launch envelope includes 30 degree off-axis shots and launch during a 5 G aircraft maneuver Shots of 12,000 feet range are tested, from a F-16 model flying 650 fps at 1000 feet altitude. It does not include maximum or minimum range shots because they are not certain in the current HVM design. A 3DOF model is used for the target. F-16, and HVM so AOA and sideslip issues are not addressed.

1.4 Summary of Current Knowledge

1.4.1 <u>Introduction</u>. The purpose of this section is to investigate work related to modeling the AFTI/F-16 and Hyper-velocity Missile (HVM) weapon system and to determine the current status of the HVM to aircraft integration technology. The HVM is a low cost, light weight anti-tank weapon that is designed to increase the kill ratio of a modern tactical air vehicle. In the attempt to make the missile as simple as possible most of the guidance responsibility has been delegated to the carrier aircraft, requiring some new technology and state-of-the-art integration. This review is an attempt to determine the current status of this integration challenge and determine the feasibility of effectively modeling the HVM guidance algorithms to be implemented by the AFTI/F-16.

To better understand the integration requirements, some articles concerning the HVM and its current status are examined first. Next, two Master's theses applicable to this problem are reviewed as a first step in the understanding of the integration issues. This literature review shows that research work has been done on the HVM integration but there has been no analysis of the proposed HVM guidance solutions for the current missile design.

1.4.2 <u>The HVM Concept</u>. The HVM concept has matured since T.C. Aden explained it in his Hyper-velocity Missile paper [2], but his work still details the heart of the weapon system. Aden's technical description of the HVM and the aircraft requirements for an effective launch are altered only because some of the missile guidance and communication details have been revised. His paper presents the historical problems of the Close Air Support (CAS) and battlefield interdiction using expensive and heavy conventional precision guided munitions (i.e., MAVERICK and HELLFIRE missiles) and then presents the HVM as an attractive, affordable solution for multiple target kills in one pass.

The concept of operation is discussed in great detail with excellent coverage of the Active Electro-Optical Guidance System (AEOGS). The responsibilities of the carrier aircraft and its AEOGS are outlined very well by Aden [2]; however, some critical emerging technologies are glazed over without much detail. The first of these is the ability of the AEOGS to place several LASER rasters within the field of view of the flying missiles, a course raster for all airborne missiles and a fine raster, centered on the target, for each individual missile. (The HVM concept is a multi-target kill with track-until-impact requirements.) Secondly, the missile has to interpret this raster into a position update with timing information alone. This requirement entails some very fine time synchronization that is not often achieved on airborne platforms, but will directly affect the probabilities of kill for an individual missile.

The article then examines the HVM in greater detail with an emphasis on the guidance and control concept. The guidance and control concept explained by Aden was abandoned during early development testing according to several conversations with Mr. Boone of the AFTI/F-16 SPO and Mr. Reilly of the Eglin AFB, HVM SPO. Off-angle problems with the beam rider technique and timing problems with the laser raster scheme led to a current concept where the aircraft performs all guidance calculations and sends updates to the missile in flight.

Aden's paper provides good coverage of most of the HVM concepts but it is dated because of the new guidance concept and increased carrier platform responsibilities. Although this type of conceptual data is required to construct a functional model it is only a first step.

1.4.3 The HVM Development. The DMS Market Intelligence Report on missiles [3] was consulted for the current status of the Hyper-velocity Missile development. DMS Market Intelligence Reports are periodicals that give the latest status of most DOD research and development projects. The report on the HVM is dated Sep 1988 and provides a very compact but

informative outline of the development phases. It consists of two sections entitled Data and Analysis.

The Data section of the DMS report is an outline of the pertinent program data. It lists the Armament Test & Development Center, at Eglin AFB, FL, as the executive developer and LTV Corporation, Missiles Division, Dallas, Texas, as the manufacturer. The data section lists possible launch platforms, gives the missile characteristics and provides good coverage of the development timetable and forecast. It lists the ground test demonstration completed in June of 1987 and a flight test demonstration completion in April, 1989, with a FSD decision in FY '92.

The Analysis section is a general system description followed by program history, plans, current status and outlook. This section also covers several related development activities and gives a DMS analysis of the program. The system description, although not extremely technical, makes reference to a Multifunctional Infrared Coherent Optical Scanner (MICOS), a CO_2 laser sensing device. The MICOS is said to receive pulses containing position information that must be time translated into the missile aim point. It is not clear from this report what changes to the guidance scheme were implemented during ground testing, but the report says the program has good joint service support and will proceed to the full scale development decision. That decision will require information from system models.

1.4.4 Past HVM Modeling. In 1981 Captain Donald Capps and Captain Donald Nelson, in a MS thesis, developed a systematic procedure to design Kalman Filters for the HVM system [4]. This pioneer research work developed a workable three degree-of-freedom (DOF) model of the HVM and applied the latest Kalman Filter modeling tools to the problem of guiding this missile to a target. Capps and Nelson assumed a smart missile, with a proportional guidance that did not account for the aircraft calculating a missile to target line-of-sight rate. Although this research speculated

about some of the missile parameters and the missile guidance technique, it is a major asset in developing much of the weapon system model.

Their work put much effort in building an accurate truth model of the HVM. It also evaluated some line-of-sight and inertial navigation system Kalman Filters in an attempt to come up with a reduced order Kalman Filter that could accurately estimate the system performance. A line of sight Kalman filter was determined as the best method of tracking the HVM missile. This is the tracking method to be used in this guidance algorithm analysis.

The work done in Capps' thesis used guidance concepts that required a guidance system within the missile, and assumed a proportional guidance algorithm. Although it is a major stepping off point for the full development of an AFTI/F-16 and HVM weapon system model, it did not explore the guidance solutions applicable for the current HVM developments.

1.4.5 AFTI/F-16 Modeling Effort. Captain David Michalk, in a MS thesis, investigated the target state estimation techniques for the AFTI/F-16 automated maneuvering and attack system [5]. This investigative work provides excellent coverage of the AFTI/F-16 sensor suite, the target state estimator, and the on-board implementation of a Kalman Filter. Although this work was done for the Air-To-Air mode, the details of the document provide many of the current modeling techniques, and an insight to unique AFTI/F-16 capabilities that can directly relate to the Air-to-Ground mode modeling for an HVM analysis. It is expected that the AFTI/F-16 FLIR capabilities will be strained attempting to track a small fast missile that is in the line of sight of the target. No other documentation addressing this problem appears to be available.

1.4.6 Review Conclusions. Much work has been accomplished in the modeling of AFTI/F-16 and HVM systems. It is necessary to pull this work together into a weapon system model that explores pertinent guidance

algorithm sensitivities before base line fire control algorithms are developed. Research was conducted during the conceptual phase of the HVM development, but there is no current analysis that fully explores the risky integration issues. The HVM flight demonstration program may soon be underway, and the AFTI/F-16 to HVM integration effort needs some up-front research to select a guidance scheme. There are related analysis efforts with spin-offs that might be directly applicable to such an effort and the modeling tools required to perform this analysis are in place. Further research with the latest missile parameters and the current guidance techniques can greatly enhance this integration process and more fully demonstrate the effectiveness of this weapon system.

1.5 Approach Methodology

1.5.1 Introduction. This research takes the first step of an algorithmic analysis. The examination of the algorithms and the analysis accomplished amount to the preliminary evaluation of the candidate algorithms under no-noise conditions. This step is important because a guidance algorithm can do no better than the controlling physics involved. Even at this level the differences discovered in the guidance algorithms performance for a hyper-velocity missile are striking and informative. A more in-depth analysis with both system noise and measurement noise is required on the algorithm selected after this cursory analysis.

The approach taken in the development and analysis of the weapon system guidance algorithms may have some unique situations and parameters but it is a standard weapon system modeling approach. It consists of building an aircraft, missile, and target model that interact dynamically to provide a weapon system simulation. The simulation begins with the use of position truth models for the launch aircraft, the target vehicle and the missile. A radar and FLIR tracker model takes this true position data and calculates the line of sight and range parameters that would be available to the guidance algorithms. The selected guidance algorithm then provides

the guidance command data to the missile truth model. The missile truth model applies this command to a second order response and continues the missile flight until ground impact. The miss distance to the target is the measure of effectiveness for each simulation. A block diagram of this simulation is shown in Figure 1-1. It is explained in greater detail below with a discussion of the analysis effort undertaken in this research.

1.5.2 The Truth Model. The truth model calculates the position and velocity of the aircraft, the target, and the missile. The aircraft model uses the scenario setup variables to establish a three dimensional, three-degree-of-freedom (3DOF) flight profile for the aircraft. The target model does the same for the target but its vertical plane is held constant. The missile model is of higher fidelity than the aircraft or target models. The missile acceleration calculations must include the rocket motor thrust, air drag, lateral acceleration commands, and aerodynamic turning drag. Once these are calculated the missile model also computes the current missile position and velocity in the three dimensional, three-degree-of-freedom reference system.

The truth models take scenario inputs and missile parameters from the Scenario Setup, and missile commands are received from the selected guidance algorithm. Aircraft, target, and missile position and velocity are sent to the measurement model at regular time intervals established by the Scenario Setup.

1.5.3 The Measurement Model. The measurement model implemented in this analysis is a simple coordinate transformation that calculates a relative LOS, LOS rate, Range and Range rate from the aircraft to both the target and the missile. The LOS and LOS rate are calculated in the horizontal plane as azimuth, and in the vertical plane as pitch. The measurement model provides identical data to each of the algorithms under test with a flavor of realism. For this initial and simple analysis, signal noise is
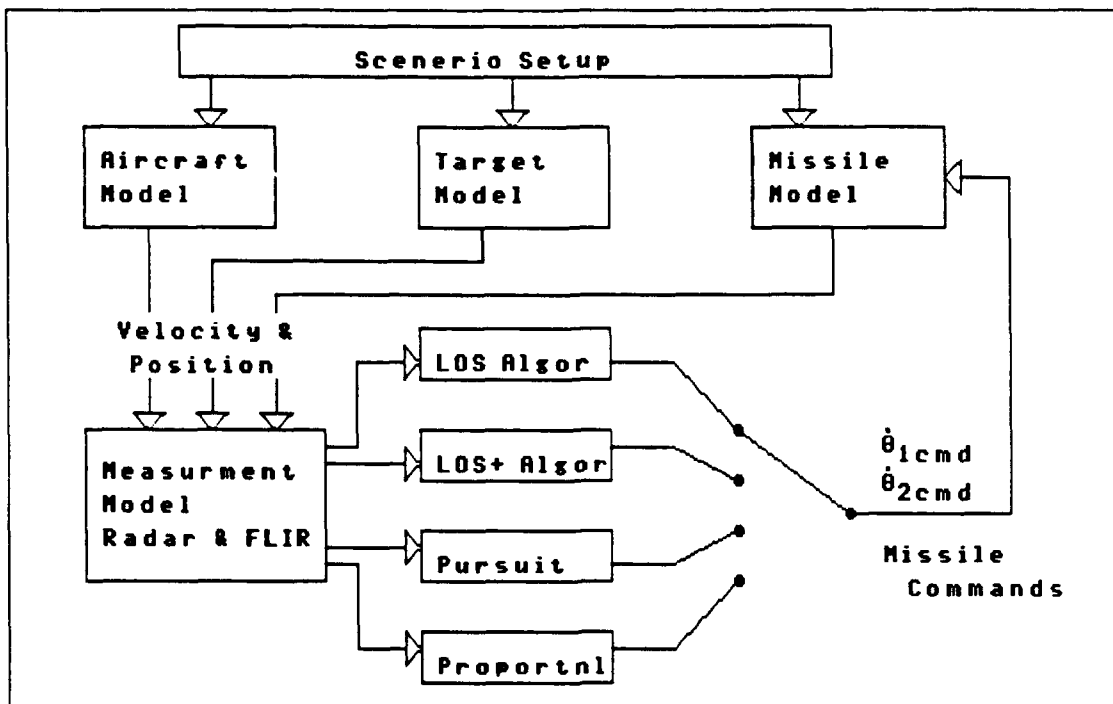
Figure 1-1 Weapon System Model Block Diagram

not accounted for, and the construction of a Kalman filter that would smooth the actual measurement data is not accomplished. The accurately calculated truth data is initially input into the guidance algorithm to establish the upper limit of performance.

The measurement model uses the inertial position and velocity data of the aircraft, the target, and the missile. It then outputs the relative LOS, LOS rate, Range, and Range rate data to the selected guidance algorithm. The time rate at which the measurement model performs the transformation is established by the Scenario Setup.

1.5.4 The Guidance Algorithm. The guidance algorithm takes the output from the measurement model and uses this data to calculate the missile commands sent to the missile truth model. A guidance algorithm must be chosen at initiation. LOS guidance, LOS+ guidance, Pursuit guidance and Proportional guidance methods are available. These guidance methods are discussed in detail in Chapter 3.

1-9

1.6 Summary

This analysis is an examination of four guidance algorithms proposed to guide a hyper-velocity missile (HVM) from a launch aircraft to a ground target. A technically risky flight demonstration program of the HVM on an AFTI/F-16 has been proposed. Chapter 2 describes the system models developed to test the guidance schemes. Chapter 3 develops the Line of Sight (LOS) (Often called the Beam Rider), the Line of Sight Plus (LOS+), the Pursuit, and the Proportional guidance algorithms. A simulation of the HVM is used to determine the no-noise capability of the algorithms within the HVM weapon system. The algorithms are each developed to exploit the launch aircraft's sensors to track the target and the missile, with only turn commands being sent to the missile. Chapter 4 documents the testing of each algorithm in several scenarios, including one where a FLIR is the only tracker used. A comparative analysis of the four algorithms is then accomplished. The conclusions and recommendations are shown in Chapter 5.

With an understanding of the background, the scope and the approach methodology it is important to understand the system truth models developed in the next chapter.

II. SYSTEM TRUTH MODEL

2.1 Introduction

The computer simulation of a system is always a compromise of fidelity. In the case of a weapons system model it is important that the truth model have greater fidelity than the algorithms under test. The model used for this simulation contains a position and velocity truth model that uses a double precision Fortran routine. The other portions of code, those that might be implemented in an airborne computer, are implemented in single precision Fortran code. To attain greater precision in the truth model the integration time is kept much smaller than the sensor or the missile time responses. Figure 1-1 is a block diagram of the general system that is built and used for preliminary tests of the four proposed algorithms. Figure 2-1 shows the geometric layout of the model scenarios. Since the simulation uses a three dimensional space there is a synonymous geometry in the vertical plane, which is shown in Figure 2-2. The coordinate system used in this work is the geographic North, East, Down (NED) coordinate system as seen in these Figures. The order of sections in this chapter are the assumptions and detailed missile, aircraft, and target truth models, and the calculations necessary to construct a measurement model. The purpose of constructing these truth and measurement models is to analyze the guidance algorithms described in the next chapter.

2.2 Model Executive and Assumptions

This model is assembled in as simple a manner as possible while affording a versatile analysis capability. This noise free model is initially constructed as a tool to test the guidance algorithm code. After only a little testing of the algorithms it became clear that a clean and simple weapon system model is adequate for the very preliminary

Figure 2-1 Weapon Model Horizontal Plane Geometry

Figure 2-2 Weapon Model Vertical Plane Geometry
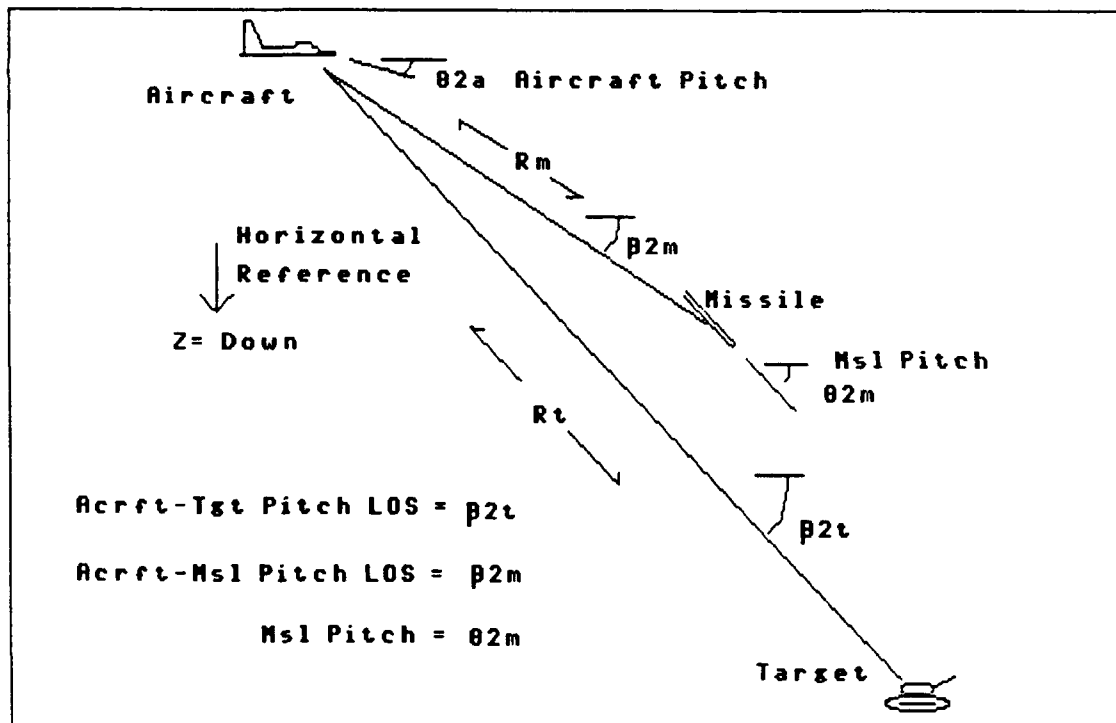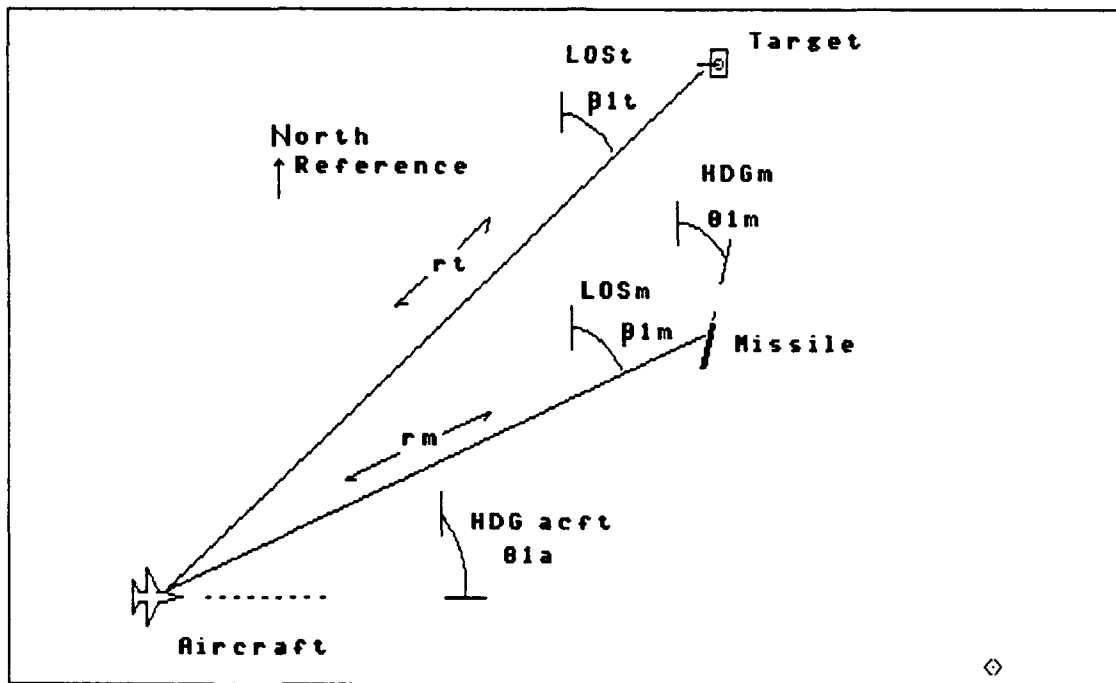
algorithm analysis that has yet to be accomplished for a hyper-velocity missile, monitored and controlled from the launch platform. Thus the model is a simple but accurate implementation that enables most of the research effort to be centered around the guidance algorithms.

The Scenario Setup block shown in Figure 1-1 allows versatile control of a missile launch scenario. The use of the I/O subroutine allows missile variables and scenario variables to be adjusted from default values before each run. The system timing and the guidance algorithm is selected and controlled via the scenario variable selection.

The truth models are stepped through their motion at a small time interval. (The default time delta is set to 2 milliseconds.) On a single pass the system time is incremented by DT (the system time interval); missile, aircraft, and target truth models are updated; a missile proximity to target check is made; excessive flight time and missile range checks are made; then the timed events are checked for their execution time. The timed events include the sensor output updates, the missile updates including guidance algorithm execution, and the recording of pertinent data. The timing of the timed events is controlled by scenario inputs. The missile and scenario inputs with their default values are shown in Table 2-1 and Table 2-2 respectively.

Throughout the simulation pertinent data is stored in a matrix for future output to a file. Each matrix can hold ten variables for 200 individual time samples. This format is ideal for future data analysis via spreadsheets. The four matrices store selected control data, the missile, aircraft and target position data, the missile, aircraft and target velocity data, and ten of the twelve measurement model states. At the end of a run the user is given the option of saving this data as a file or discarding it.

Table 2-1 Missile Input Variables

NAME	DEFAULT VALUE	UNIT	SYMBOL
MSL Thrust Time	1.5	SEC	TBURN
MSL Thrust	6000.0	LBS	THRUST
MSL Body Weight	25.9	LBS	WTBD
MSL Fuel Weight	32.17	LBS	WTFU
MSL Diameter	3.8	IN	MDIA
MSL Length	7.0	FT	MLNGTH
MSL Wn	44.0	RPS	WN
MSL Damping	0.7071	NU	ZETA
MSL Max G	100.0	G	GMAX
MSL Max Flt Time	4.0	SEC	TFLGHT
MSL Drag Constant	0.000174	NU	KDRAG

Table 2-2 Scenario Input Variables

NAME	DEFAULT VALUE	UNIT	SYMBOL
Aircraft Speed	650.0	FPS	VAC
Acft Heading	60.0	DEG	HDGA
Acft Altitude	1000.0	FT	AALT
Acft Lateral Accel	00.0	G	AACf
Acft Climb Accel	0.0	G	APITCH
Range To Target	12000.0	FT	RT
Target Speed	50.0	MPH	VTGT
Target Heading	90.0	DEG	HDGT
Target Lateral Accel	00.0	FPS^2	ATGT
Sys Integr Time	0.002	SEC	DT
MSL Update Times	0.02	SEC	DTMU
Sensor Update Times	0.02	SEC	DTSU
Output Times	0.02	SEC	DTOUT
Filter Update Times	0.02	SEC	DTKU
Correction Time	0.1	SEC	TC
Other Constant	1.5	SEC	K2
Porportional Constant	0.003	NU	K3
Algorithm Selection	1.0	NU	ALG

2.3 Missile Model

The model of the missile is an integral part of the system executive. It consists of an integration of the state vectors at an integration time of DT, the system time delta. A block diagram of this model is shown in Figure 2-3.

Several of the missile parameters are read from a data file called "msl.dat". This allows for easy change of some basic parameters. These variable and their default values are in a data file as shown in Table 2-1. At program initiation any of these variables may be altered before the program proceeds.

Before the missile states are updated in each cycle, the missile response to the turn command rates are modeled as a second order lag response. This second order model is controlled by the missile natural frequency and damping coefficient W_n and δ respectively. These are input from the data table and may be changed before a simulation. The default values used were $W_n = 44$ radians/second and $\delta = .707$, these were used in the previous HVM model by Capps and Nelson [4:D-2]. The commanded turn from the guidance algorithm is the input to this second order lag and the actual turn rate, H_{lag} is the filter output. Both the heading rate, $\dot{\Theta}_{1r}$, and the pitch rate, $\dot{\Theta}_{2m}$, are computed in the geographic NED coordinate frame. The equations for each iteration are shown below:

$$\dot{\Theta}_{1m} = \dot{\Theta}_{1r} + (W_n^2 \ (\dot{\Theta}_{1cmd} - H_{lag})) \ \tau \tag{2-1}$$

$$\dot{\Theta}_{2r} = \dot{\Theta}_{2m} + (W_n^2 \ (\dot{\Theta}_{2cmd} - P_{lag})) \ \tau \tag{2-2}$$

and

$$H_{lag} = H_{lag} + (\dot{\Theta}_{1m} - 2 \ \delta \ W_n \ H_{lag}) \ \tau \tag{2-3}$$

$$P_{lag} = P_{lag} + (\dot{\Theta}_{2m} - 2 \ \delta \ W_n \ P_{lag}) \ \tau \tag{2-4}$$

Where: $\dot{\Theta}_{1r}$ = The Actual Turn Rate (radians / sec)

$\dot{\Theta}_{2r}$ = The Actual Pitch Rate (radians / sec)

W_n = Missile Natural Frequency (radians / sec)

δ = Natural Damping of the Missile (No Units)
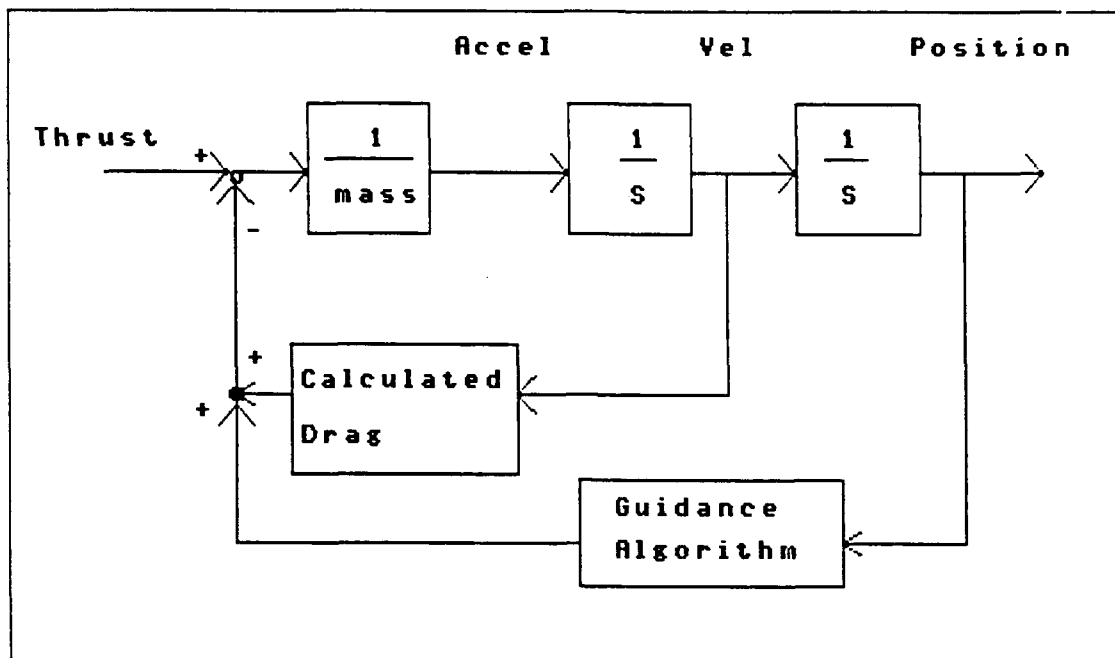
Figure 2-3 Missile Truth Model Block Diagram

$\dot{\Theta}_{1cmd}$ = The Commanded Turn rate (radians / sec)

$\dot{\Theta}_{2cmd}$ = The Commanded Pitch Rate (radians / sec)

H_{lag} = Internal 2nd order state variable

P_{lag} = Internal 2nd order state variable

τ = System integration time   time delta (sec)

The missile and aircraft flight starts at time zero, location
(x,y,z) = $(0,0,0)$. The missile has an initial velocity equal to the
aircraft velocity and an acceleration of THRUST/MASS. The missile weight
is decremented during each update during the rocket burn. The amount of
the weight decrement is calculated so the fuel weight is eliminated at
burnout time, assuming constant thrust. A linear fuel burn and a constant
thrust are normal missile design goals. The heading of the missile is
altered by the applied lateral commands. This is accomplished by turning
the missile half the distance it will turn in a time interval of τ;
applying the acceleration caused by the engine thrust; updating the

velocity and position vectors; then turning the missile the remaining commanded rotation and adjusting the velocity vector to align to this new heading. This method ensures a smooth and accurate implementation of the commanded turn. The Euler integration technique is used in this model so it is important to keep the integration step size much smaller than the time constant associated with the missile [4:B-3]. In this test a 2 msec integration time was used.

The drag on the missile is calculated much the same as Capps did except for a lift drag penalty proportional to the turn command [4:2-9 - 2-10]. The drag, μ, is calculated as follows:

$$\mu = - \sigma/2 \; S \; V_m^2 \; (V_s/V_m + \dot{\Theta}_{1m} \; V_m \; K_{dr}) / M \qquad (2-5)$$

Where: μ = Air Drag Estimate (ft/sec^2)

σ = Air density (.0023 slugs/ft^3)

S = MSL Cross-sectional Area (ft^2)

V_m = MSL Velocity (FPS)

V_s = Speed of Sound, 1087.1 (FPS)

(i.e. V_s / V_m = 1/MACH#)

$\dot{\Theta}_{1m}$ = Actual Missile Turn Rate (Radians / sec)

K_{dr} = A Lift Drag Penalty Constant (sec^2/ft)

M = Missile Mass (Slugs)

In many models the missile drag is based on only the body drag with no penalty for the lift drag caused by missile turns. The K_{dr} constant has a default setting which doubles the air drag during a 50 G turn at 5000 FPS missile velocity. This drag penalty is caused by the missiles angle of attack during turning and is added here to add fidelity to the HVM motion model. The coupling of this lift drag to the body drag through a proportion constant is better understood by examining Blackelock's development of the drag equation [8-332]. Thus, in this model there is a drag penalty added for high G turning commands.

In this manner the missile state vector is updated each cycle of the executive. The state vector includes the three dimensional position and velocity vectors tracked in double precision. The calculation of these states is straight forward.

2.4 Aircraft Model

Since the missile flight is so short (approximately 4 seconds maximum) a very simple 3DOF model is used to simulate the aircraft position. Because of its simplicity it is not a validated F-16 model, but it can simulate the position of a maneuvering F-16 during a 4 second portion of flight. The 3DOF model of the aircraft is an integral part of the system executive. It consists of an integration of the state vectors at an integration time of τ, the system time delta. A block diagram of this model is the same as the missile model shown in Figure 2-3, except the input thrust and drag are always equal and opposite. This assumption makes the aircraft maintain a constant speed during the missile flight, even if the aircraft engages in a turn. This is a realistic flight maneuver for the short engagement time.

The aircraft track is determined by the variable selection prior to the simulation run. The variables that may be altered prior to each run are shown in Table 2-2. The ones which control the aircraft model include an initial aircraft heading, speed, pitch, turn G and climb G. For a left turn or a dive the turn G and climb G are negative. These initial G maneuvers are transformed into a total G maneuver at a body angle to keep the coordinate frame proper during a pitch over maneuver. Since AOA and sideslip are not modeled in a 3DOF model it is left to the care of the user to ensure that aircraft heading or pitch does not inhibit sensor tracking bounds for the target or the missile. All maneuvers are assumed to occur at a constant speed, and the maneuver is constant throughout the short missile flight time. There is also no G onset rate so when set for

a 5 G turn (for example), the aircraft is already executing this turn at t=0, launch time.

At launch time, time zero, the aircraft position establishes the origin of the reference inertial plane. The aircraft initial velocity vector is established by the input heading, pitch and aircraft speed. The heading of the aircraft is altered by the applied maneuver commands. This is accomplished by turning the aircraft half the distance it will turn in a time interval of τ; updating the velocity and position vectors; then turning the aircraft the remaining commanded rotation and adjusting the velocity vector to align to this new heading. This method ensures a smooth and accurate implementation of the commanded turn, as discussed in the missile model description.

In this manner the aircraft state vector is updated with the Euler integration technique during each cycle of the executive. The state vector includes the three dimensional position and velocity vectors tracked in double precision. The calculation of these states is straight forward.

2.5 Target Model

The target model used in this analysis is a simple 3DOF approximation of a moving ground target. The model employes a simple Euler integration technique in the NED coordinate frame with an x and y (north and east) plane and a constant vertical plane assumed. The form of the Euler integration is as follows:

$$V_x(t+1) = V_x(t) + A_x \, dt \tag{2-6}$$

$$V_y(t+1) = V_y(t) + A_y \, dt \tag{2-7}$$

$$X_t(t+1) = X_t(t) + V_x(t+1) \, dt \tag{2-8}$$

$$Y_t(t+1) = Y_t(t) + V_y(t+1) \, dt \tag{2-9}$$

The initial conditions and the acceleration terms are calculated from the scenario input variables LOS_t, R_t, V_{tgt}, H_{tgt} and A_{tgt} shown in Table 2-2.

These calculations are shown below.

$$A_x = A_{tgt} \sin(H_{tgt}) \qquad\qquad A_y = A_{tgt} \cos(H_{tgt})$$

$$V_x(0) = V_{tgt} \cos(H_{tgt}) \qquad\qquad V_y(0) = V_{tgt} \sin(H_{tgt})$$

$$X_t(0) = R_t \cos(LOS_t) \qquad\qquad Y_t(0) = R_t \sin(LOS_t)$$

Where: LOS_t = Line of Sight angle from Aircraft to Target

$\qquad R_t$ = Range from Aircraft to Target

$\qquad V_{tgt}$ = Velocity of Target

$\qquad H_{tgt}$ = Heading of Target

$\qquad A_{tgt}$ = Acceleration of Target

In this manner the target is given motion for the algorithm evaluation. The target integration is accomplished each cycle of the execution as is the aircraft and missile Euler integrations. The measurement model is used to calculate the missile and target position relative to the aircraft and to put these in an angle and range format as would be done by a FLIR and a radar. Since the aircraft attitude is not calculated in the 3DOF model, these lines of sight measurements are not in the aircraft tracking frame as done by some models. In the NED coordinate frame the line of sight measurements are the angle from north, and the angle above the horizon, as shown in Figure 2-1 and 2-2.

2.6 Measurement Model

The Measurement model is made up of a 14 state matrix and the calculations required to update the matrix from the inertial data. The states selected for the model are as follows:

$x(1) = \beta_{1t}$ = Azimuth LOS aircraft to target

$x(2) = \dot{\beta}_{1t}$ = Azimuth LOS rate aircraft to target

$x(3) = \beta_{2t}$ = Pitch LOS aircraft to target

$x(4) = \dot{\beta}_{2t}$ = Pitch LOS rate aircraft to target

$x(5) = R_t$ = Range aircraft to target

$x(6) = \dot{R}_t$ = Range rate aircraft to target

$x(7) = \beta_{1m}$ = Azimuth LOS aircraft to missile

$x(8) = \dot{\beta}_{1m}$ = Azimuth LOS rate aircraft to missile

$x(9) = \beta_{2m}$ = Pitch LOS aircraft to missile

$x(10) = \dot{\beta}_{2m}$ = Pitch LOS rate aircraft to missile

$x(11) = R_m$ = Range aircraft to missile

$x(12) = \dot{R}_m$ = Range rate aircraft to missile

$x(13) = R_{mest}$ = Range estimate, aircraft to missile

$x(14) = V_{mest}$ = speed estimate of the missile relative to aircraft

These last two states are constructed from a very simple missile model in order to test the algorithm with FLIR inputs only, i.e. no radar range or range rate data available. The simplified missile model assumes that the missile has constant acceleration and constant drag, and that it flies directly away from the launching aircraft. As expected it accumulates error rapidly, and this error is used to demonstrate guidance algorithm sensitivity to poor range data.

The aircraft could use a Kalman filter to provide a best estimate of these values to the guidance algorithm. In this simplified model single precision 'perfect' measurements approximate the data that would be available to the guidance algorithms on the aircraft. The single precision used is an 8 bit exponent and a 24 bit mantissa. This gives a range accuracy of 7×10^{-4} feet, range rate of 4×10^{-4} fps, and angle measurements of 6×10^{-7} rad. Though noise free, the modeled state measurements are adequate for the this first level evaluation of the guidance algorithms.

The calculations of these states is accomplished at an update rate as specified in the scenario input. The states are shown in Figure 2-1 and 2-2 and are calculated from the geographic NED x, y, and z values as follows:

2-11

$$\beta_{1t} = \tan^{-1}((Y_t - Y_a)/(X_t - X_a)) \tag{2-10}$$

$$\beta_{1m} = \tan^{-1}((Y_m - Y_a)/(X_m - X_a)) \tag{2-11}$$

$$r_t = ((X_t - X_a)^2 + (Y_t - Y_a)^2)^{1/2} \tag{2-12}$$

$$\beta_{2t} = \tan^{-1}((Z_t - Z_a)/r_t) \tag{2-13}$$

$$r_m = ((X_m - X_a)^2 + (Y_m - Y_a)^2)^{1/2} \tag{2-14}$$

$$\beta_{2m} = \tan^{-1}((Z_m - Z_a)/r_m) \tag{2-15}$$

$$R_t = ((Z_t - Z_a)^2 + r_t^2)^{1/2} \tag{2-16}$$

$$R_m = ((Z_m - Z_a)^2 + r_m^2)^{1/2} \tag{2-17}$$

$$\dot{\beta}_{1t} = \frac{(V_{yt} - V_{ya})\cos(\beta_{1t}) - (V_{xt} - V_{xa})\sin(\beta_{1t})}{r_t} \tag{2-18}$$

$$\dot{\beta}_{1m} = \frac{(V_{ym} - V_{ya})\cos(\beta_{1m}) - (V_{xm} - V_{xa})\sin(\beta_{1m})}{r_m} \tag{2-19}$$

$$\dot{\beta}_{2t} = (V_{zt} - V_{za})/R_t\,\cos(\beta_{2t}) -$$
$$(V_{xt} - V_{xa})/R_t\,\cos(\beta_{1t})\,\sin(\beta_{2t}) -$$
$$(V_{yt} - V_{ya})/R_t\,\sin(\beta_{1t})\,\sin(\beta_{2t}) \tag{2-20}$$

$$\dot{\beta}_{2m} = (V_{zm} - V_{za})/R_m\,\cos(\beta_{2m}) -$$
$$(V_{xm} - V_{xa})/R_m\,\cos(\beta_{1m})\,\sin(\beta_{2m}) -$$
$$(V_{ym} - V_{ya})/R_m\,\sin(\beta_{1m})\,\sin(\beta_{2m}) \tag{2-21}$$

$$\dot{R}_t = (V_{zt} - V_{za})\,\sin(\beta_{2t}) + (V_{xt} - V_{xa})\,\cos(\beta_{1t})\,\cos(\beta_{2t}) +$$
$$(V_{yt} - V_y)\,\sin(\beta_{1t})\,\cos(\beta_{2t}) \tag{2-22}$$

$$\dot{R}_m = (V_{zm} - V_{za})\,\sin(\beta_{2m}) +$$
$$(V_{xm} - V_{xa})\,\cos(\beta_{1m})\,\cos(\beta_{2m}) +$$
$$(V_{ym} - V_{ya})\,\sin(\beta_{1m})\,\cos(\beta_{2m}) \tag{2-23}$$

For the 3DOF implementation of this model the missile attitude is not calculated. Instead, the missile NED x, y, and z values are taken from the missile truth model and used to calculate the parameters needed by the guidance algorithms.

2.7 System Truth Model Summary

The 3DOF truth model constructed for this analysis is adequate for algorithm familiarity and preliminary test. The model is not intended for the full error sensitivity analysis where a 6DOF model is needed for angle measurement analysis. This sensitivity analysis needs to be accomplished on guidance algorithms which, in this preliminary test, are most effective.

The measurement model is made to use the range and velocity estimates for its range and range rate measurements during some tests. This simulated the elimination of the radar sensor and tested the guidance algorithms dependence on range and range-rate measurements. For more details on this analysis see Chapter 4.

The models constructed here are simple but useful for performing the initial comparative analysis of the four guidance algorithms. The next chapter gives a detailed explanation of the guidance algorithm development.

III. Guidance Algorithm Development

3.1 Introduction

The guidance algorithms tested in this study have been tested in many applications. The Line-Of-Sight (LOS) algorithm, sometimes called a beam rider algorithm, is very common in surface to air missile applications [6:158]. The LOS+ algorithm is similar to the LOS algorithm with a predictor that estimates the final line of sight to the target and guides the missile down this line to the target. The pursuit algorithm is an old standby used because of its very simple implementation. This algorithm is implemented by causing the missile to continually steer towards the target. The proportional guidance algorithm is a low control energy guidance algorithm based on the fact that if the LOS between a missile (or originally a ship) and a target does not change they are on a collision course. (This is preferred by the missile-target scenario, but dreaded by the ship-to-ship scenario.)

A different application of these algorithms is represented here because they are being used in a system quite foreign to their original development. The LOS algorithm has been developed and used largely for a stable platform tracking a moving target, here we have a moving platform tracking a relatively stable target. The pursuit and proportional guidance algorithms were built for a missile sensor tracking a target, here a third party is involved, an aircraft, trying to sense the targets location relative to the missile's. In each application the guidance algorithms must deal with an extremely fast missile that uses only turn or climb commands. In this sense then, this is a new test of these algorithms.

The development of these algorithms is discussed in the sections that follow. It should be remembered again that the geometry of the scenario takes a little effort to understand in each discussion. These changes in

the basic scenario geometry cause the algorithms to react differently than in their normal implementation, as seen in the analysis section of this report.

3.2 Line of Sight Algorithm Development

The LOS guidance principle is often called the beam rider method and was developed fo. ground to air applications [6:158]. It involves keeping the missile on a line projected from the shooter to the target. Note that this is different than a pursuit guidance scheme where the missile is pointed down to its own line of sight to the target. The geometry of the LOS guidance scheme is shown in Figure 3-1.

In both snapshots of this figure a missile steering correction is required to move the missile onto the line between the aircraft and the target. The calculation of this steering command is the task of the LOS guidance algorithm. A concern with the LOS guidance scheme is that some missile control energy must be used to keep the missile on a rotating LOS. How much control energy this takes was not clear prior to this effort, but the missile control energy consumed is one of the measures of effectiveness in this study. This was a concern because the current missile design turns with a limited supply of pyrotechnic cartridges. A second concern with this guidance method involved the missile's rocket plume standing between the target and the FLIR assigned to track the target. This problem is not addressed in this study, except to note that the LOS+ guidance algorithm was devised to avoid this problem. The ability of the FLIR to track a target through the missile plume, or to detect a burned out missile overlaying a target is a problem which requires further study. The LOS algorithm analysis of Chapter 4 and the conclusions and recommendations of Chapter 5 address these concerns further.

In working with the LOS guidance concept some geometry problems are discovered that were not discussed in any of the literature uncovered on
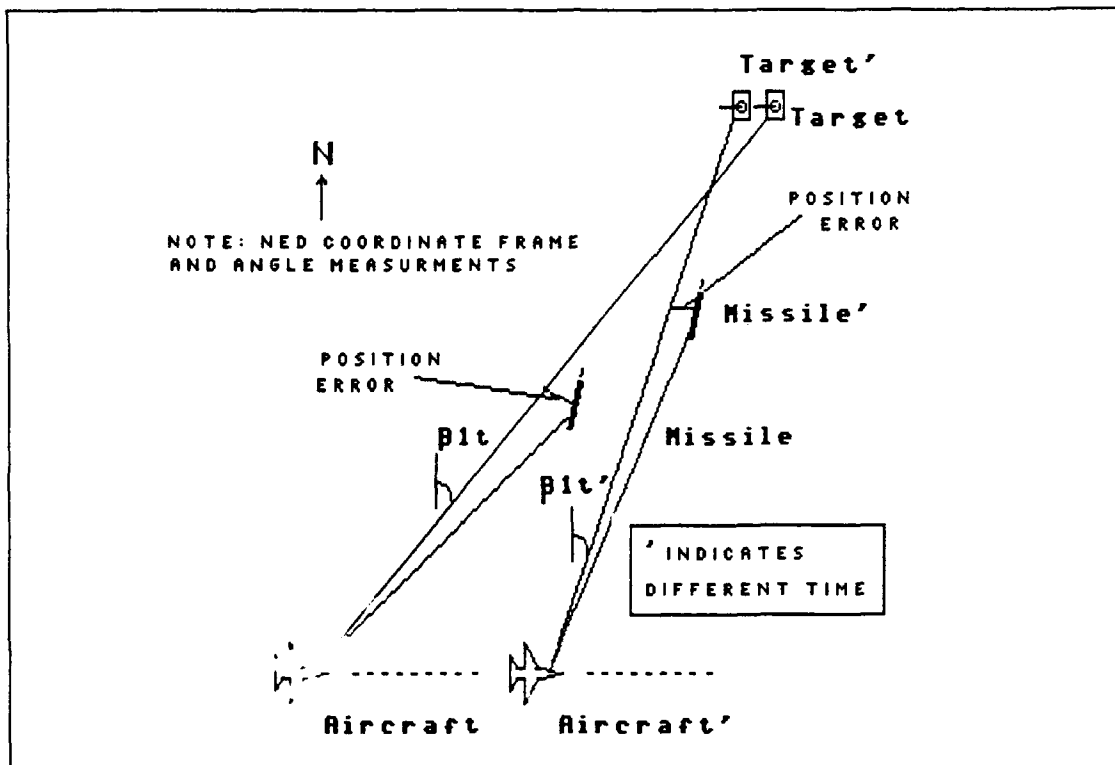
Figure 3-1 Rotating β_{1t} Geometry

beam riders. The algorithm development proceeded as did some of the early ballistic missile algorithms, with what is called a nominal velocity and the calculation of a velocity to be gained [7:65-70].

The dot product of this velocity vector to be gained with the current missile velocity vector provides the missile steering commands. The nominal velocity is calculated in two parts. A missile that is on the nominal course, i.e. on the LOS between the aircraft and the target, will have a component of velocity keeping it on the rotating LOS, and a component of velocity directing it down the LOS to the target. These components are shown in Figure 3-2 as V_{1n} and V_{2n}. The first component can be calculated from the LOS rate and the range from the aircraft to the missile, Rm. The second component, moving the missile down the line of sight, is simply the remaining missile velocity magnitude. An additional correction term must be added to this otherwise nominal velocity, to

NOMINAL MSL VELOCITY

$$\overline{V}_n = V1n \, \hat{r} + V2n \, \hat{t}$$

ACTUAL MSL VELOCITY

$$\overline{V}_m = V1'_m \, \hat{r}' + V2'_m \, \hat{t}'$$

$$\overline{V}_m = V1m \, \hat{r} + V2m \, \hat{t}$$

'INDICATES CHANGED COORDINATE SYS
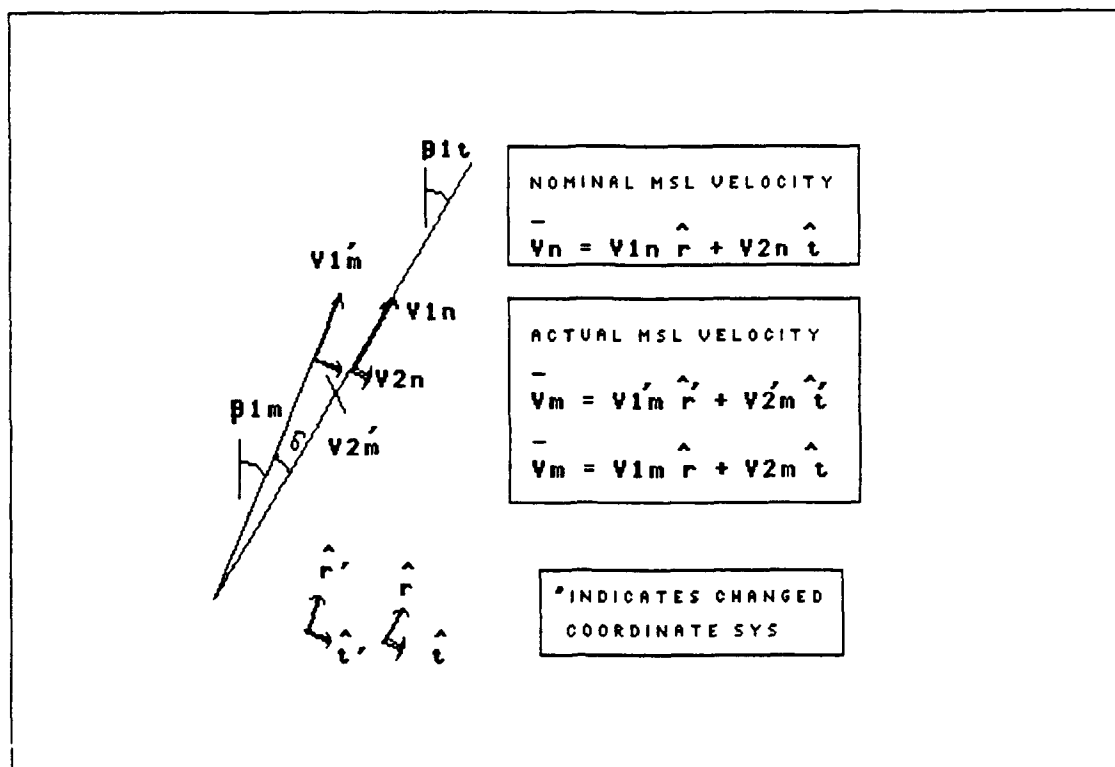
Figure 3-2 Differing Coordinate System of V_m

compensate for missile position and bring the missile onto the target line of sight. This correction term is the distance to the line of sight (labeled position error in Figure 3-1) divided by a correction time, t_c. This is the time allowed for this position error correction and it is a predominate algorithm control parameter. Thus the nominal velocity vector is calculated as follows:

$$\overline{V}_n = V_{2n} \, \hat{t} + V_{1r} \, \hat{r}$$

$$\overline{V}_n = (r_m \, \beta_{1t} + r_m \, \delta/t_c) \hat{t} + (V_m^2 - (r_m \, \beta_{1t})^2)^{1/2} \, \hat{r} \tag{3-1}$$

Where: $\overline{V}_n$ = Nominal velocity vector for on track missile

   V_{2n} = the V_n tangent to the line of sight

   V_{1r} = the V_n radial along the line of sight

   $\delta = \beta_m - \beta_{1t}$

   t_c = an input control parameter of correction time

   r_m = horizontal range from aircraft to missile

3-4

$\dot{\beta}_{1t}$ = LOS angle rate from aircraft to target

$\hat{t}$ = unit vector component tangent to β_{1t}

V_m = Velocity of missile with respect to aircraft

$\hat{r}$ = unit vector component radial along β_{1t}

Note that the correction for the position error is assumed to be entirely in the tangent component of the nominal velocity. This is true if the difference angle, δ, is small. Should this angle become to large, as in the LOS+ guidance algorithm discussed later, the portion of this position correction that lies in the radial direction must also be calculated. If the difference angle, δ, grows large, a radial component of the correction term is required to maintain this algorithm accurately. (It can be seen that when δ approaches 90 degrees a tangent term will pull the missile back towards the aircraft rather than towards the target. This problem is encountered during the LOS+ development because a forecast position is used which caused δ to exceed 90 degrees.) For a normal LOS guidance application, where the target and missile remain in the same line-of-sight angle quadrant, this tangent component is all the correction term that is necessary. With a nominal velocity calculated, one must now calculate the velocity of the missile and translate it into the same reference frame. The missile velocity is calculated from the measurement model parameters as follows:

$$\overline{V}_m = r_m \, \dot{\beta}_{1m} \, \hat{t}' + \dot{r}_m \, \hat{r}' \qquad (3-2)$$

Where: $\overline{V}_m$ = missile velocity with respect to the aircraft

r_m = horizontal range form aircraft to missile

$\dot{\beta}_{1m}$ = LOS angle rate from aircraft to missile

$\hat{t}'$ = unit vector component tangent to β_{1m}

$\hat{r}'$ = unit vector component radial along β_{1m}

It can be seen in Figure 3-2 that a rotation of the coordinate system is required before mathematical operations can be accomplished on the missile LOS vector. This vector rotation is accomplished as follows:

$$\overline{V}_m = (r_m \, \dot{\beta}_{1m} \cos(\delta) + \dot{r}_m \sin(\delta)) \, \hat{t}$$
$$+ (r_m \, \dot{\beta}_{1m} \sin(\delta) + \dot{r}_m \cos(\delta)) \, \hat{r} \tag{3-3}$$

Where: δ = the angle between $\hat{r}$ and $\hat{r}'$

In order to understand the control problem and construct the control block diagram a small angle approximation can be made if the missile is close to its nominal position on the aircraft to missile line-of-sight. This approximation is accurate for angles of less than 10 degrees. With this assumption the missile velocity vector of equation (3-3) reduces to:

$$\overline{V}_m = r_m \, \dot{\beta}_{1m} \, \hat{t} + \dot{r}_m \, \hat{r} \tag{3-4}$$

Now that the velocity of the missile and the desired, or nominal velocity are in the same coordinate system the velocity to be gained (V_g) is simply the difference:

$$\overline{V}_g = \overline{V}_n - \overline{V}_m$$

Combining equations (3-1) and (3-4):

$$\overline{V}_g = r_m \, (\delta/t_c + \dot{\beta}_{1t} - \dot{\beta}_{1m}) \, \hat{t} + (\dot{r}_n - \dot{r}_m) \, \hat{r} \tag{3-5}$$

Where: $\dot{r}_n = (V_m^2 - (r_m \, \dot{\beta}_{1t})^2)^{1/2}$

Once the velocity to be gained vector is computed the heading change may be computed by taking the cross product as follows:

$$\Theta_{1cmd} = K3/|\overline{V}_m| \; (\overline{V}_g \times \overline{V}_m) \tag{3-6}$$

$$\Theta_{1cmd} = K3 \, r_m/|V_m| \; (r_m \, (\dot{\beta}_{1t} + \delta/t_c) - \dot{r}_n \, \dot{\beta}_{1m}) \tag{3-7}$$

This is the equation used in the LOS guidance algorithm. Notice that the missile velocity magnitude is normalized out of the heading command but the velocity to be gained magnitude is not. The algorithm gain control, K3, must be quite small to account for this remaining magnitude. Some dot product steering methods normalize to one and use K3 to control

all the loop gain. The magnitude of Vg was left in the command because it represents a magnitude of required error correction.

Notice that these equations handle the azimuth guidance in the horizontal plane. An identical set of these equations has to be implemented in the vertical plane to calculate the missile pitch rate command, Θ_{2cmd}.

Notice also that care is taken to implement this algorithm using only the variable states available from the measurement model described in Paragraph 2.6. Thus the LOS guidance algorithm is tested with identical scenarios available to the other guidance algorithms.

3.2.1 LOS Algorithm Control Parameters. The algorithm allows two variable inputs, K3 and t_c, that change the dynamics of the guidance algorithm. By studying the block diagram of Figure 3-3 it can be seen that these parameters control the system gain and a control loop zero. To derive the block diagram and the root locus plots requires some assumptions shown in the following development.

Equation (3-7) can be simplified by assuming that the LOS angle to the target and the LOS angle to the missile will always be close to each other, say within 0.17 radians. This is true when the missile is being properly guided down the line-of-sight. It is not true during the first moments after launch for an off angle shot (i.e. an off angle of greater than 0.17 radians) but the missile quickly comes into this limitation so the general control principle being developed here is effective. This small angle assumption used to analyze the control problem yields $\sin(\delta) \approx \delta$ and $\cos(\delta) \approx 1$. Assuming the missile is heading almost directly away from the aircraft, a typical guidance situation, r_m rate $\approx r_t$ rate $\approx V_r$. Using these approximations to simplify equation (3-7) we see that:

$$r_r \; \dot{\beta}_{1r} = V_r \; \sin(\Theta_{1r} - \beta_{1m})$$

solving for $\dot{\beta}_{1m}$ and applying the small angle assumption yields:

$$\dot{\beta}_{1r} \approx V_m/r_m \; (\Theta_{1m} - \beta_{1r})$$
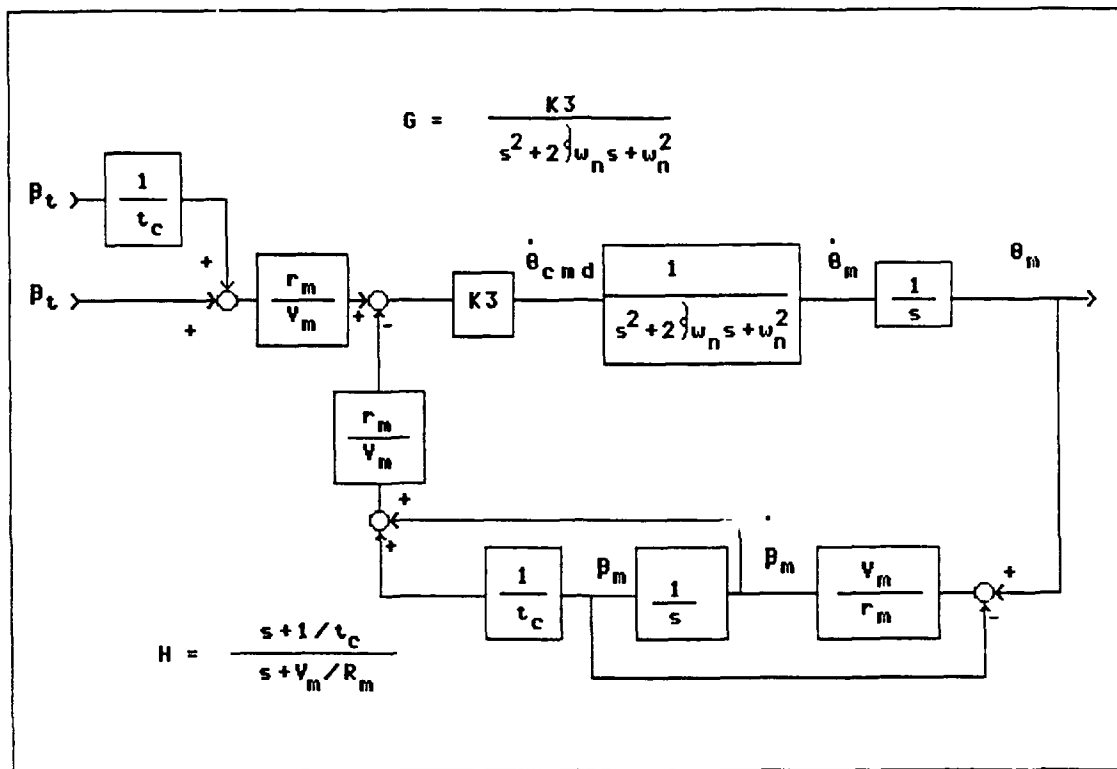
Figure 3-3 LOS Control Block Diagram

With the velocity assumption this simplifies equation (3-7) into:

$$\dot{\Theta}_{1cmd} \approx K3 \; r_m \; (\dot{\beta}_{1t} - \dot{\beta}_{1m} + \beta_{1m}/t_c - \beta_{1t}/t_c \;)$$

With these simplifications in place the block diagram of Figure 3-3 is constructed. The poles and zeros of this control system are plotted, and it is seen that t_c controls a zero placement. The plotting of the root locus here is not a trivial matter because there is a pole location at $-V_m/r_m$. As the missile accelerates and leaves the aircraft this pole location moves and causes the root locus plot to have a time dependence. V_m/r_m changes according to Table 3-1. As the missile gets farther away from the aircraft the LOS guidance control characteristics change. Three snapshots of the root locus plots are shown in Figure 3-4. The three plots represent times of .06, .5, and 1.0 seconds, with a zero set by t_c at -10. These plots are representative of the root locus variations during a launch with a LOS guidance scheme. They reveal the time variation of this

Table 3-1 Typical flight V_m/R_m pole values

Time sec	V_m ft/sec	R_m k ft	$- V_m/R_m$ /sec
0.02	55	0.005	-11.83
0.04	110	0.006	-17.80
0.06	166	0.009	-18.69
0.08	227	0.013	-17.28
0.10	284	0.018	-15.52
0.12	340	0.025	-13.87
0.14	398	0.032	-12.44
0.16	455	0.041	-11.23
0.18	508	0.049	-10.30
0.20	567	0.060	-9.43
0.50	1562	0.368	-4.24
1.00	3322	1.574	-2.11
1.50	5565	3.777	-1.47
2.00	5123	6.445	-0.795
2.50	4720	8.892	-0.531
2.89	4431	10.66	-0.416

root locus throughout the flight. A more efficient control could be developed by tuning the system gain for various phases of the flight. The gain could then be adjusted to provide the desired damping for the entire flight. In this development a constant gain was used to provide favorable damping over the range of control characteristics found in a typical flight of the defined missile. The placement of the zero and the gain is controlled by varying t_c and K3. This is accomplished to give best algorithm performance and is the first thing explored in the analysis section of Chapter 4.

3.3 Line-of-sight Plus (LOS+) Algorithm Development

The LOS+ algorithm is a unique solution devised to move the missile off the target line-of-sight (in an attempt to ease the FLIR target and missile discrimination) and to reduce the control energy involved in following a rotating line-of-sight [1]. The LOS+ guidance algorithm is not new but no references were found that give its description or document
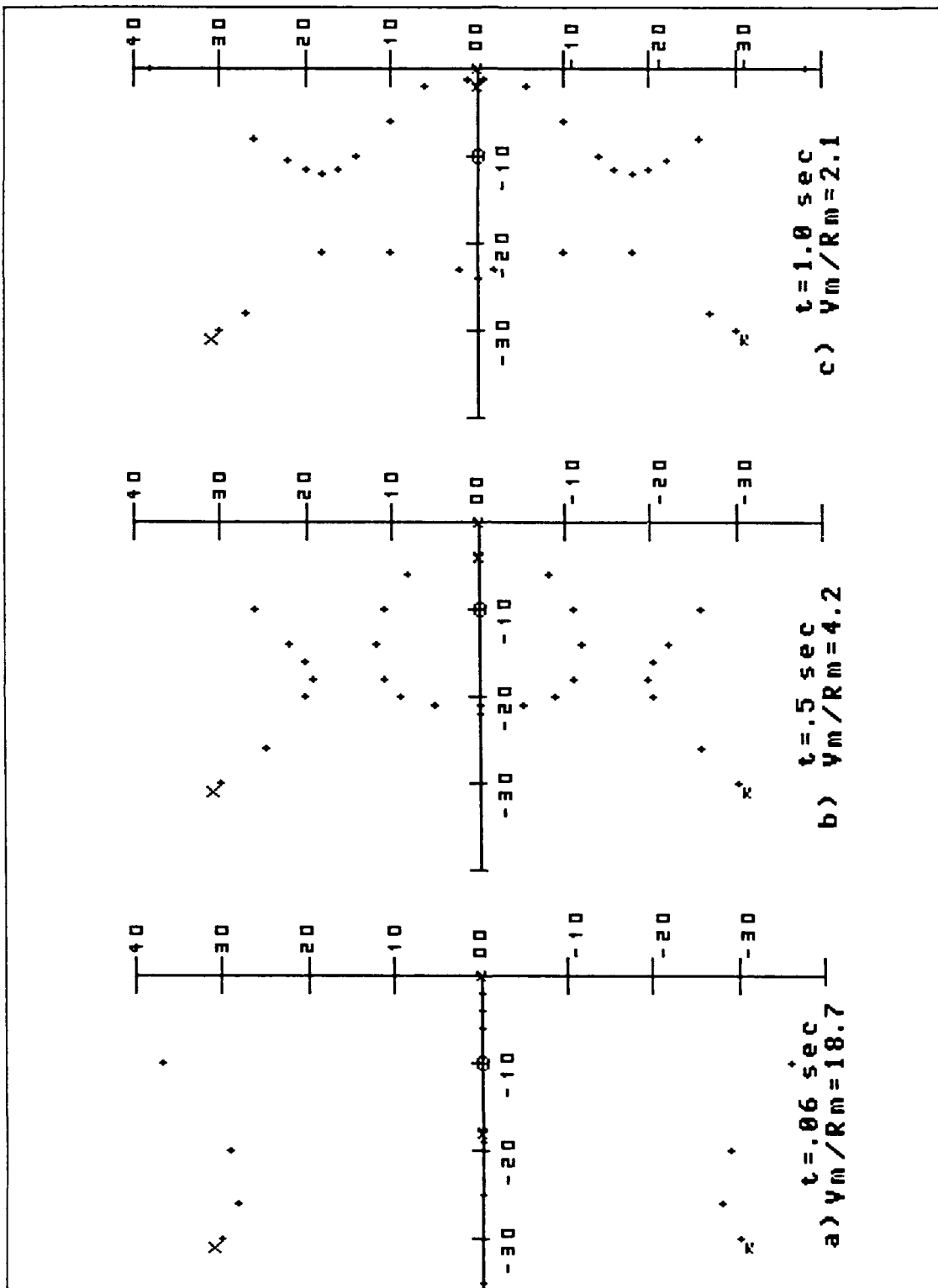
Figure 3-4 Root Locus Plots During a Typical Flight

its use. As with the LOS guidance, however, the application of the algorithm, with a moving tracker, is unique. The principle involved in this guidance concept requires forecasting the aircraft position and the LOS to the target, β_{1t} and β_{2t}, at the time of missile intercept and flying the missile down this reasonably stable line-of-sight into the target. Figure 3-5 is a layout of this concept.

Two challenges evident in this concept are the requirement to calculate the time to missile impact and the control problem involved in guiding the missile on to this future line-of-sight. In the very early development of this guidance algorithm its inefficiencies began to show through. The first evident drawback is the missiles high velocity when the first major turn onto the future line-of-sight is encountered. This high velocity causes this turn to impose a high control energy requirement as seen in the analysis. Figure 3-5 shows this problem, though somewhat exaggerated because of the high off angle shot pictured.

Attempts were made to "aim" for different intercept points on the future line-of-sight but each solution is a compromise in either accuracy or control energy. Because of its high velocity and short flight time an optimal solution must be developed to efficiently put the missile on the future line-of-sight. Since the optimal solution will involve a time varying gain and Locus pole/zero placement (reference the LOS control parameters of Para 3.2.1) it is considered beyond the scope of this research. The other guidance algorithms developed here were considered more advantageous than spending much effort on this algorithm development.

A second drawback to the LOS+ algorithm is its sensitivity to the aircraft's maneuvers after launch. Yogi Bera once said "the future is not what it used to be," and this is especially true of a future line-of-sight when a pilot pulls an unpredicted 5 G turn. The other algorithms developed here are intuitively more independent of the launch aircraft's maneuvers. Again the LOS+ algorithm could be better tuned to account for
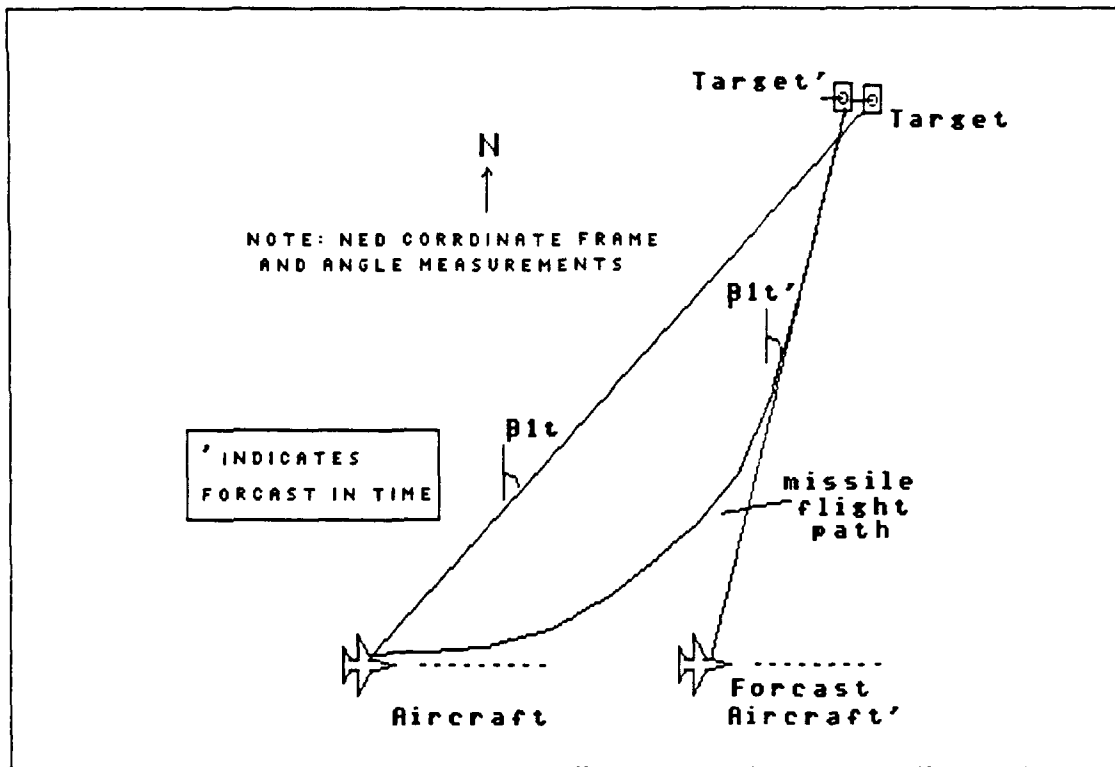
Figure 3-5 LOS+ Implementation Geometry

aircraft acceleration but the work involved is deemed more tedious than advantageous, given the shortfalls of this algorithm. The challenges of calculating an impact time and guiding to the future line-of-sight are discussed in the following paragraphs.

3.3.1 Missile Impact Time Calculation. The missile impact time must be calculated in order to project the aircraft position properly. The missile impact time is calculated with a simple binary search iteration technique. The time to go, t_g is calculated as follows:

$$t_g = R_g / |V_{mt}| \qquad (3-8)$$

Where R_g = range to go i.e. missile to target range (see equation (3-9))

$|V_{mt}|$ = Average missile Velocity (see equation (3-10))

A simple conversion to the NED x, y, and z coordinates and a magnitude calculation of their differences is used in this calculation. This is accomplished using the following equations:

$$R_g = [(r_t \sin(\beta_{1t}) - r_m \sin(\beta_{1m}))^2 +$$

$$(r_t \cos(\beta_{1t}) - r_m \cos(\beta_{1m}))^2 +$$

$$(R_t \sin(\beta_{2t}) - R_m \sin(\beta_{2m}))^2]^{1/2} \qquad (3\text{-}9)$$

The average missile velocity is calculated by a weighted time average of the acting accelerations as follows:

IF $t < t_{BURN}$:

$$|V_{mt}| = V_0 + 1/2 [a_{th} (t_{BURN} - t) + a_{dr} t_g] \qquad (3\text{-}10)$$

IF $t >= t_{BURN}$:

$$|V_{mt}| = V_0 + 1/2 a_{dr} t_g \qquad (3\text{-}11)$$

Where: V_0 = missile velocity at time of calculation (see equation (3-14))

t = time of calculation

t_g = time to go before impact

t_{BURN} = time of rocket burn

a_{th} = Average accel caused by missile thrust (see equation (3-15))

a_{dr} = Average accel caused by missile drag (see equation (3-16))

The present missile velocity is: $V_0 = |V_m - V_t|$

To perform this subtraction the target velocity term is rotated into the line-of-sight to the missile as follows:

$$V_m = \dot{r}_m \hat{1}_1 + r_m \dot{\beta}_{1m} \hat{1}_2 + R_m \dot{\beta}_{2m} \hat{1}_3 \qquad (3\text{-}12)$$

$$V_t = [\dot{r}_t \cos(\delta) + r_t \dot{\beta}_{1t} \sin(\delta)] \hat{1}_1 +$$

$$[\dot{r}_t \sin(\delta) + r_t \dot{\beta}_{1t} \cos(\delta)] \hat{1}_2 +$$

$$R_t \dot{\beta}_{2t} \hat{1}_3 \qquad (3\text{-}13)$$

Subtracting the terms and taking the magnitude yields:

$$V_0 = \{(\dot{r}_m - (\dot{r}_t \cos(\delta) + r_t \dot{\beta}_{1t} \sin(\delta)))^2 +$$

$$(r_m \dot{\beta}_{1m} - (-\dot{r}_t \sin(\delta) + r_t \dot{\beta}_{1t} \cos(\delta)))^2 +$$

$$(R_m \dot{\beta}_{2m} - R_t \dot{\beta}_{2t})^2]^{1/2} \qquad (3\text{-}14)$$

Where: r_m = horizontal range from aircraft to missile

$\dot{r}_m$ = horizontal range rate from aircraft to missile

β_{1m} = LOS angle from aircraft to missile

$\dot{\beta}_{1m}$ = LOS angle rate from aircraft to missile

3-13

r_t = horizontal range from aircraft to target

$\dot{r}_t$ = horizontal range rate from aircraft to target

β_{1t} = LOS angle from aircraft to target

$\dot{\beta}_{1t}$ = LOS angle rate from aircraft to target

R_m = range form aircraft to missile

$\dot{\beta}_{2m}$ = Pitch LOS angle rate from aircraft to missile

R_t = range form aircraft to target

$\dot{\beta}_{2t}$ = Pitch LOS angle rate from aircraft to target

The acceleration and drag terms required for equation (3-10) and (3-11) are averages calculated from missile input parameters. The use of these average accelerations over the remaining time of flight meets the accuracy requirements of this simple time to go calculation. The acceleration and drag terms are calculated as follows:

$$a_{th} = (TH) * G / (W_{TBD} + 1/2 W_{TFU}) \qquad (3-15)$$

AND:

$$a_{dr} = \frac{-\sigma \pi D^2 V_s (V_a + 1/2 a_{th} t_{BURN})}{8 * WTBD/G} \qquad (3-16)$$

Where: TH = Rocket Thrust input from missile data file

G = Gravitational constant

W_{TBD} = missile body weight input from missile data file

W_{TFU} = missile fuel weight input from missile data files

σ = air density (.0023 slugs/ft^3)

D = missile diameter input from missile data files

V_s = Speed of Sound at average altitude, 1087 ft/sec

V_a = aircraft velocity

These equations are now used in a binary search iteration to calculate the time to go, t_g. The binary search is implemented as follows:

Step 1: Calc R_g and V_c and guess at time to go, t_{guess}

Step 2: Calculate $|V_{mt}|$ via equation (3-10) or (3-11)

Step 3: Calculate t_g via equation (3-8)

Step 4: Set $t_{guess} = t_{guess} + 1/2(t_g + t_{guess})$

3-14

Step 5: IF ABS(t_g-t_{guess}) > Tolerance Repeat from Step 2

This method converged on to the missile time to go value in about 10 iterations in each case tested. It also makes the assumption that the missile is using all its velocity to get straight to the target.

3.3.2 LOS+ Control Challenge. Getting a missile of this speed to fly down a predicted aircraft-to-target LOS in the short time allowed, turns out to be a challenge. The approach taken here is one of several that could work, but others were not attempted because there are more efficient optimal control solutions that should be used if this guidance methodology were to be considered further.

This approach follows the footsteps of the previous LOS development that used a nominal velocity calculation, a velocity to be gained, and a dot product steering command calculation. The complete nominal velocity calculation involves two factors. A nominal velocity for an on track missile and a position correction term are required to move the missile towards this 'on track' condition. The nominal velocity for an on track missile is simply a velocity moving the missile down the stable future LOS to the target. The nominal velocity magnitude is set equal to the current missile velocity magnitude. So its calculation requires only a rotation of the missile velocity onto the future LOS. This rotation is accomplished as follows. The future LOS is calculated assuming a constant β_{1t} rate:

$$\beta'_{1t} = \beta_{1t} + \beta_{1t} t_g$$

The horizontal missile velocity magnitude is calculated:

$$v_m = [r_m^2 + (r_m \beta_{1m})^2]^{1/2}$$

and the velocity is rotated into this velocity frame:

$$\overline{V}_{na} = v_m \cos(\beta_{1m}-\beta'_{1t}) \; \dot{r} + v_m \sin(\beta_{1m}-\beta'_{1t}) \; \dot{t} \qquad (3-17)$$

where: β'_{1t} = Future LOS to target (from North)

v_m = Horizontal missile velocity magnitude

V_{na} = Nominal velocity without position correction

$\dot{r}$ = unit vector along missile velocity path

$\dot{t}$ = unit vector tangent to missile velocity path

There are several ways to calculate the position error. They depend on where the missile is projected on the future LOS. The selected scenario based on performance, is shown in Figure 3-6. The correction distance, R_c, is calculated as follows:

$$R_c = V_{ac} \, t_g - d$$

where: $d = R_m \cos(\Theta_{la} - \beta_{lm}) - a$

and: $\tan(\Theta_{la} - \beta'_{lt}) = R_m \sin(\Theta_{la} - \beta_{lm}) / a$

Combining these terms yields:

$$R_c = v_{ac} t_g - R_m [\cos(\Theta_{la} - \beta_{lm}) - \sin(\Theta_{la} - \beta_{lm}) / \tan(\Theta_{la} - \beta'_{lt})]$$

As shown in the figure the direction of R_c is chosen parallel to the aircraft heading. Expressing R_c as a vector in the β_{lm} frame and dividing by the time allowed for the position correction yields:

$$\overline{V}_{nb} = R_c / t_c \, [\cos(\Theta_{la} - \beta_{lm}) \, \dot{r} + \sin(\Theta_{la} - \beta_{lm}) \dot{t}] \qquad (3\text{-}18)$$

where: V_{nb} = position correction portion of nominal velocity

The total nominal velocity is now:

$$\overline{V}_n = \overline{V}_{na} + \overline{V}_{nb}$$

$$\overline{V}_n = |\overline{V}_m| \, \cos(\beta_{lm} - \beta'_{lt}) + R_c / t_c \, \cos(\Theta_{la} - \beta_{lm}) \, \dot{r}$$
$$+ |V_m| \, \sin(\beta_{lm} - \beta'_{lt}) + R_c / t_c \, \sin(\Theta_{la} - \beta_{lm}) \, \dot{t} \qquad (3\text{-}19)$$

The velocity to be gained is $\overline{V}_g = \overline{V}_n - \overline{V}_m$ and the commanded missile heading rate is proportional to the dot product of $\overline{V}_m$ with $\overline{V}_g$ as follows:

$$\dot{\Theta}_{lcmd} = K3 \, (\overline{V}_g \star \overline{V}_m) \qquad (3\text{-}20)$$

To make this algorithm perform better it is necessary to weight the position correction term more heavily during the final stage of the engagement than at the beginning. This is not attempted in this research because this algorithm is inferior to the LOS and Proportional guidance algorithms.
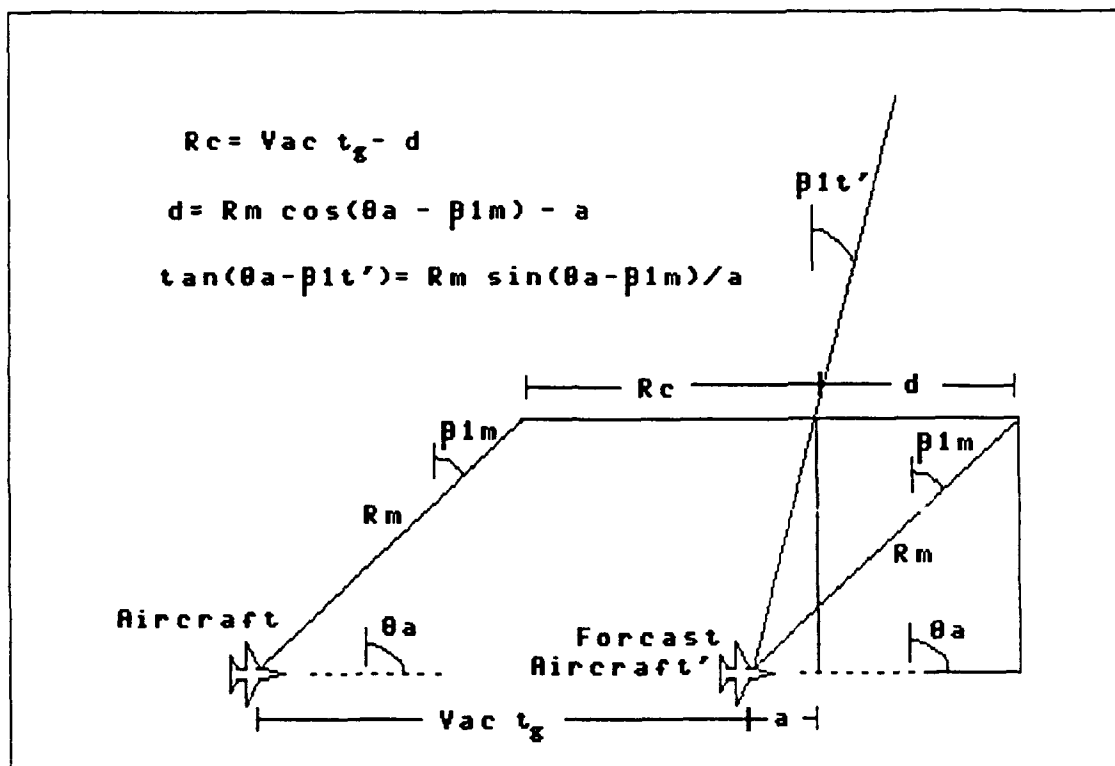
Figure 3-6 LOS+ Position Correction Geometry

Notice that these equations handle the azimuth guidance in the horizontal plane. An identical set of equations must be implemented in the vertical plane to calculate the missile pitch rate command, Θ_{2cmd}.

Care is taken to implement this algorithm using only the variable states available from the measurement model described in Paragraph 2.6. Thus the LOS+ guidance algorithm is tested with identical scenarios available to the other guidance algorithms.

3.4 Pursuit Guidance Algorithm Development

The pursuit guidance algorithm is an old and simple guidance solution whereby the missile is continually flown at the known target position. This is a relatively easy implementation to use and the geometry is shown in Figure 3-7. The algorithm requires the calculation of the missile to target line-of-sight and the missile heading, or at least its velocity vector. These two calculations are accomplished as follows:

Figure 3-7 Pursuit Algorithm Geometry

From Figure 3-7 it is seen that:

$$\alpha_1 = \tan^{-1}\left[\frac{r_t \sin(\delta)}{r_t \cos(\delta) - r_m}\right] \tag{3-21}$$

$$\alpha_2 = \tan^{-1}(r_m \dot{\beta}_{1m}/ \dot{r}_m) \tag{3-22}$$

where: $\delta = \beta_{1m} - \beta_{1t}$

Then the commanded azimuth turn is made proportional to $\alpha_1 + \alpha_2$ as follows:

$$\dot{\Theta}_{1cmd} = -K_3 (\alpha_1 + \alpha_2) \tag{3-23}$$

Notice that these equations handle the azimuth guidance in the horizontal plane. An identical set of equations are implemented in the vertical plane to calculate the missile pitch rate command, $\dot{\Theta}_{2cmd}$. The Pursuit guidance algorithm is a straight-forward implementation. Again notice that care is taken to implement this algorithm using only variables available from the measurement model described in paragraph 2.6. Thus the pursuit guidance algorithm is tested with the same scenarios and data calculations as the other algorithms under test.

3.5 Proportional Guidance Algorithm Development

The proportional guidance algorithm uses the line-of-sight rate as a guidance parameter instead of the line-of-sight angle used in the pursuit guidance [8:198]. The geometry of the problem is identical to the pursuit geometry layout shown in Figure 3-7 above. Here the guidance algorithm commands a missile heading rate-of-change which is proportional to the rate-of-change of the line-of-sight from the missile to the target. The proportional constant, K3, is called the navigation constant [8:199]. A computational challenge is the need to calculate the missile-to-target line-of-sight rate $\dot{\beta}_{lmt}$. In the normal implementation of this guidance algorithm $\dot{\beta}_{lmt}$ rate is simply measured from the missile's target tracker. In this application this value is constructed from the measured missile velocity and target velocity. Thus the proportional guidance algorithm is implemented as follows:

$$\dot{\Theta}_{lcmd} = K_3 \ \dot{\beta}_{lmt} \tag{3-24}$$

where: $\dot{\Theta}_{lcmd}$ = the missile azimuth turn command

K_3 = the navigation constant

$\dot{\beta}_{lmt}$ = the missile to target line-of-sight rate

$\dot{\beta}_{lmt}$ rate remains to be calculated. The calculation of the target velocity relative to the missile is accomplished using the V_m and V_t as expressed in equation (3-12) and (3-13). It follows then, that the target velocity relative to the missile is:

$$V_{tr} = V_m - V_t = V_1 \ l_1 + V_2 \ l_2 \tag{3-25}$$

Where: $V_1 = r_m - r_t \cos(\beta_{lt} - \beta_{lm}) - r_t \dot{\beta}_{lt} \sin(\beta_{lt} - \beta_{lm})$

$V_2 = r_m \dot{\beta}_{lm} - r_t \sin(\beta_{lt} - \beta_{lm}) - r_t \dot{\beta}_{lt} \cos(\beta_{lt} - \beta_{lm})$

The component of this relative velocity that causes a rotation of the missile-to-target line-of-sight is tangent to the missile-to-target line-of-sight, β_{lmt}. This tangent velocity term can be expressed two ways, as follows:

3-19

$$r_{mt} \, \dot{\beta}_{1mt} = V_2 \cos(\beta_{1m} - \beta_{1mt}) + V_1 \sin(\beta_{1m} - \beta_{1mt}) \qquad (3-26)$$

Solving these two for $\dot{\beta}_{1mt}$ yields:

$$\dot{\beta}_{1mt} = \frac{V_2 \cos(\beta_{1m} - \beta_{1mt}) + V_1 \sin(\beta_{1m} - \beta_{1mt})}{r_{mt}} \qquad (3-27)$$

The β_{1mt} angle used in this equation is calculated from the NED X and Y coordinates as follows:

$$\beta_{1mt} = \tan^{-1}\left[\frac{x_t - x_m}{y_t - y_m} \right]$$

$$\beta_{1mt} = \tan^{-1}\left[\frac{r_t \sin(\beta_{1t}) - r_m \sin(\beta_{1m})}{r_t \cos(\beta_{1t}) - r_m \cos(\beta_{1m})} \right] \qquad (3-28)$$

Once β_{1mt} is calculated the range from the missile to the target, r_{mt}, used in equation (3-20) is calculated via the law of sines as follows:

$$r_{mt} = \frac{r_t \sin(\beta_{1t}) - r_m \sin(\beta_{1m})}{\sin(\beta_{1mt})} \qquad (3-29)$$

where: β_{1mt} = azimuth line-of-sight missile to target

$\dot{\beta}_{1mt}$ = azimuth line-of-sight rate, missile to target

r_t = horizontal range, aircraft to target

$\dot{r}_t$ = horizontal range rate, aircraft to target

β_{1t} = azimuth line-of-sight, aircraft to target

$\dot{\beta}_{1t}$ = azimuth line-of-sight rate, aircraft to target

r_m = horizontal range, aircraft to missile

$\dot{r}_m$ = horizontal range rate, aircraft to missile

β_{1m} = azimuth line-of-sight, aircraft to missile

$\dot{\beta}_{1m}$ = azimuth line-of-sight rate, aircraft to missile

Notice that these equations handle the azimuth guidance in the horizontal plane. An identical set of these equations are implemented in the vertical plane to calculate the missile pitch rate command, Θ_{2cmd}.

Again care is taken to implement this algorithm using only the variable states available from the measurement model described in paragraph 2.6.

Thus the proportional guidance algorithm is tested with the same scenarios and data calculations as the other algorithms under test.

3.6 Range and Range Rate Estimator

In the event that the aircraft will launch without electromagnetic emittions it is necessary to test each algorithm's performance with a range estimator rather than range and range rate from a radar. To accomplish this test, a very simple range and velocity estimator is built to use in place of the radar measurements. To do this average thrust and drag, calculated in equation (3-15) and (3-16), is used. An Euler integration is used to calculate the velocity and another to calculate the range. This rough estimator assumes the missile is always accelerating directly away from the launch aircraft, an assumption that is accurate
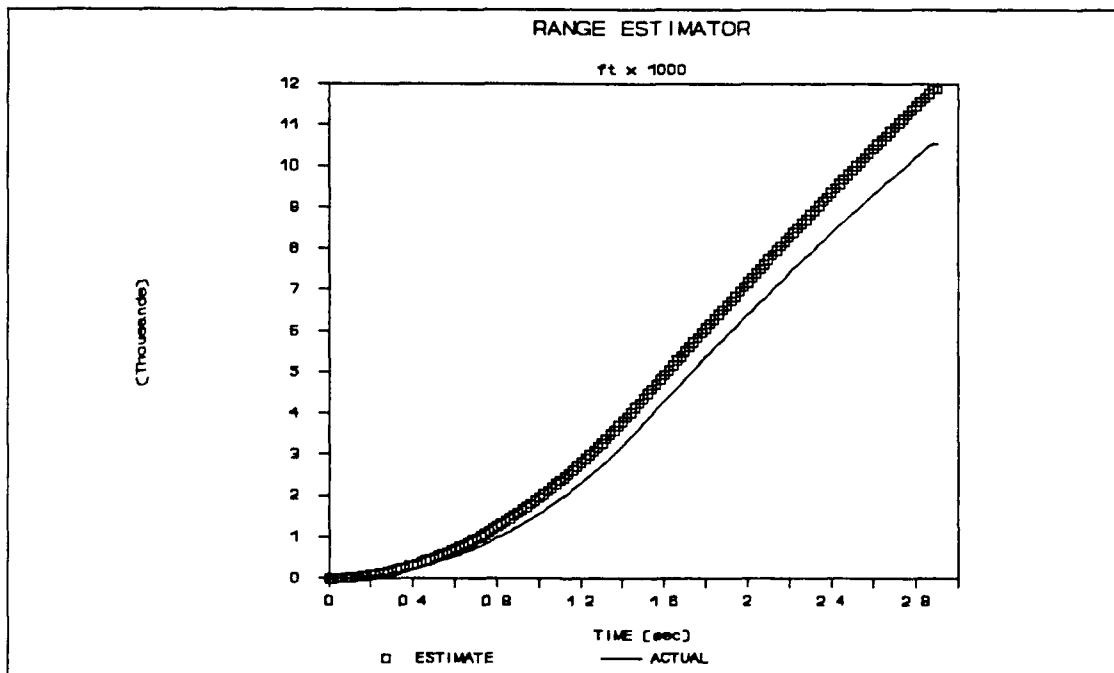

Figure 3-8 Range Estimator Performance Comparison

except for high off-angle shots. A graph of this range estimation is shown in Figure 3-8. The actual range shown in this graph is taken from a

3-21

LOS guidance shot with a 30 degree off angle initial heading. The range

rate estimation is made by taking the estimated missile velocity and

backing out the components causing the azimuth rate and pitch rate. This

is done because a missile azimuth and pitch rate can be obtained from the

FLIR. Thus the range rate is calculated as follows:

$$R_m = [V_{est}^2 - [\beta_{1m} R_{est} \cos(\beta_{2m})]^2 - (\beta_{2m} R_{est})^2]^{1/2} \qquad (3-30)$$
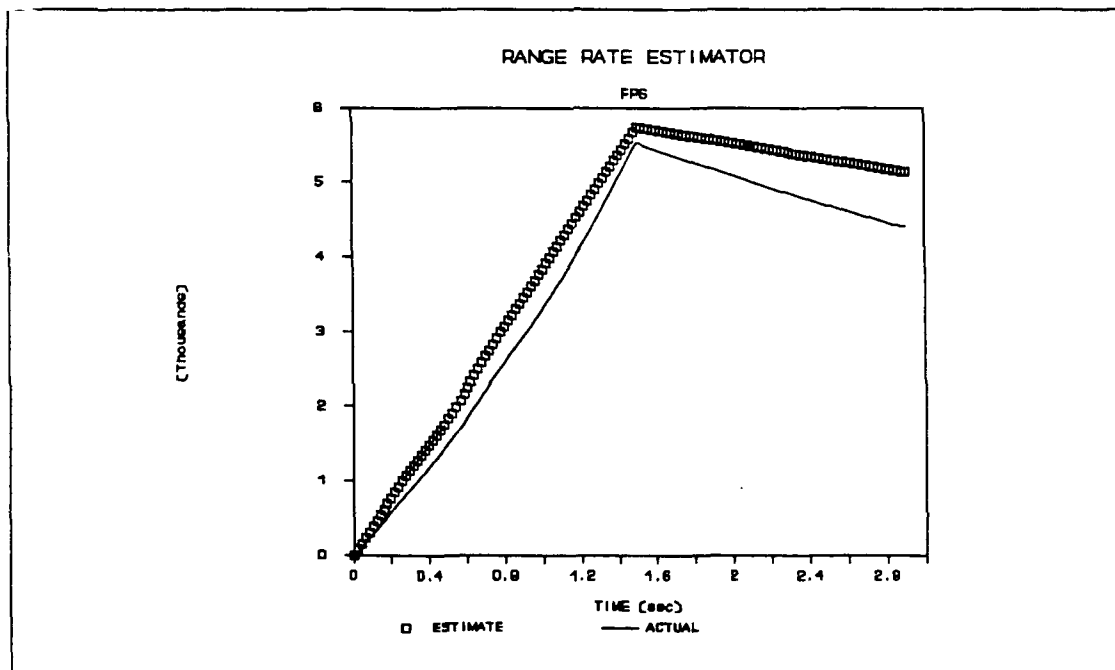
Figure 3-9 Range Rate Estimator Performance Comparison

This range-rate estimate as well as the actual range-rate from the LOS

guidance shot is shown in Figure 3-9. Although more accurate on-board

estimates of missile range and range rate could easily be developed, this

one is used to demonstrate some of the algorithms dependence on range and

range rate. The objective here is not to build an accurate estimator,

just a consistent one that can be used in each test.

IV. Algorithm Analysis

4.1 Introduction

The performance of each algorithm developed in chapter 3 is tested and the results are explained in this section. In performing analysis there are always more scenarios desired than one can possibly evaluate. For the initial analysis a 30 degree off-angle shot is chosen because it strains the algorithms initial correction capabilities. This is used to test and establish the gain and/or control parameters for each algorithm. For this shot the target is at 030 degrees LOS with a heading of due east, (i.e. 090 degrees). The aircraft and missile initial heading is 060 degrees. Then a simpler 5 degree off-angle scenario is used to test reactions to an aircraft 5-G turn during the missile flight. Here the target is at 055 degrees LOS with a heading of due west, (i.e. 270 degrees). The aircraft and missile initial heading is 060 degrees. Finally the aircraft's radar is turned off and a simple missile range and velocity estimator is used to 'sense' the missile range and range rate. This process shows the error in the algorithms when accurate range and range rate are not available to the algorithm. The "radar off" test repeated the 30 degree off-angle scenario. The only algorithm that has performance reasonably independent of these range parameters is the LOS algorithm. This chapter is organized to analyze the data for each of these algorithm tests.

4.2 Figures of Merit

The missile miss distance and the amount of expended control force is used as the primary figures of merit (FOM) for this analysis. Each algorithm can be adjusted from an under-damped to an over-damped condition with the control parameters. In general this changed the miss distance from small to large and the control energy from large to small. So by

observing the primary FOMs a cont ol parameter can be chosen to obtain the best algorithm performance. Thus, minimizing these two FOMs forms the basis for most of this analysis.

The missile miss distance is measured during the missile flight by recording the missiles closest approach to the target. There is no consideration given for a missile impacting the ground before it reaches this closest approach. One should exercise caution in using this FOM to obtain a probability of kill. The miss distance FOM is a tool to evaluate the guidance algorithm accuracy.

The amount of control force required to steer the missile is the FOM used to measure the guidance algorithms efficiency. This control force is measured by integrating the commanded turn rates throughout the missile flight. This is accomplished with the following equation:

$$E_n = E_n + |V_m| \; (\Theta_{1cmd}^2 + \Theta_{2cmd}^2)^{1/2} \; M \; dt$$

Where: E_n = total control moment commanded (lbs sec)

$\quad V_m$ = total missile velocity (ft/sec)

$\quad \Theta_{1cmd}$ = commanded missile heading rate (rad/sec)

$\quad \Theta_{2cmd}$ = commanded missile pitch rate (rad/sec)

$\quad M$ = missile mass (slugs)

$\quad dt$ = integration time of one execution cycle (sec)

Although this symbology hints that this is a measure of the control energy, it is not. Monitored here is the time integral of turning force commanded, integrated over the time of the flight. To calculate the control energy requires more information on how efficiently the missile transforms the commands to turning motion, which requires much more detail than is available about the missile. The measure of the total force and time product that it is commanded gives a force time unit (FTU) measure that is useful in comparing the algorithms even if it is not physically realizable. The control FTU is a useful FOM for determining the guidance algorithms efficiency.

4.3 LOS Control Parameter Testing

The various runs used to establish the LOS algorithm control parameters K_3 and t_c, are shown in Figure 4-1 through 4-5. The only parameters changed for these runs are the control parameters. Included in these figures is a scenario ground map that pictures the aircraft track, the target track, and the missile flight path. In the upper left corner of this map is the type of algorithm used, some figures of merit and the control parameters. Inset into each of the scenario maps is a graph of the heading rate commands and a graph of the missile heading and pitch.

The graph of the missile heading shows the effect of the LOS control variables t_c and K_3. In Figure 4-1 notice the slight heading overshoot around the 0.8 second TOF and the quick settling on to a steady heading rate that effectively brings the missile into the target. Notice also the change of heading from about 32 degrees to about 28 degrees during the last two seconds of flight. This is caused by the rotating aircraft to target line of sight as explained in chapter three.

A change in the heading command is evident at the 1.5 sec TOF, the time that the missile rocket engine burns out. This is caused by the step change in the missile acceleration that occurs at this point. Recall that the missile accelerations were not accounted for in the algorithm development, but it does effect the missile LOS and LOS rate. This causes the control system to have an increase in accuracy when the unaccounted for acceleration just decreased drastically. This step through the control system settles quickly and is barely discernable in the heading plot.

Figure 4-2 through 4-5 show various stages of control damping from under-damped to over-damped. Recall from chapter three, that a control zero is at $-1/t_c$ and the gain varies with K_3, and that a pole, located at $-V_m/R_m$, moves during the missile flight. A typical pole location for several TOF values is shown in Table 3-1. This "movement" of the control

4-3
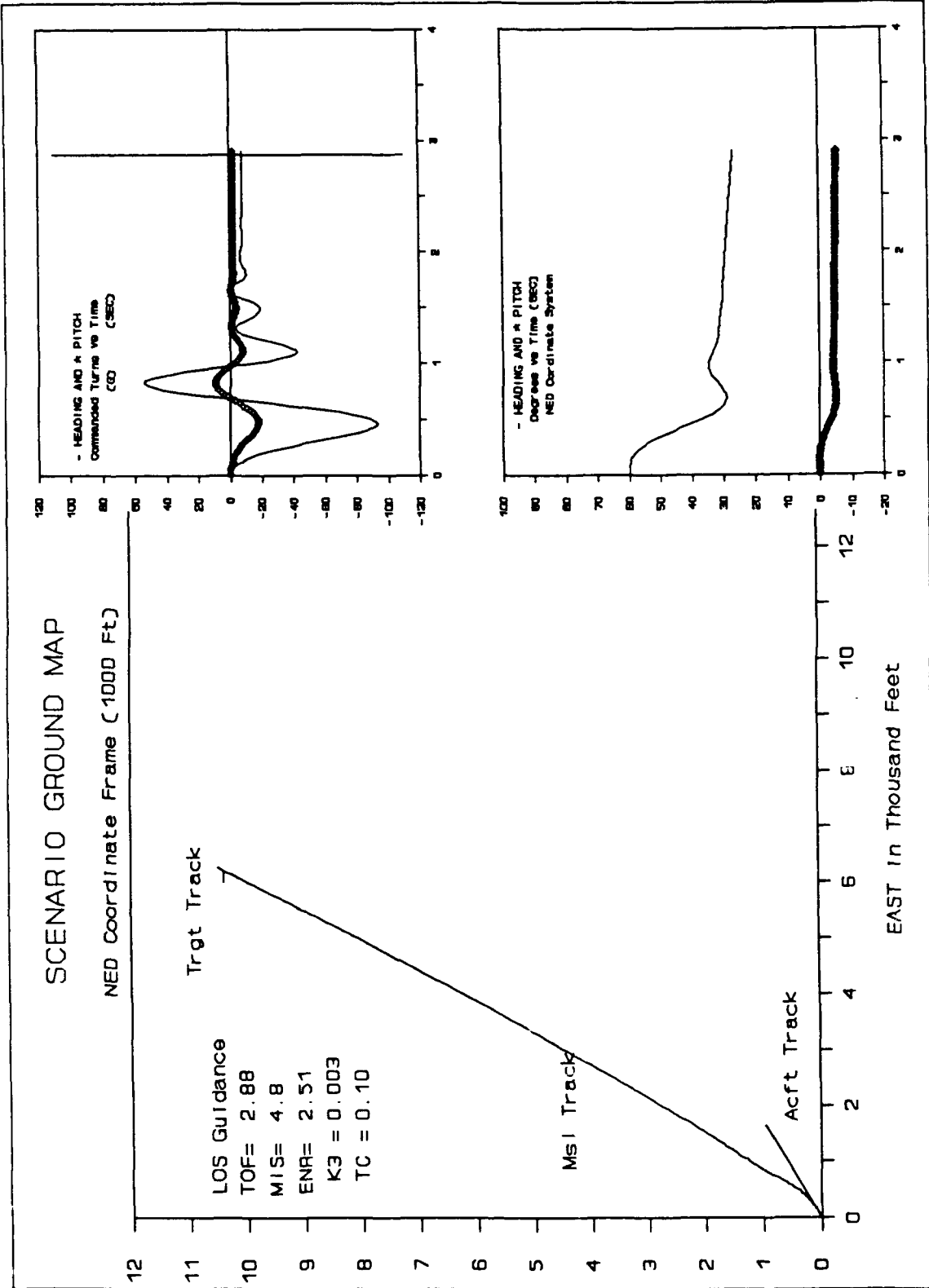
Figure 4-1 LOS Control Parameter Test #1
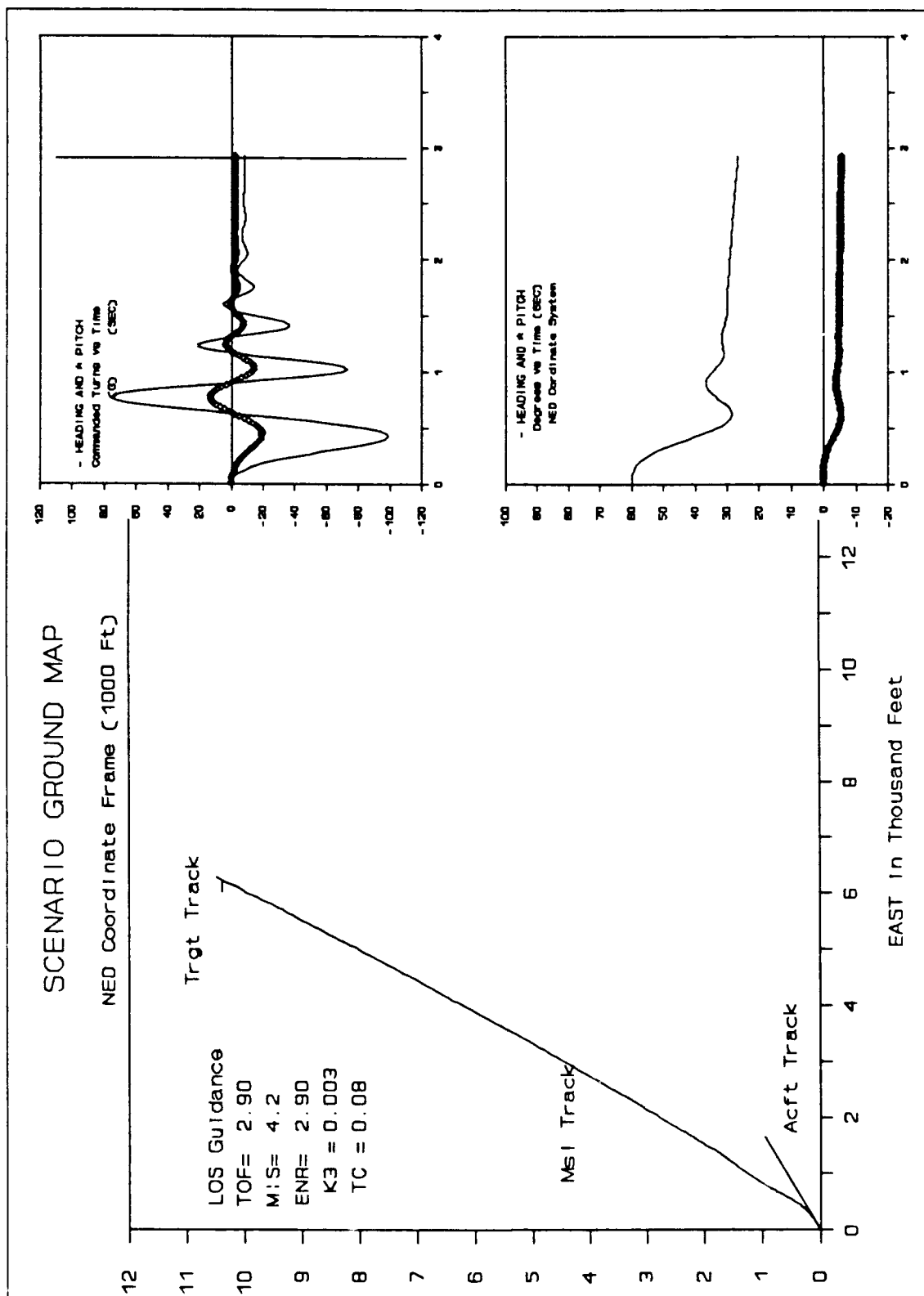
Figure 4-2 LOS Control Parameter Test #2

SCENARIO GROUND MAP

NED Coordinate Frame (1000 Ft)

Trgt Track

LOS Guidance
TOF= 2.91
MIS= 5.2
ENR= 2.92
K3 = 0.002
TC = 0.10

Msl Track

Acft Track

EAST In Thousand Feet

- HEADING AND ∧ PITCH
Commanded Turns vs Time
(Deg) (SEC)

- HEADING AND ∧ PITCH
Degrees vs Time (SEC)
NED Coordinate System
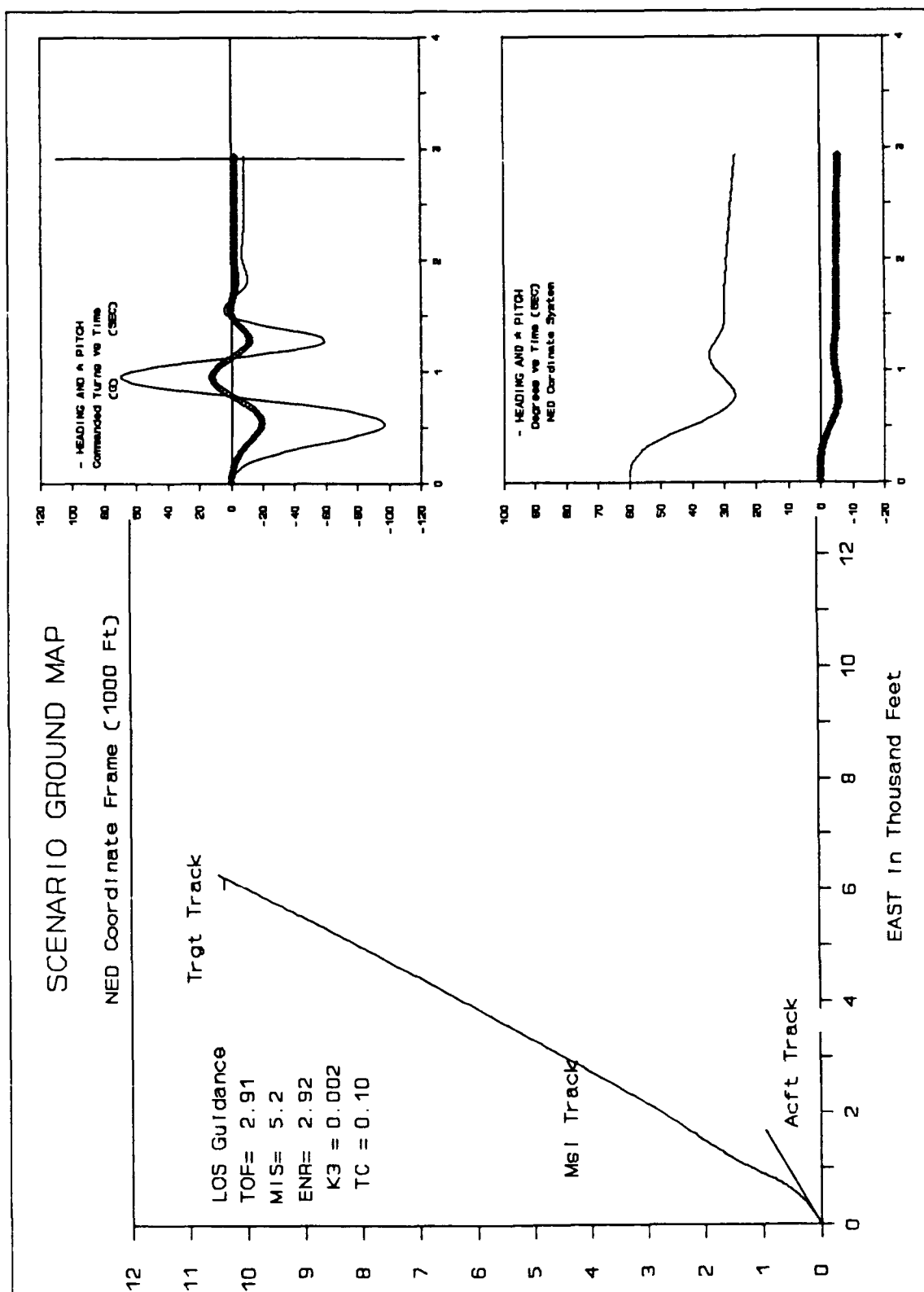
Figure 4-3 LOS Control Parameter Test #3

4-6

SCENARIO GROUND MAP

NED Coordinate Frame (1000 Ft)

Trgt Track

LOS Guidance
TOF= 2.87
MIS= 1.6
ENR= 2.27
K3 = 0.004
TC = 0.10

Msl Track

Acft Track

EAST In Thousand Feet

- HEADING AND * PITCH
Commanded Turns vs Time
(CQ CSEC)

- HEADING AND * PITCH
Degrees vs Time (SEC)
NED Coordinate System

Figure 4-4 LOS Control Parameter Test #4

4-7

SCENARIO GROUND MAP

NED Coordinate Frame (1000 Ft)

Trgt Track

LOS Guidance
TOF= 2.84
MIS= 3.5
ENR= 1.84
K3 = 0.004
TC = 0.20

Msl Track

Acft Track

- HEADING AND * PITCH
Commanded Turns vs Time
(C) (SEC)

- HEADING AND * PITCH
Degrees vs Time (SEC)
NED Coordinate System

EAST In Thousand Feet
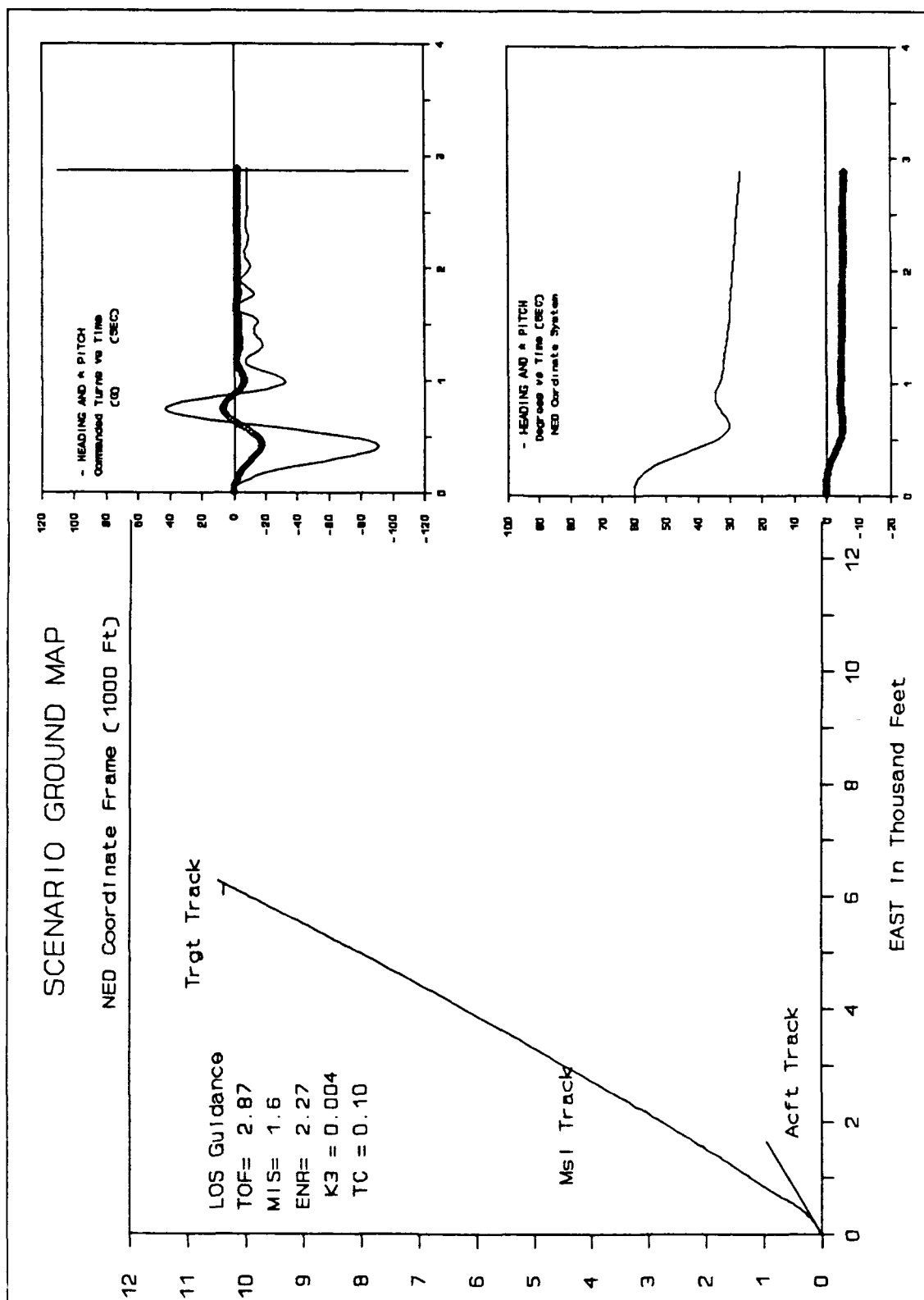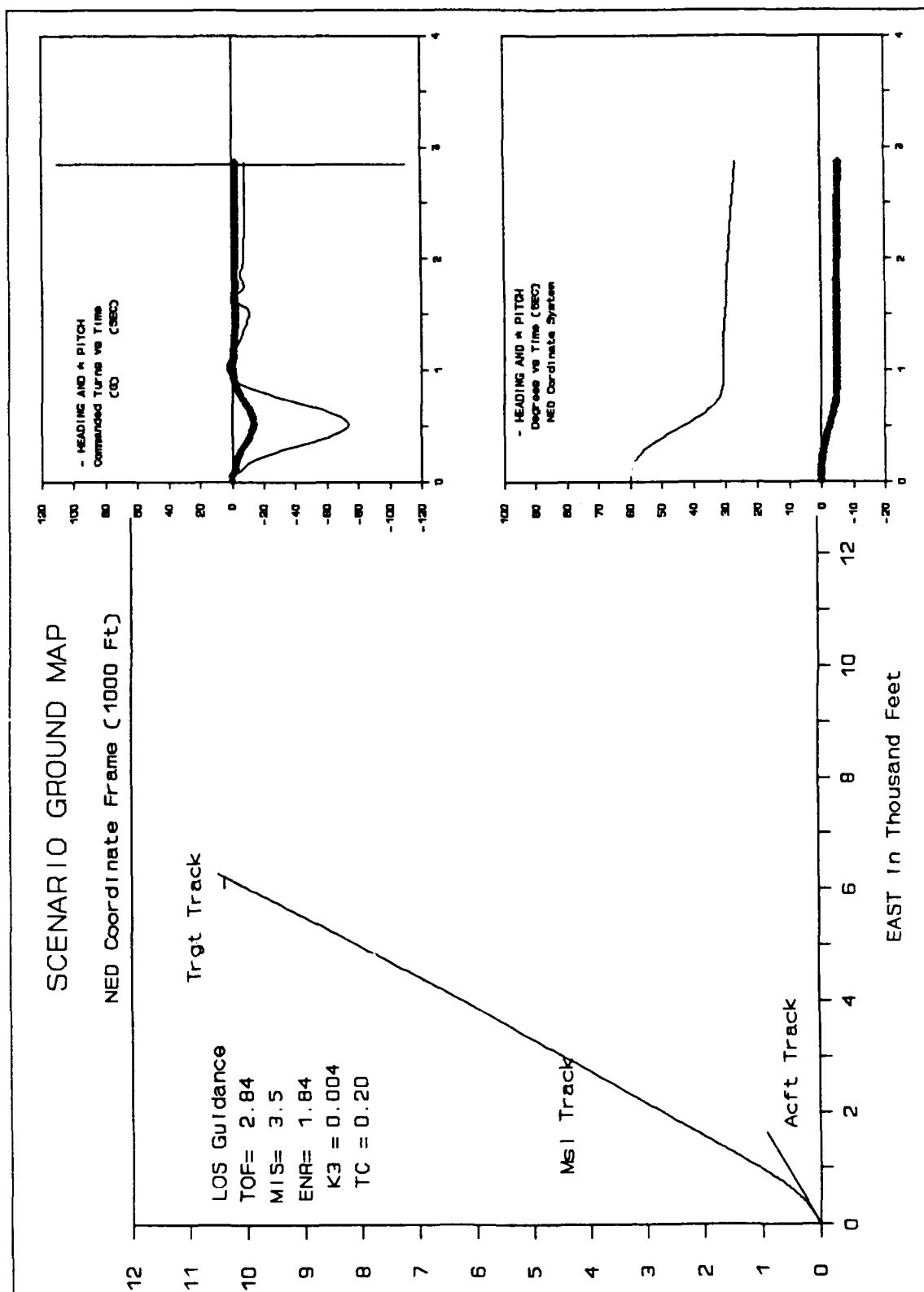
Figure 4-5 LOS Control Parameter Test #5

4-8

pole location causes the control characteristics to change during the missile flight. It is very difficult to see this change in control characteristic in the figures, but the objective is an average control response that acts critically damped throughout the flight.

Figure 4-6 shows all the FOM results for the LOS algorithm runs. The first five graphs show the tests run for control parameter selection. By analyzing the results it is apparent that the best shot is obtained with $t_c = 0.1$ and $K_3 = 0.004$. However, the best overall performer is $t_c = 0.1$ and $K_3 = 0.003$. Notice from the control graphs that these control parameters give smoother damped sinusoidal control curves. In running with $K_3 = 0.004$ the control is more erratic and did not perform well in all the other scenarios. (Additional scenario runs are presented in Appendix A.) The runs with $K_3 = 0.003$ show the good FOM values as well as the best damped control responses. The remainder of the LOS guidance tests are run using $t_c = 0.1$ and $K_3 = 0.003$.

4.4 LOS 5 Degree Off-Angle Tests

The less dynamic 5 degree off-angle shot is run to test the algorithm with less stringent initial control requirements, and to test the effect of a 5-G aircraft turn on the guidance situation. The bar graph labeled Sen #1 and Sen #2 in Figure 4-6 represent these two tests. Figure 4-7 and 4-8 give the ground map and control graphs of these two runs. In the non-maneuvering shot of Figure 4-7 a slight overshoot and very quick settling onto an almost constant heading to the target are evident.

Figure 4-8 illustrates the heading changes more dramatically as the turning aircraft causes a change in the LOS from the aircraft to the target. The missile commands are a lot less stable in this shot, in fact the step from the engine burnout at the 1.5 sec TOF point is more noticeably pronounced. The algorithm is strained here to account for a change in the aircraft to target LOS rate that is not accounted for in its development. Thus the position correction portion of the algorithm is
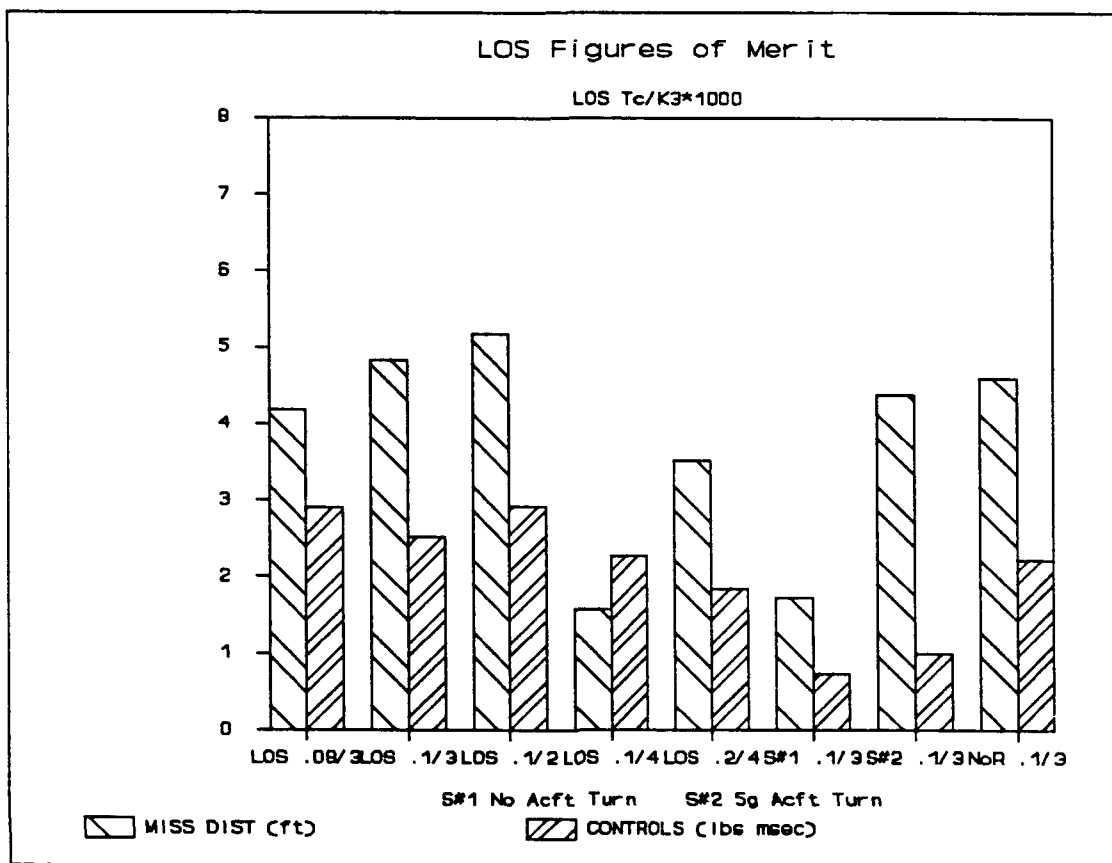
LOS Figures of Merit

Figure 4-6 FOM for All LOS Guidance Runs

exercised to make corrections that are not considered in the algorithm development, where accelerations are not figured into the LOS rate calculations. Notice that the accuracy decreases in this shot for the same reason.

Aircraft acceleration could be accounted for in the algorithm since it is measured on board. Acceleration is not incorporated into the LOS algorithm because it is not predictable and because its effect can be corrected via the position correction portion of this algorithm. The requirement to further tune the algorithm to account for aircraft acceleration may depend on the algorithm's sensitivity to sensor errors which have not yet been explored.
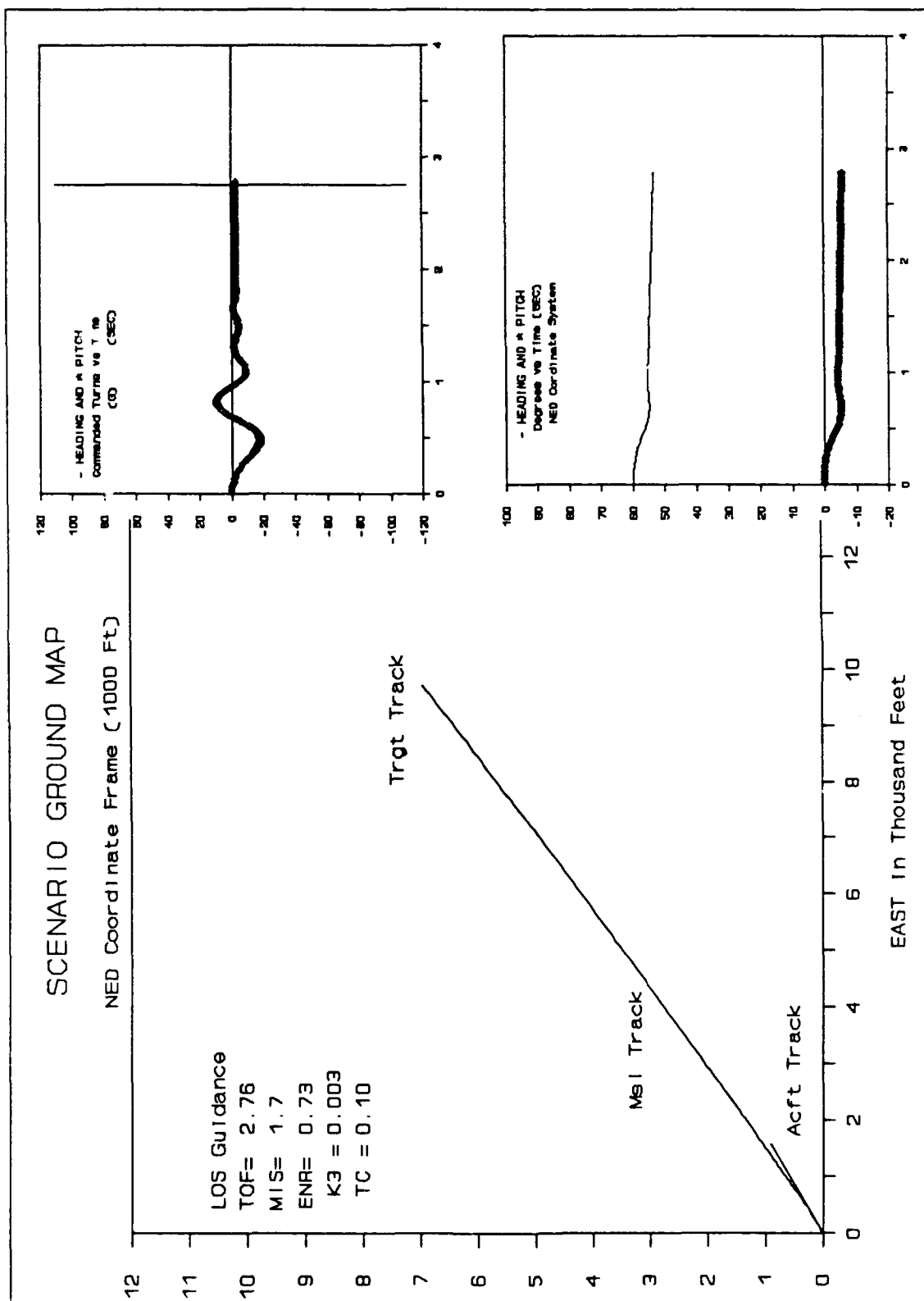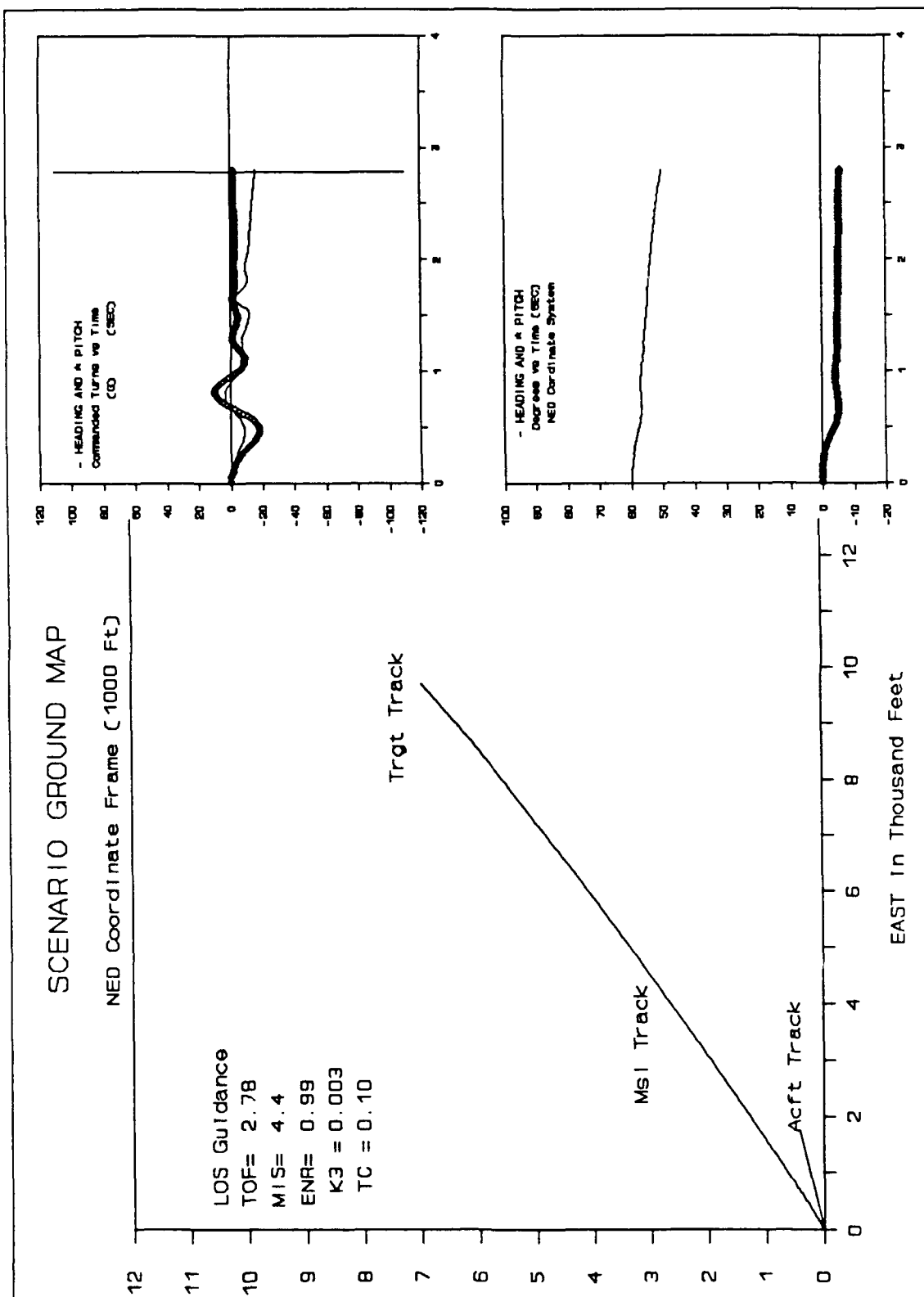
Figure 4-7 LOS 5 Degree Off Angle Test

Figure 4-8 LOS 5 Degree Off Angle Test, 5-G Turn

The performance of the LOS algorithm with critical damping and no sensor error appears to be superb in this benign engagement. However with the introduction of an aircraft acceleration the miss distance doubles. This emphasizes that a hyper-velocity missile strains the very best of the guidance algorithms.

4.5 Radar Off LOS Tests

When the sensor model uses a very simple 3DOF missile model to estimate the range and range rate measurements, the algorithm's dependence on accurate range data is examined. Figure 4-9 shows the no-radar scenario and it should be compared to Figure 4-1 which shows the same shot with accurate range and range-rate data.

Although there is an increase in the miss distance the algorithms performance is relatively unaffected by poor range and range rate data. Poor range data causes the LOS position calculations to have a proportional error but the rest of the algorithm is independent of the radar range. Recall from chapter 3 that the missile range from the aircraft does not affect algorithm performance, the algorithms only purpose is to keep it on the LOS between the aircraft and the target. Since obtaining an accurate radar measurement on this very fast and small missile is a concern, it is a comfort that the LOS algorithm is not dependent on an accurate radar. In fact it can operate effectively without a radar.

4.6 LOS+ Control Parameter Testing

The various runs used to establish the LOS+ algorithm control parameters K_1 and t_c, are shown in Figure 4-10 through 4-13. The only parameters changed for these runs are the control parameters. As before a scenario ground map is included that pictures the aircraft track, the target track and the missile flight path. In the upper left corner of this map is the type of algorithm used, some figures of merit, and the
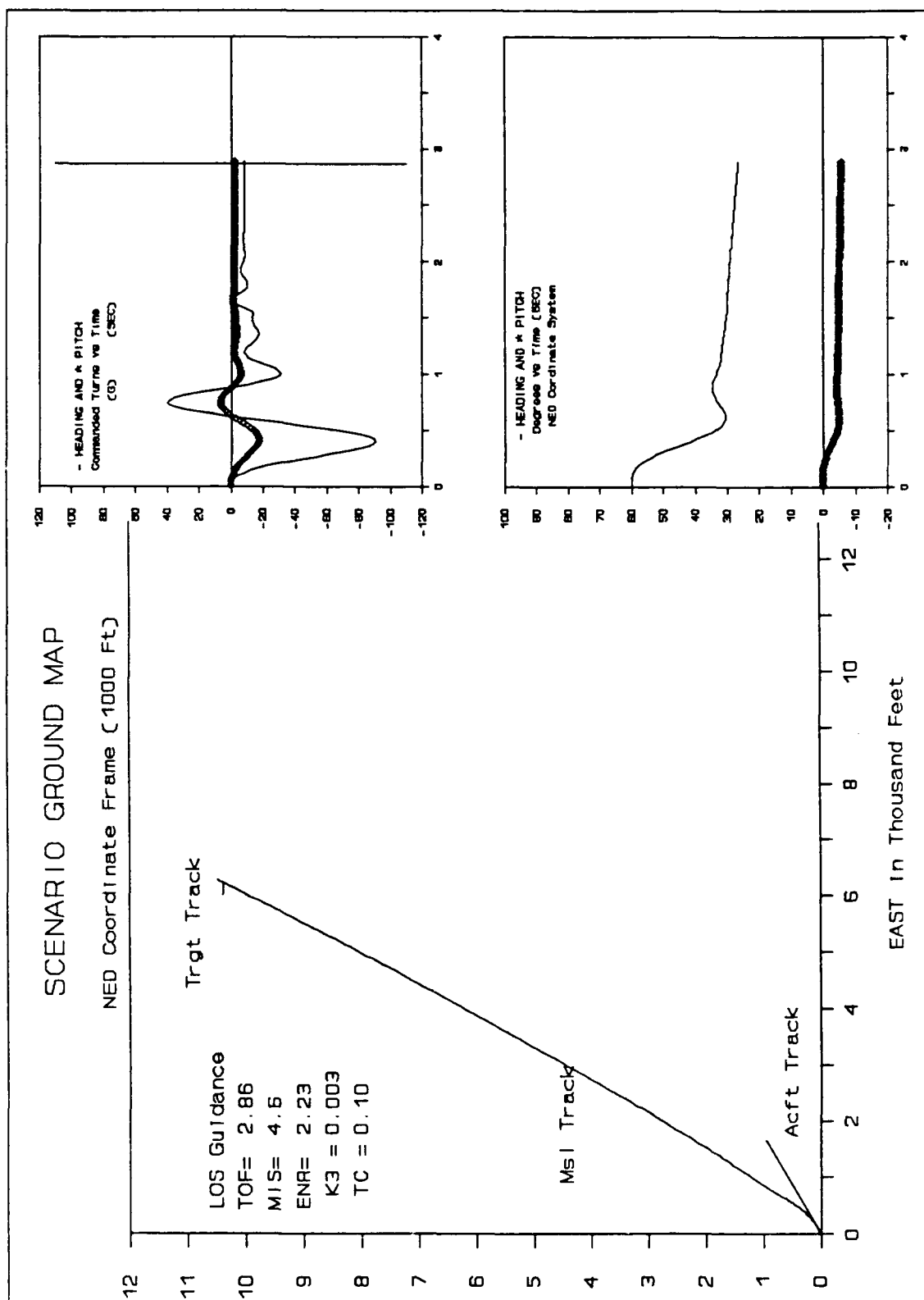
Figure 4-9 LOS No Radar Range Test

control parameters. Inset into each of the scenario maps is a graph of the heading rate commands and graph of the missile heading and pitch.

The conglomerations of flight paths and control graphs found in these four figures only begin to illustrate the difficulty in tuning and developing this algorithm. Figure 4-10 illustrates that the best accuracy did not coincide with a very efficient flight path. In progressing toward a better flight path, poor control of the position error gives unacceptable accuracy. Since the algorithm is proposed partly to reduce wasted control energy, effort is given to find the control values that minimize the control force FOM. This is shown in Figure 4-13 but notice that the control force FOM doubles those used in the LOS algorithm.

The effort involved trying to guide this missile to a future line of sight and balance its efficiency and accuracy. The sensitivities caused dynamic fine tuning of the control parameters to be required for this approach. If it is still deemed necessary to keep the missile off the target line of sight, a variable gain will be required.

Examining Figure 4-13, the shot that flew most efficiently (but missed by the most) one can see the sharp turn onto the predicted LOS. The commanded control then causes an overshoot and quick settling onto the correct heading at about the 2 second TOF point. At about 1/2 seconds before impact one see the commanded heading rate increase. This is where the time-to-go prediction is discontinued and the algorithm strives to keep the missile on the current target LOS. Recall that the time to go calculation is abandoned when $t_g < 0.5$ sec. This is to keep the t_g calculation errors from effecting accuracy. (In hindsight the author feels that it will not effect it greatly.) To improve accuracy the control parameters need to be altered during the final engagement. The best method of doing this might involve an optimal control design.
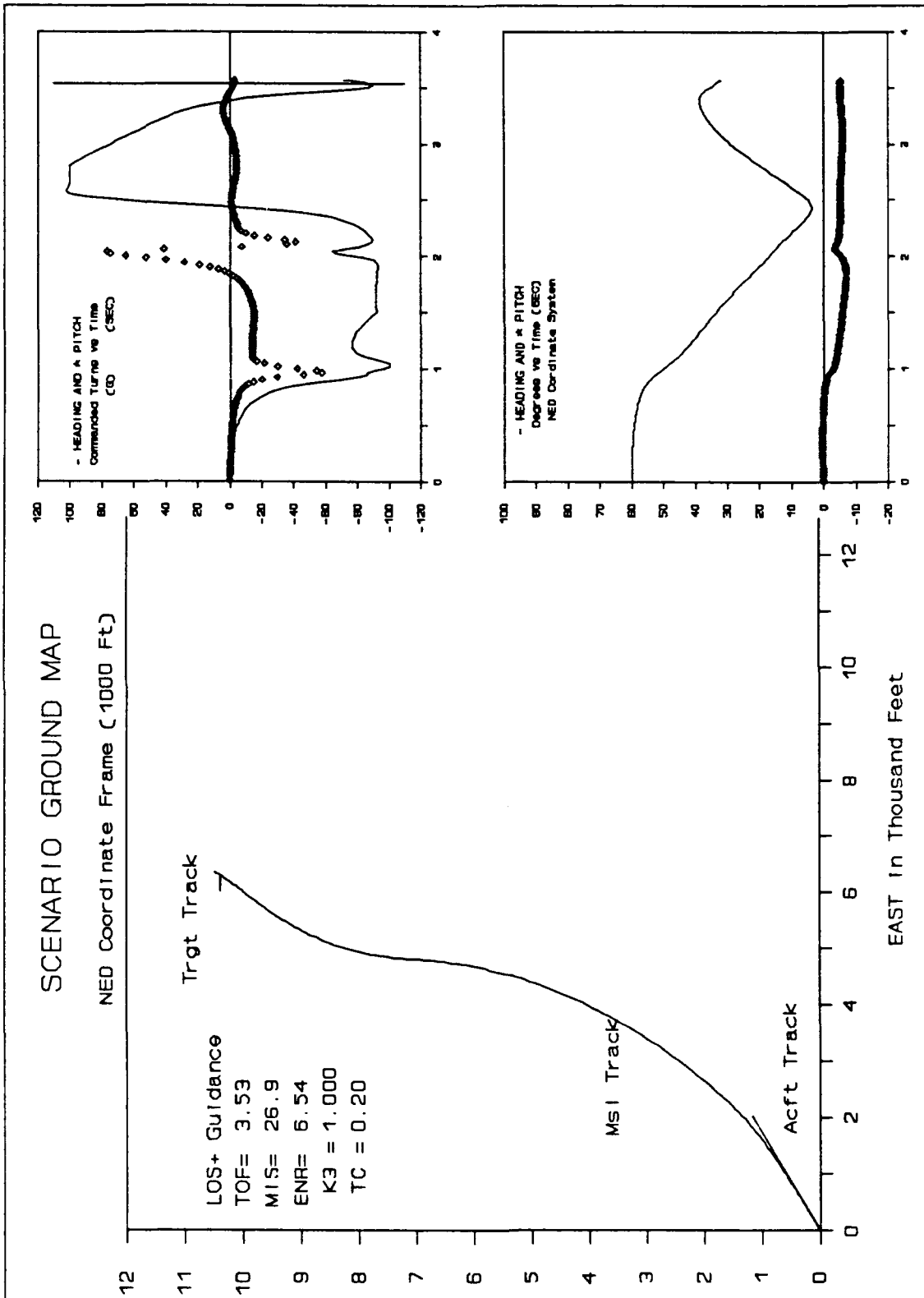
Figure 4-10 LOS+ Control Parameter Test #1

Figure 4-11 LOS+ Control Parameter Test #2

SCENARIO GROUND MAP

NED Coordinate Frame (1000 Ft)

Trgt Track

LOS+ Guidance
TOF= 3.16
MIS= 106.7
ENR= 5.78
K3 = 4.000
TC = 0.40

Acft Track

Msl Track

EAST In Thousand Feet

- HEADING AND ⋆ PITCH
Commanded Turns vs Time
(CG) (CSEC)
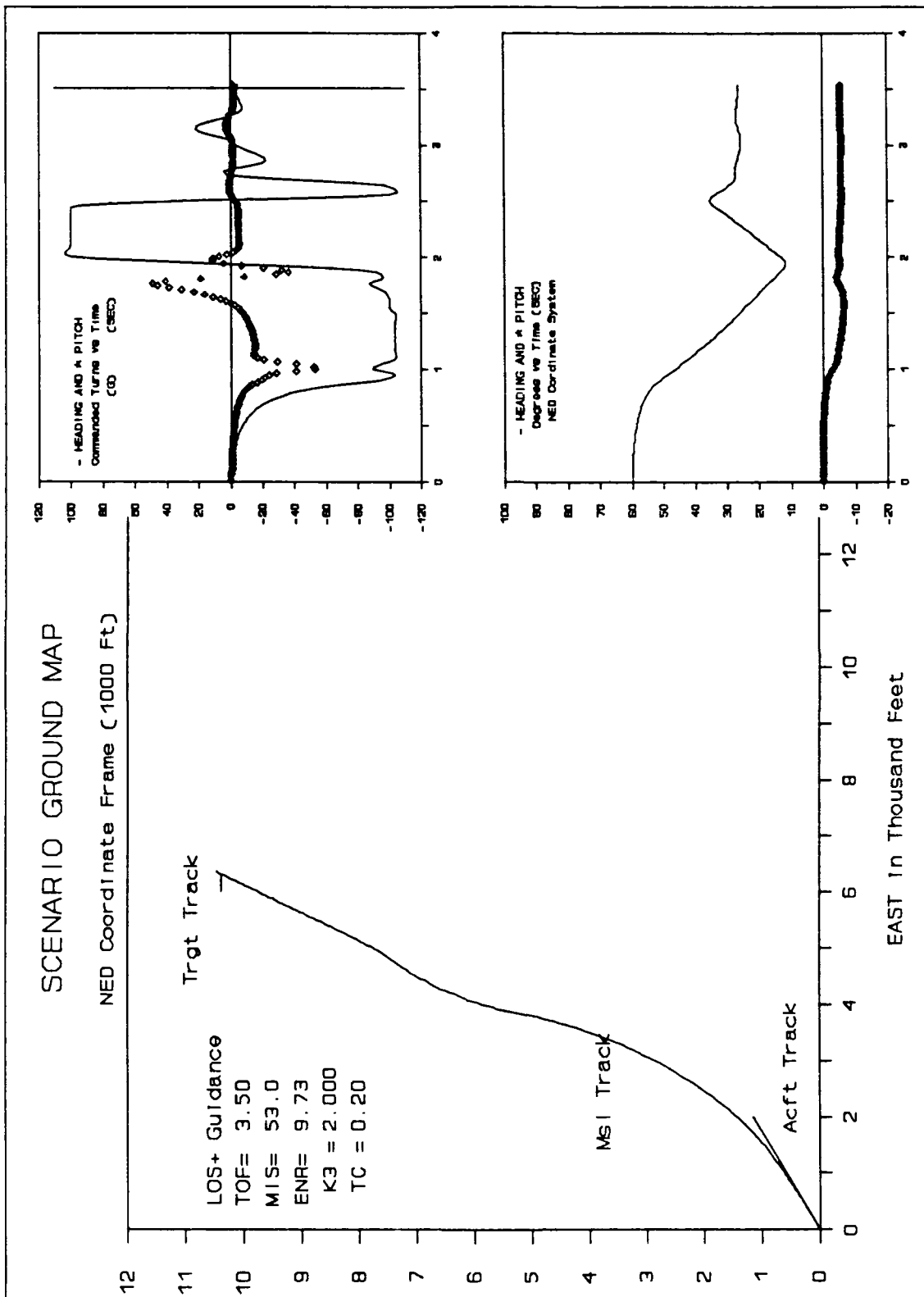
- HEADING AND ⋆ PITCH
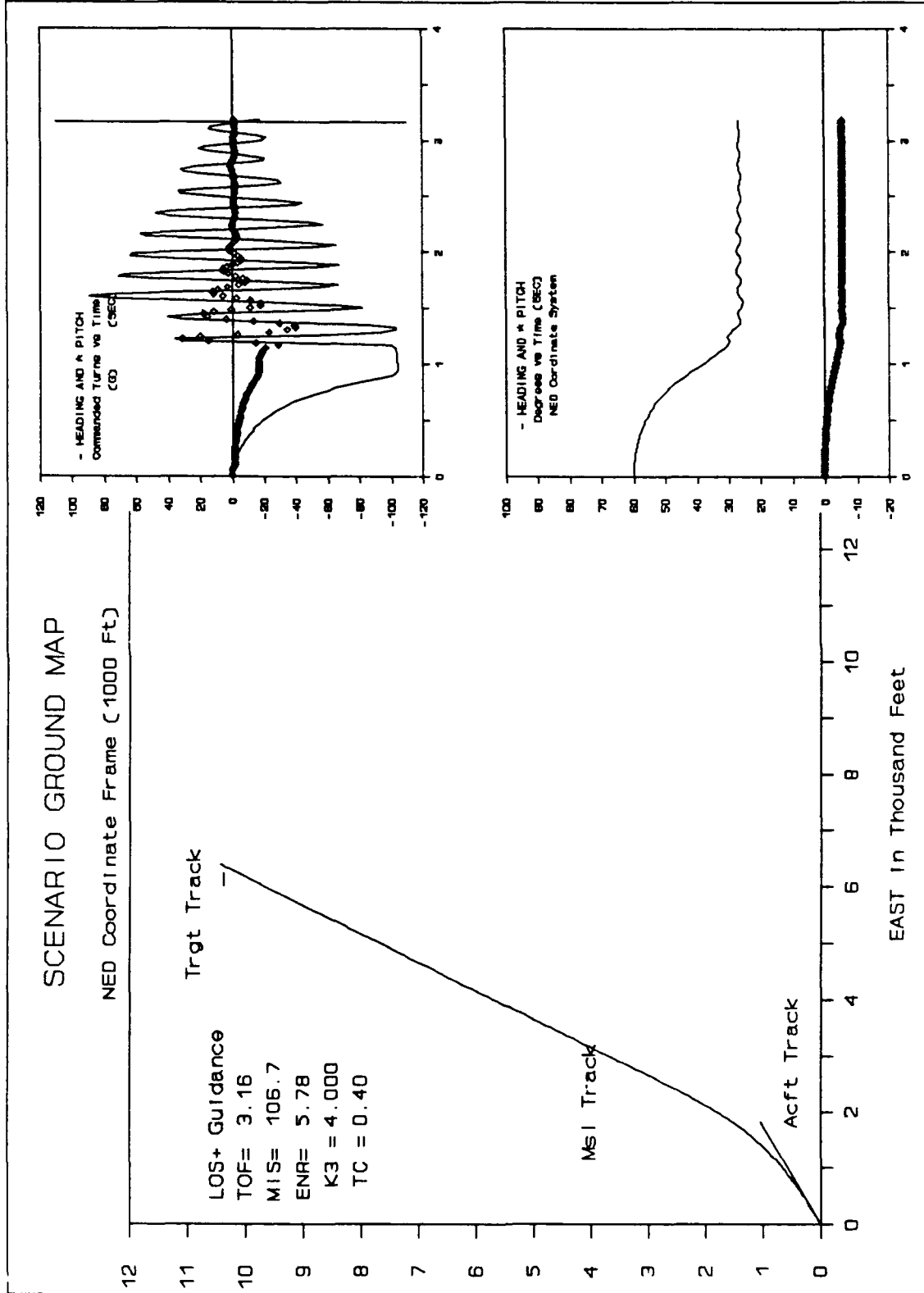Degrees vs Time (CSEC)
NED Coordinate System
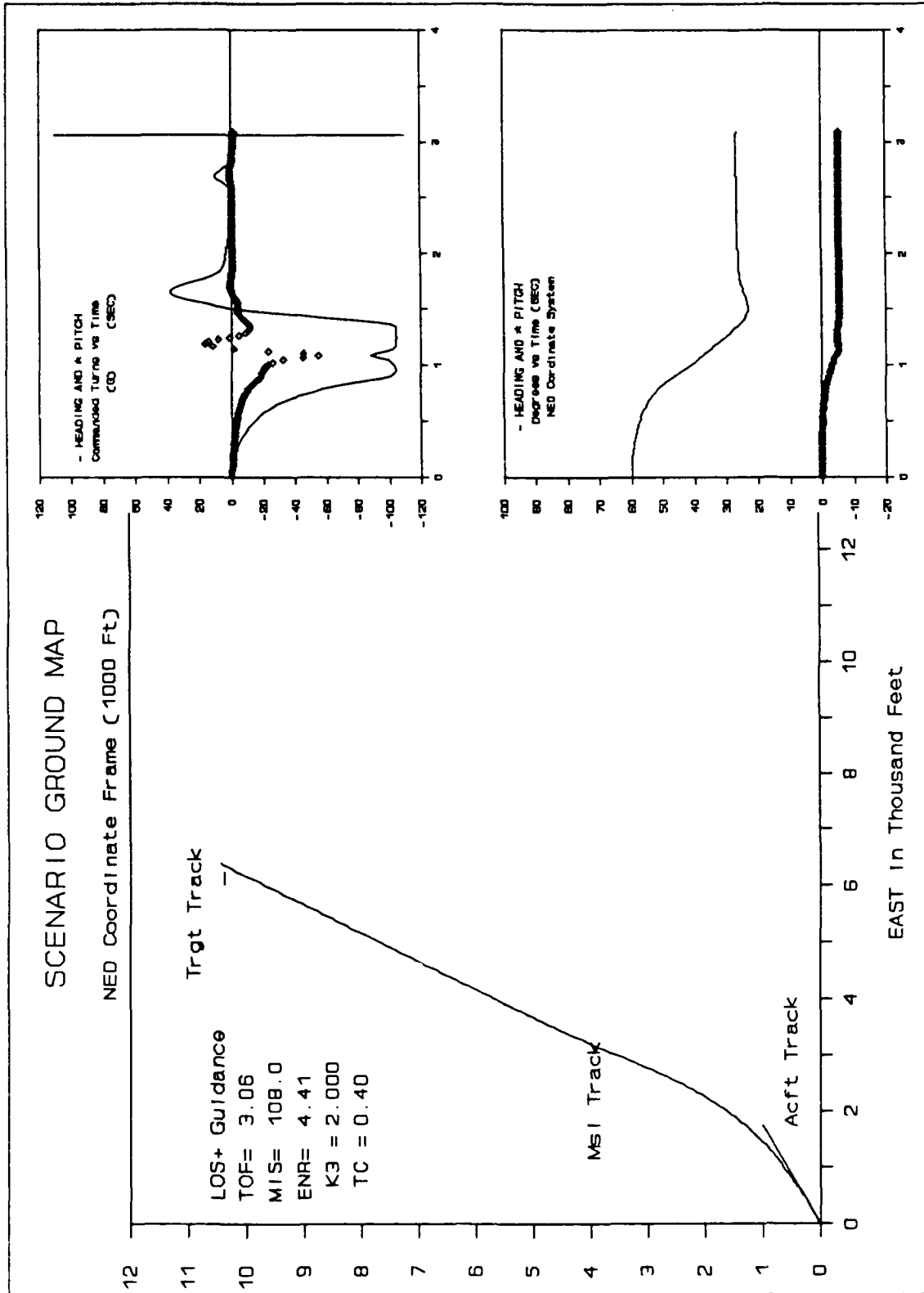
Figure 4-12 LOS+ Control Parameter Test #3

Figure 4-13 LOS+ Control Parameter Test #4

Figure 4-14 shows all the FOM results for the LOS+ runs. The first four graphs show the tests run for control parameter selection. By analyzing the results of the first four runs it is apparent that the best results depend on what you wish to accomplish. Values of $K_3 = 2.0$ and $t_c = 0.4$ seem to show the best damped control responses, but values of $K_3 = 1.0$ and $t_c = 0.2$ gave the best accuracy. The remainder of the LOS+ guidance algorithm tests are run using the best accuracy results.

LOS+ Figures of Merit
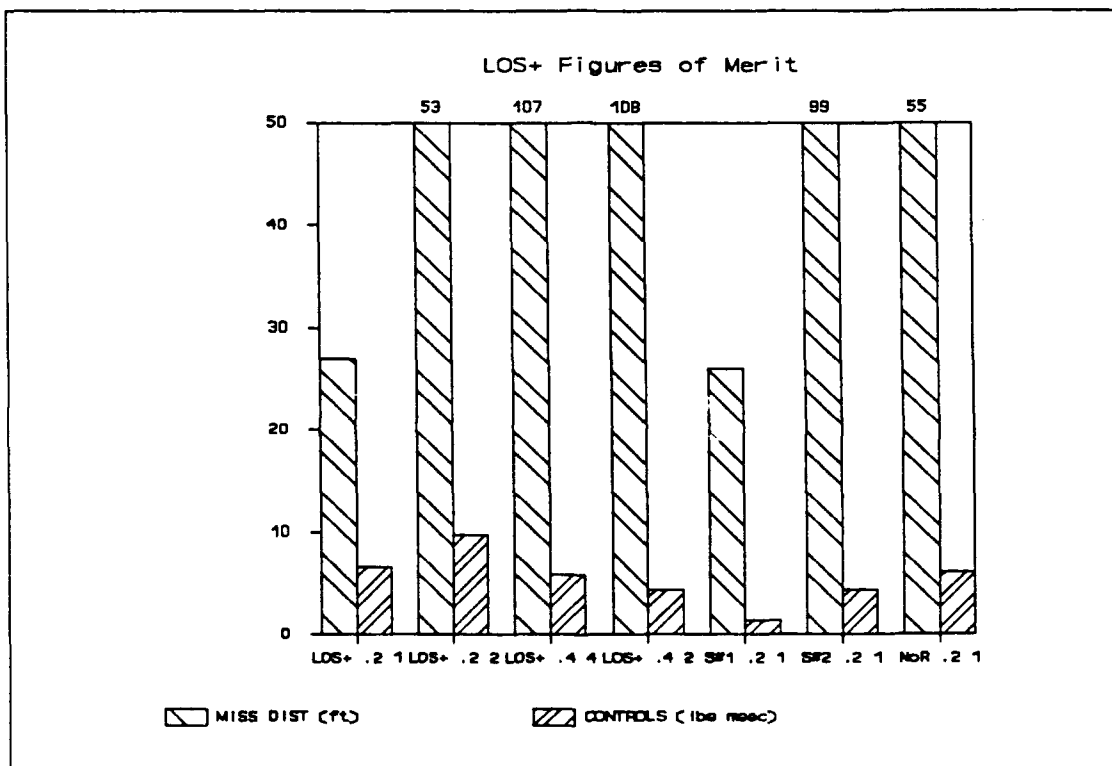
Figure 4-14 FOM For All LOS+ Guidance Runs

4.7 LOS+ 5 Degree Off-Angle Tests

The less dynamic 5 degree off-angle shot is run to test the algorithm with less stringent up-front control requirements, and to test the effect of a 5 G aircraft turn on the guidance situation. The bar graph labeled Sen #1 and Sen #2 in Figure 4-14 represent these two tests. Figure 4-15 and 4-16 give the ground map and control graphs of these two runs. In the non-maneuvering shot of Figure 4-15 some erratic behavior in the heading

and pitch graph appears as a glitch between the first and second TOF points. Although the data in the range is confirmed by hand calculations, an error or a cause for this behavior is not determined. This phenomenon shows up equally in the azimuth and pitch aspect of the algorithm leading suspicion to a dynamic pole location (as seen in the LOS algorithm development) as the cause. This is supported by the fact that this phenomena changes as the different control parameters are used in Figure 4-10 through 4-13.

In Figure 4-16 one can see the effect on this algorithm when the aircraft maneuvers. This is a special problem for this algorithm because it causes motion in the future LOS to the target; motion that is not accounted for in the algorithm development. The result is an erratic flight path that is attempting to settle on an unpredicted future line-of-sight. Notice also the pitch channel is unchanged from the previous shot since the scenario does not change appreciably in pitch. Although this is a less dynamic control challenge the results of this algorithm are unimpressive. The shots are useful for better understanding the LOS+ guidance algorithms shortfalls.

4.8 Radar Off LOS+ Tests

When the sensor model uses a very simple 3DOF missile model to estimate the range and range rate measurements, the algorithm's dependence on accurate range data is examined. Figure 4-17 shows the no-radar scenario and it should be compared to Figure 4-10 which shows the same shot with accurate range and range rate data. Although there is an increase in the miss distance the algorithms performance is relatively unaffected by poor range and range rate data. Poor range data causes the time to go calculation to suffer but if the guidance commands are released from that dependence the results can be relatively independent of range and range rate. (Much the same as the LOS guidance was.) Recall that the time-to-go accuracy dependence is forced to zero for the last half second of

4-21
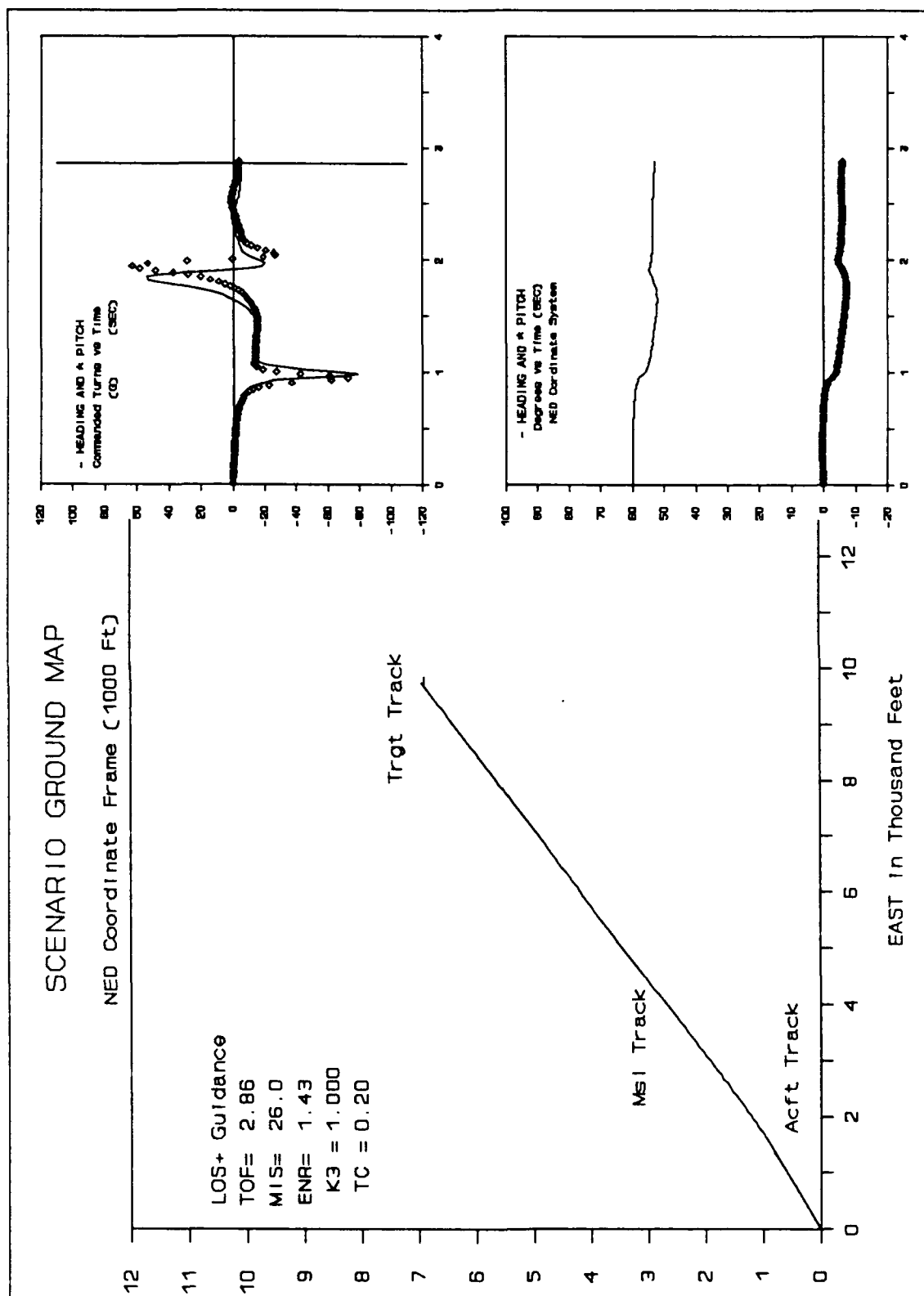
Figure 4-15 LOS+ 5 Degree Off Angle Test
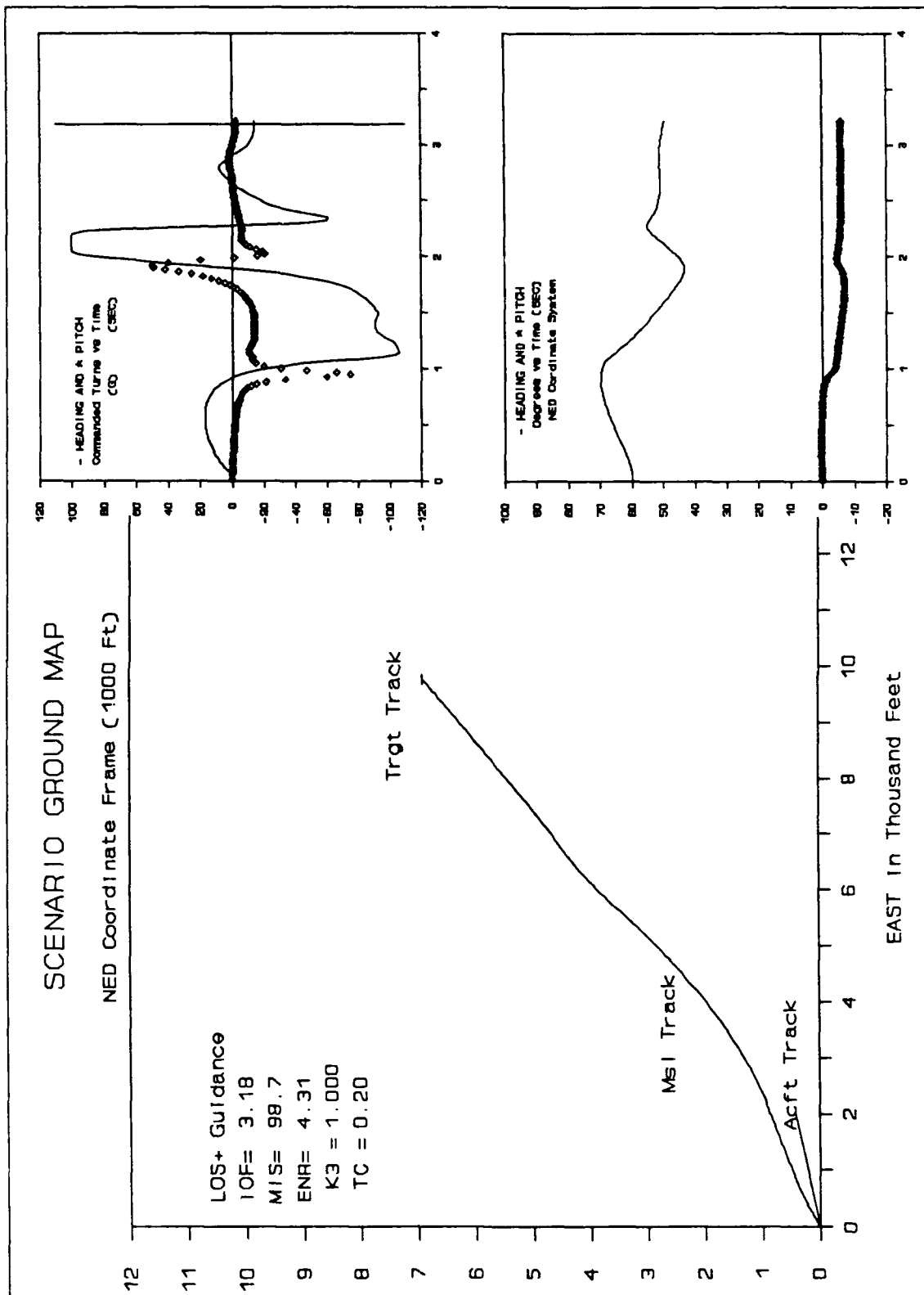
Figure 4-16 LOS+ 5 Degree Off Angle Test, 5-G Turn

SCENARIO GROUND MAP

NED Coordinate Frame (1000 Ft)

LOS+ Guidance
TOF= 3.46
MIS= 54.7
ENR= 6.14
K3 = 1.000
TC = 0.20

Trgt Track

Msl Track

Acft Track

EAST In Thousand Feet

- HEADING AND A PITCH
Commanded Turns vs Time
(DEG) (SEC)

- HEADING AND A PITCH
Degrees vs Time (SEC)
NED Coordinate System

Figure 4-17 LOS+ Radar Off Test

flight. Although this algorithm does not have a strong range and range rate dependence it has enough other drawbacks to dwarf this advantage.

4.9 Pursuit Control Parameter Testing

The runs used to establish the pursuit algorithm control gain are shown in Figure 4-18 through 4-22. The only parameter changed for each of these shots is K_3, the gain for the pursuit guidance algorithm. It is typical for the pursuit algorithm to have a large acceleration towards the end of its flight. This is caused by an increase in the missile-to-target line-of-sight rate as the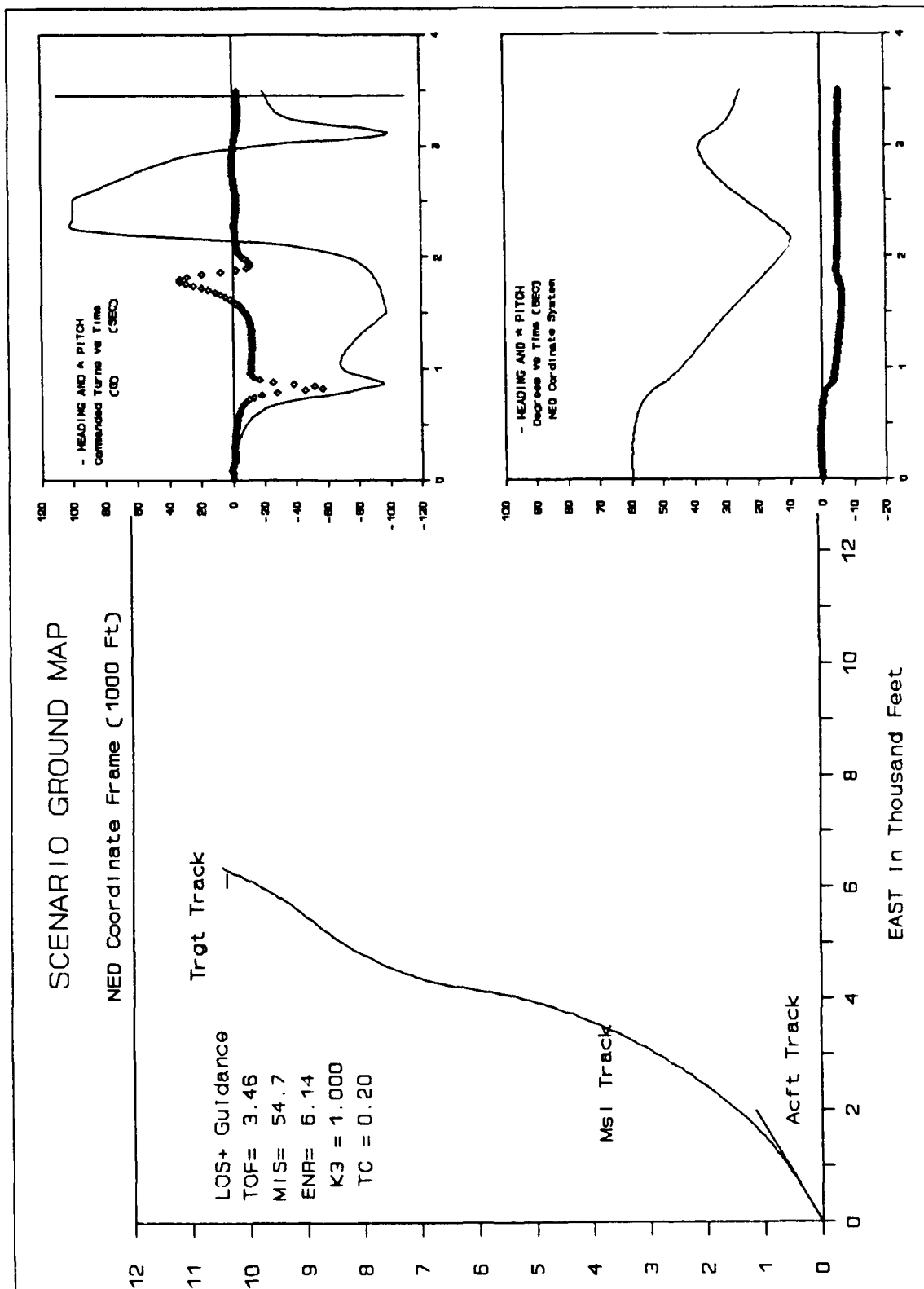 missile range to the target decreases. In Figure 4-18 one can see this high-G turn commanded at the end of the missile flight.

An interesting aspect of this "end game" turn is that it is in the opposite direction of a normal pursuit engagement. In the normal pursuit engagement, i.e. where a missile sensor gives the LOS to the target, the missile ends up pursuing the target, and flying up its tail. (Thus the name of the engagement.) In our engagement notice that the tank is moving east and the missile requires a negative heading command to strike the target; bringing it into the nose of the tank. This interesting situation is brought about by the fact that the aircraft is doing the tracking, not the missile. Thus, in relation to the aircraft, the tank is moving west and the pursuit algorithm is performing normally.

In Figure 4-19 through 4-22 are some runs with various gains to show the inability to correct the large miss distances by increasing the gain. Figure 4-23 shows the FOMs for all the pursuit algorithm shots. Notice that a gain of $K_3 = 8$ gives the best performance obtainable with this algorithm. When firing a hyper-velocity missile it is not wise to put your most strenuous turn in the end game as the pursuit algorithm does.

4-25

Figure 4-18 Pursuit Control Parameter Test #1

SCENARIO GROUND MAP

NED Coordinate Frame (1000 Ft)

Trgt Track

PURSUIT

TOF= 2.87
MIS= 65.6
ENR= 4.95
K3 = 8.000
TC = 0.10

Msl Track

Acft Track

EAST in Thousand Feet

- HEADING AND * PITCH
Commanded Turns vs Time
(CG)   (SEC)

- HEADING AND * PITCH
Degrees vs Time (SEC)
NED Coordinate System
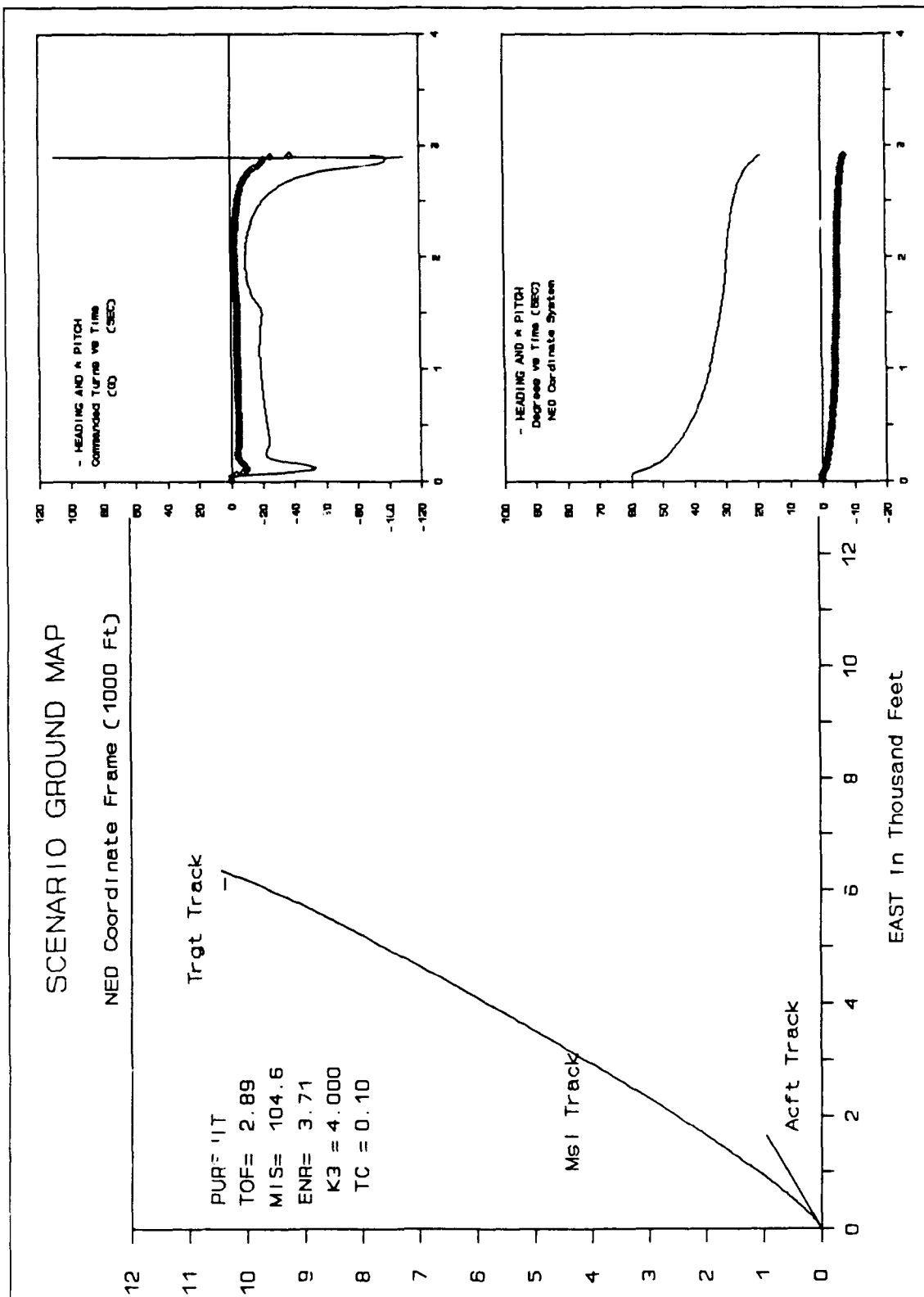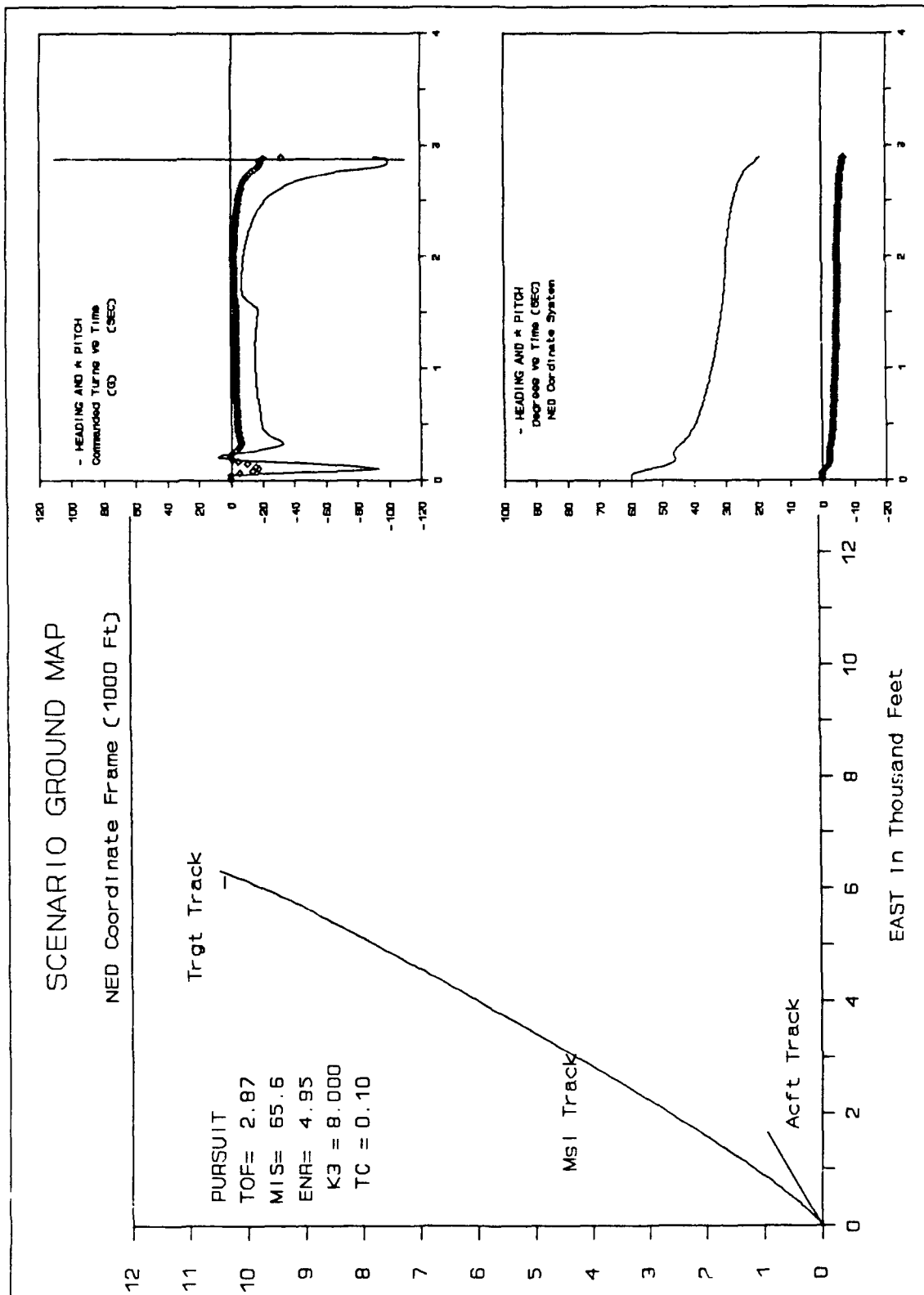
Figure 4-1%, Pursuit Control Parameter Test #2
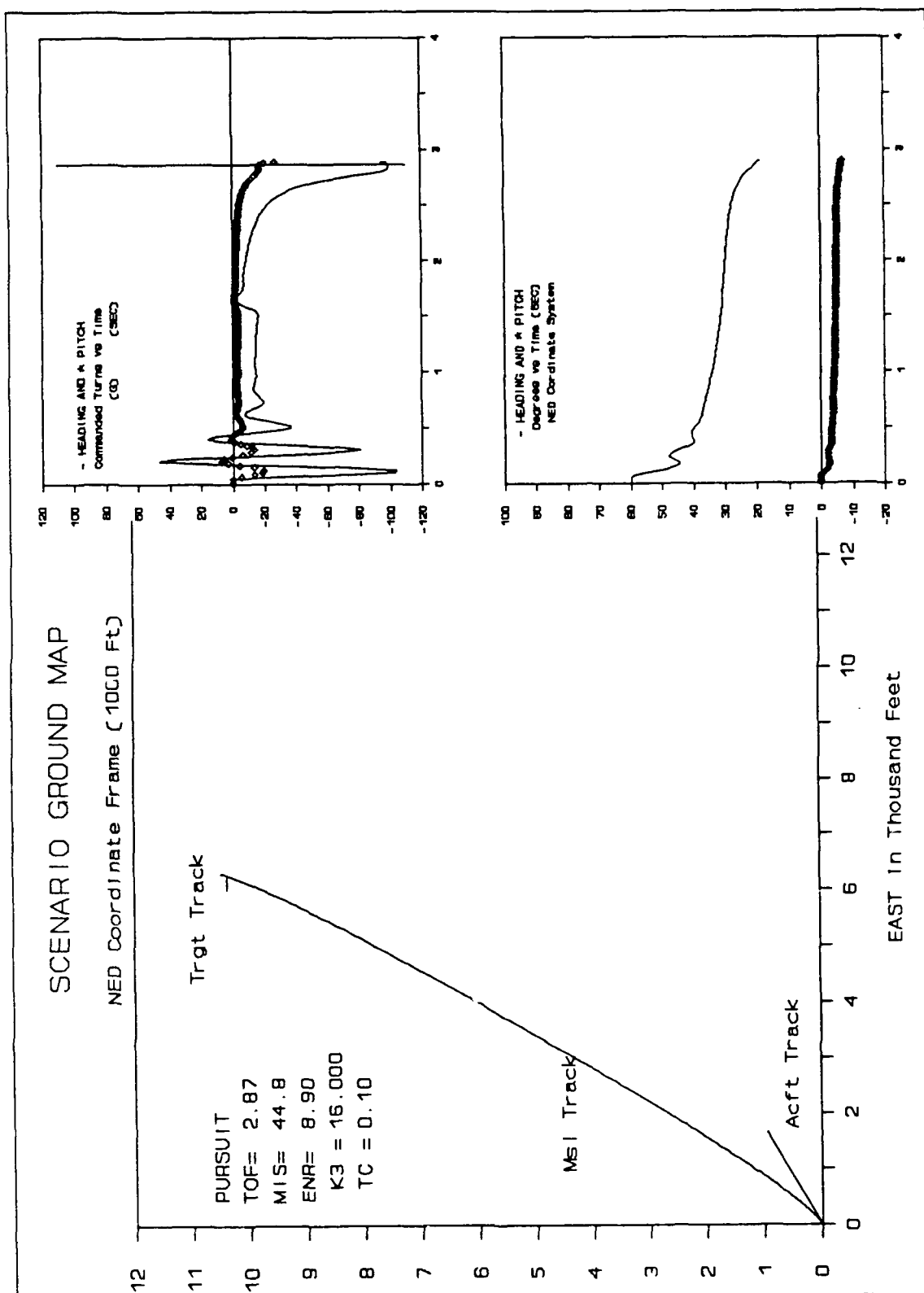
Figure 4-20 Pursuit Control Parameter Test #3
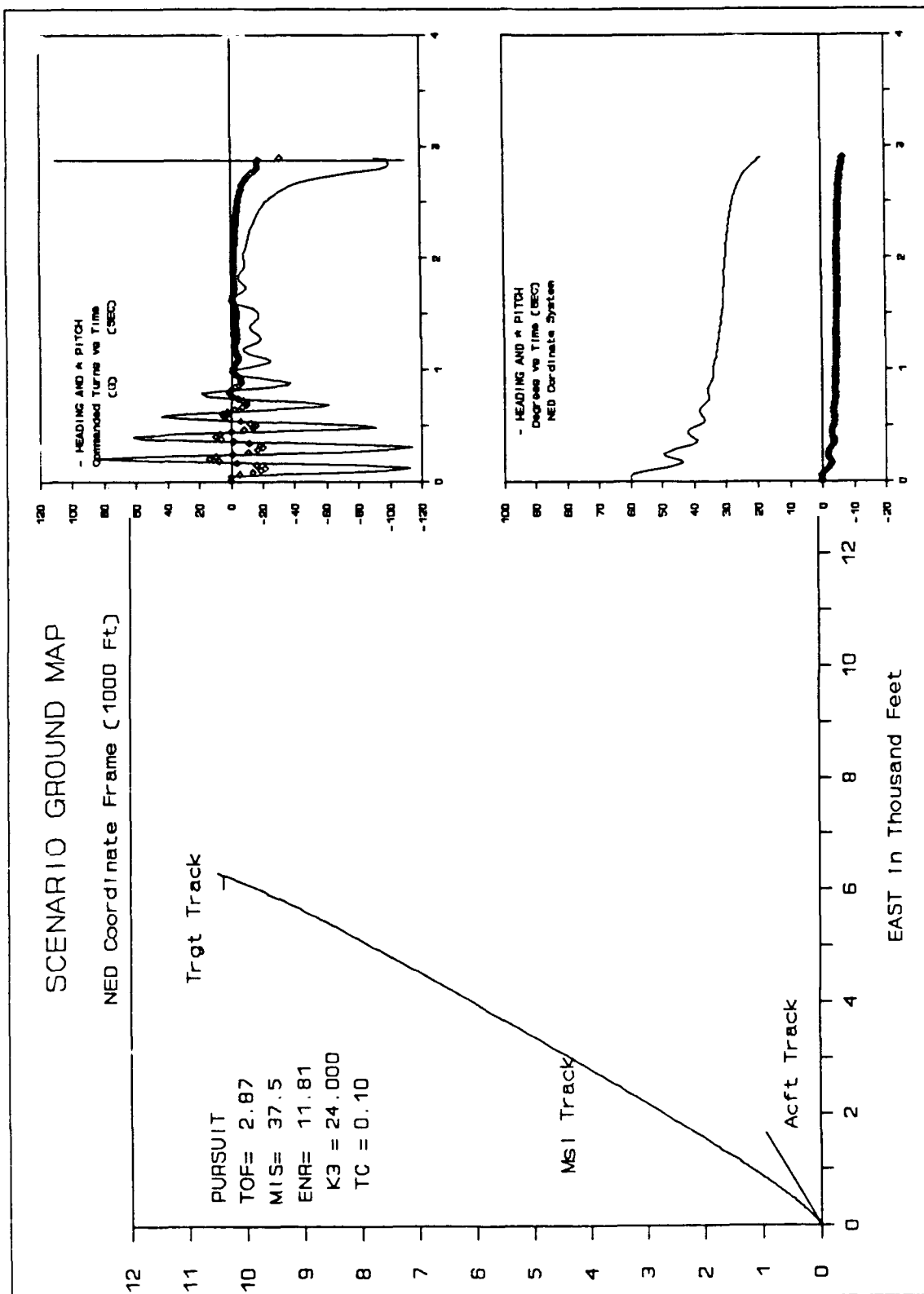
Figure 4-21 Pursuit Control Parameter Test #4
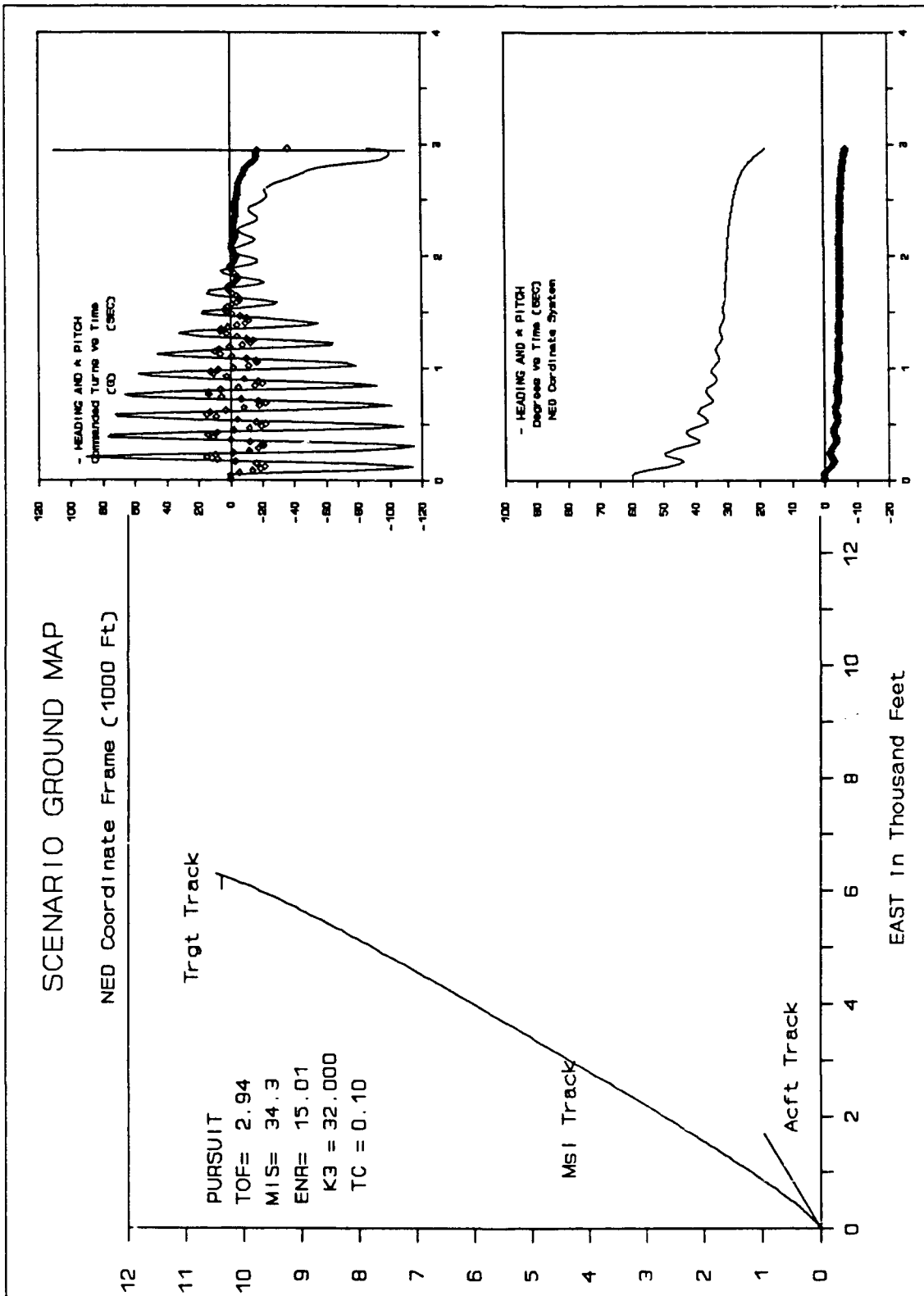
Figure 4-2∠ Pursuit Control Parameter Test #5
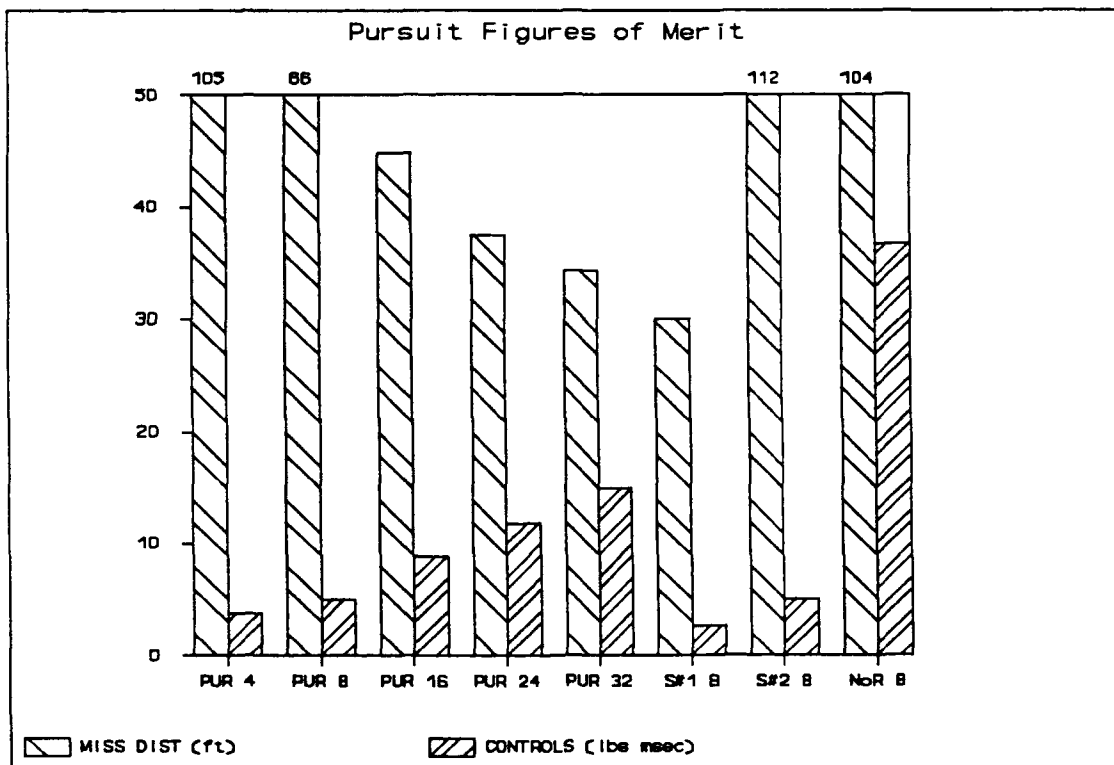
Figure 4-23 FOM For All Pursuit Guidance Runs

4.10 Pursuit 5 Degree Off-Angle Test

The less dynamic 5 degree off-angle shot is run to test the algorithm with less stringent up-front control requirements, and to test the effect of a 5-G aircraft turn on the guidance situation. The bar graph labeled Sen #1 and Sen #2 in Figure 4-23 represent these two tests. Figure 4-24 and 4-25 give the ground map and control graphs of these two runs.

In the non maneuvering shot of Figure 4-24 one can still see a large "end game" acceleration commanded. Again this is caused by the missile to target line of sight rate approaching infinity as the missile closes on the target. Remember that the HVM missile is a hit or miss "bullet" and here, even with no sensor errors and benign launch conditions, the missile only passed within 30 feet of the target.
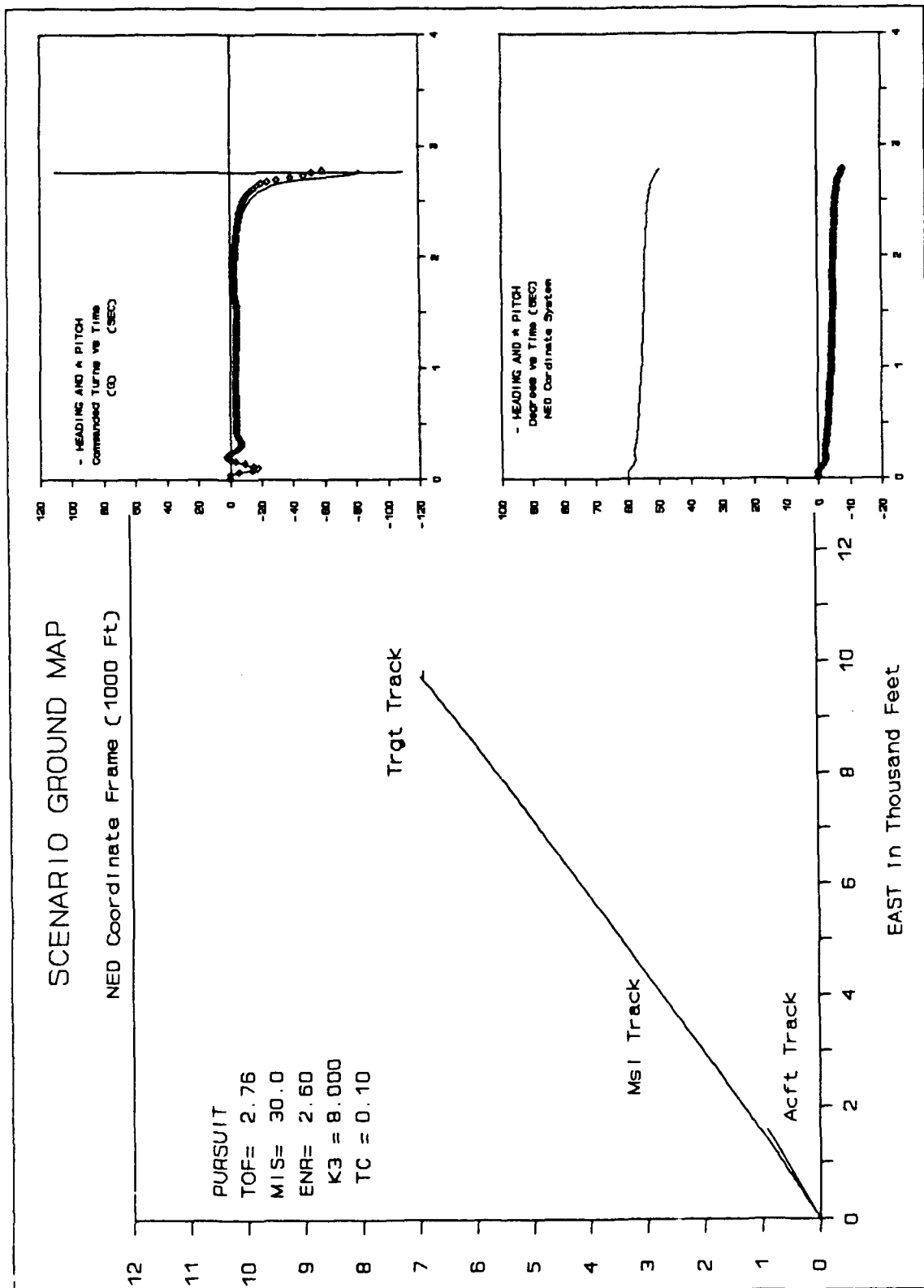
Figure 4-24 Pursuit 5 Degree Off Angle Test
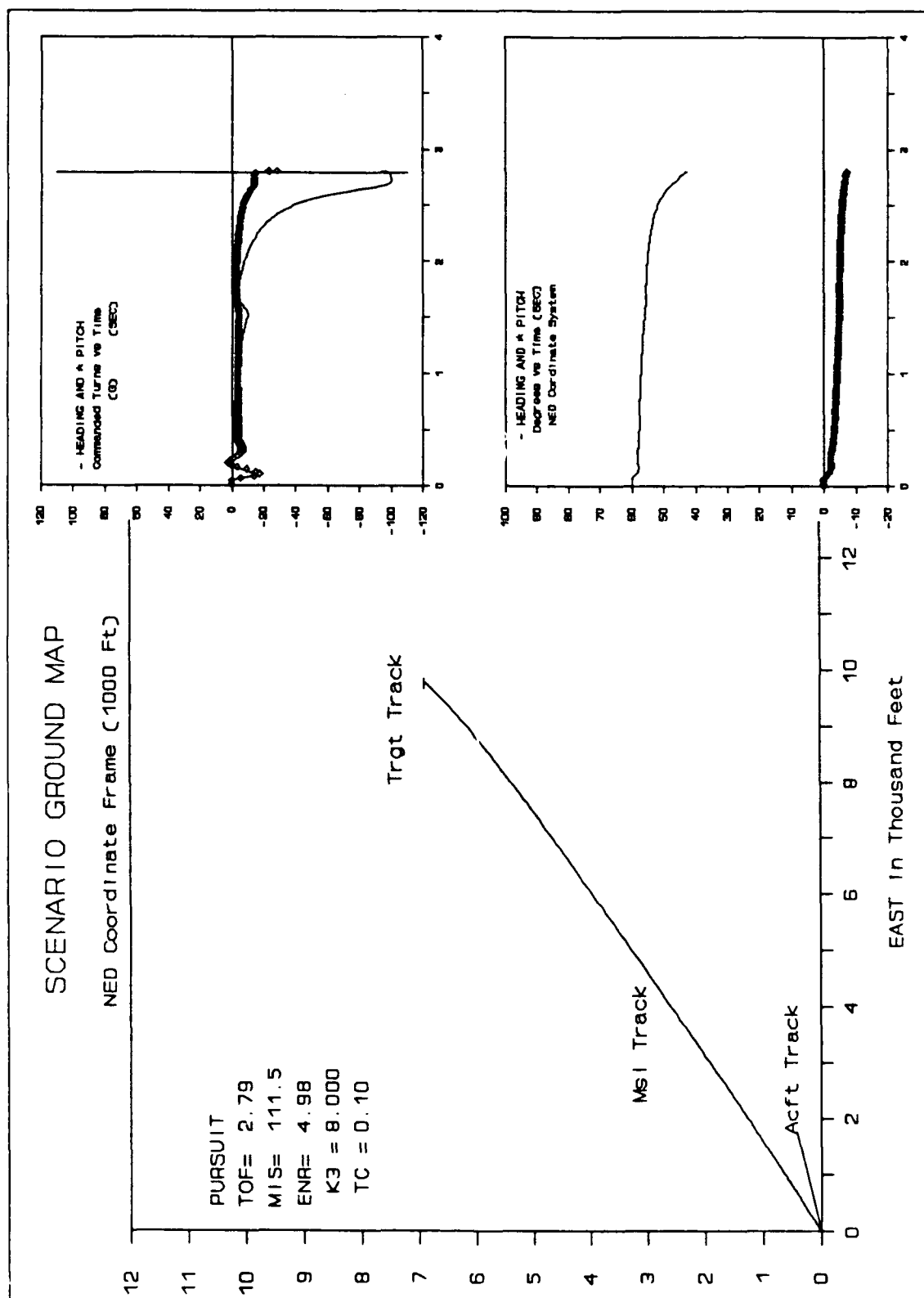
Figure 4-25 Pursuit 5 Degree Off Angle Test, 5-G Turn

When the 5-G aircraft maneuver is included in the shot the miss distance increases. Comparing Figure 4-25 with 4-24 gives some insight to the reason. A first impulse for this shot is that it is independent of an aircraft maneuver since the aircraft is only the sensor in charge of calculating the missile-to-target line-of-sight and this calculation should be relatively independent of the aircraft's acceleration, and to some extent independent of its position. But recalling the argument that the target is sensed in the aircraft reference frame, what changes here is the sensed target velocity. Or, in reference to our sensor the missile is chasing an accelerating target and this causes the increased miss distance. One can see the increased "end game" correction attempt when comparing it to the non-maneuvering shot. Other than this perceived accelerating target problem the pursuit algorithm operates the same for a maneuvering aircraft.

4.11 Radar Off Pursuit Tests

Once again a very simple 3DOF missile model is used to estimate the range and range rate measurements to examine the algorithm's dependence on accurate range data. Figure 4-26 shows the no-radar scenario and it should be compared to Figure 4-18 which shows the same shot with accurate range and range rate data. Since the pursuit algorithm calculates the missile velocity vector direction using missile range and range rate, i.e. see equation (3-21) and (3-22), the algorithm performance is directly dependent on the accuracy of this data. An interesting anomaly can be seen in Figure 4-26. Notice that the commanded left turn increases as the missile approaches the target. Then, the range estimator says the missile has past the target and the command abruptly turns the missile into a right turn. This last right turn does, coincidentally, bring the missile
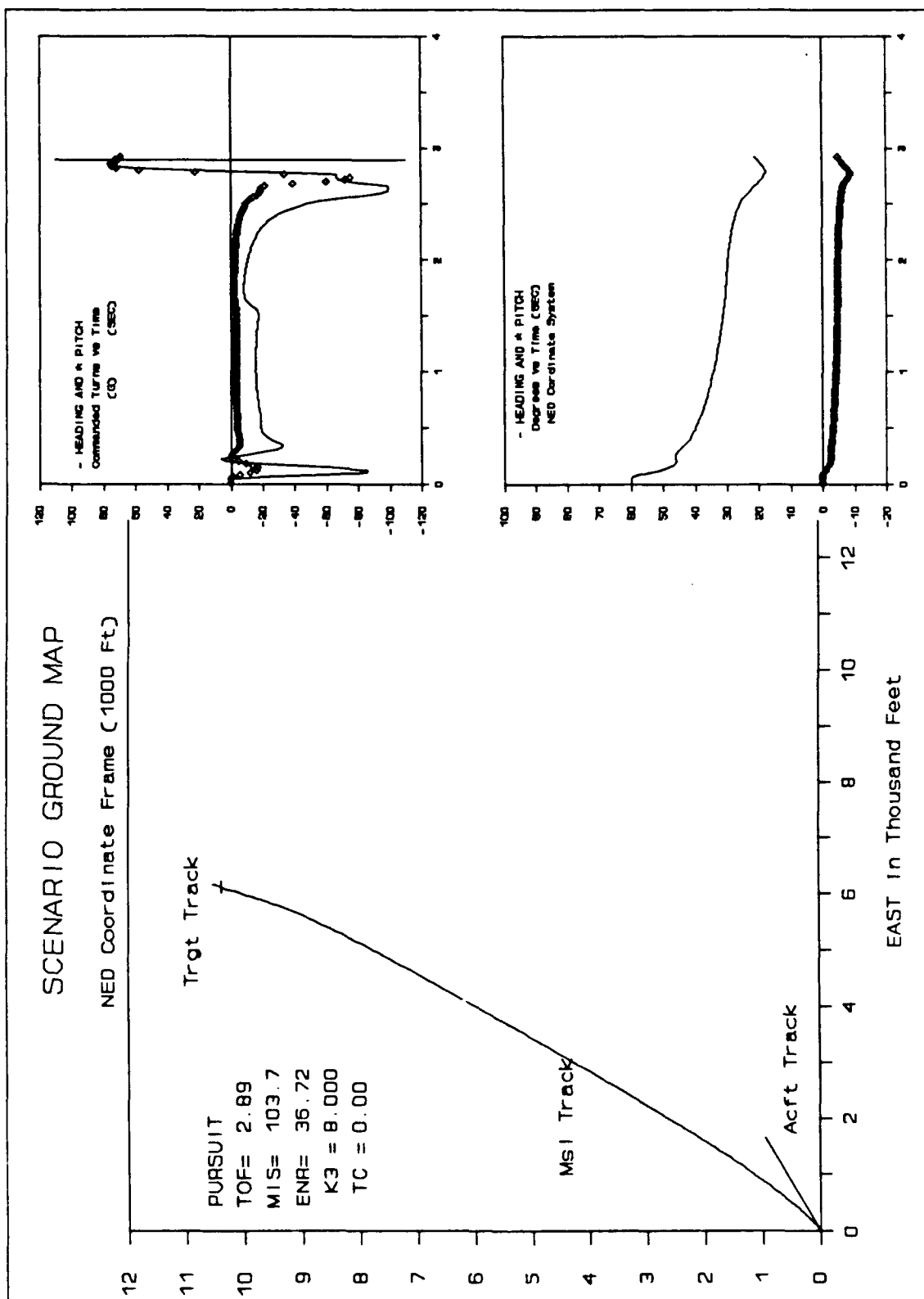
Figure 4-26 Pursuit Radar Off Test

towards the target, but not because the algorithm knows the missile to target line of sight. It has been unable to calculate that line of sight because of inaccurate range and range rate data. This algorithm needs an accurate range and range rate measurement to calculate the missiles heading in reference to the target.

4.12 Proportional Control Parameter Testing

The various runs used to test the navigation constant, K_3, for the proportional guidance algorithm are shown in Figure 4-27 through 4-31. The only guidance parameter changed for these runs is K_3, the input variable used as the navigation constant when the proportional algorithm is selected. As before in these figures a scenario ground map that pictures the aircraft track, the target track and the missile flight path is included. In the upper left corner of this map is the type of algorithm used, some figures of merit and the control parameters. Inset into each of the scenario maps is a graph of the heading rate commands and graph of the missile heading and pitch.

The normal navigation constant for this algorithm ranges from 2.5 to 3.5 and Figure 4-27 shows test results with $K_3 = 3$. This shot shows a very smooth flight path that takes the missile to an interception point with the target as designed. The miss distance of 2.7 feet with "perfect" single precision sensor measurements is from calculation round-offs and represents an equivalent pointing error of .26 mrad.

Some other navigation constant runs are shown in Figures 4-28 through 4-31. Notice that the form of the commanded heading rates follows a similar pattern. In Figure 4-31 the navigation constant of $K_3 = 6$ is used and the miss distance and control efficiency FOMs reach another minimum.
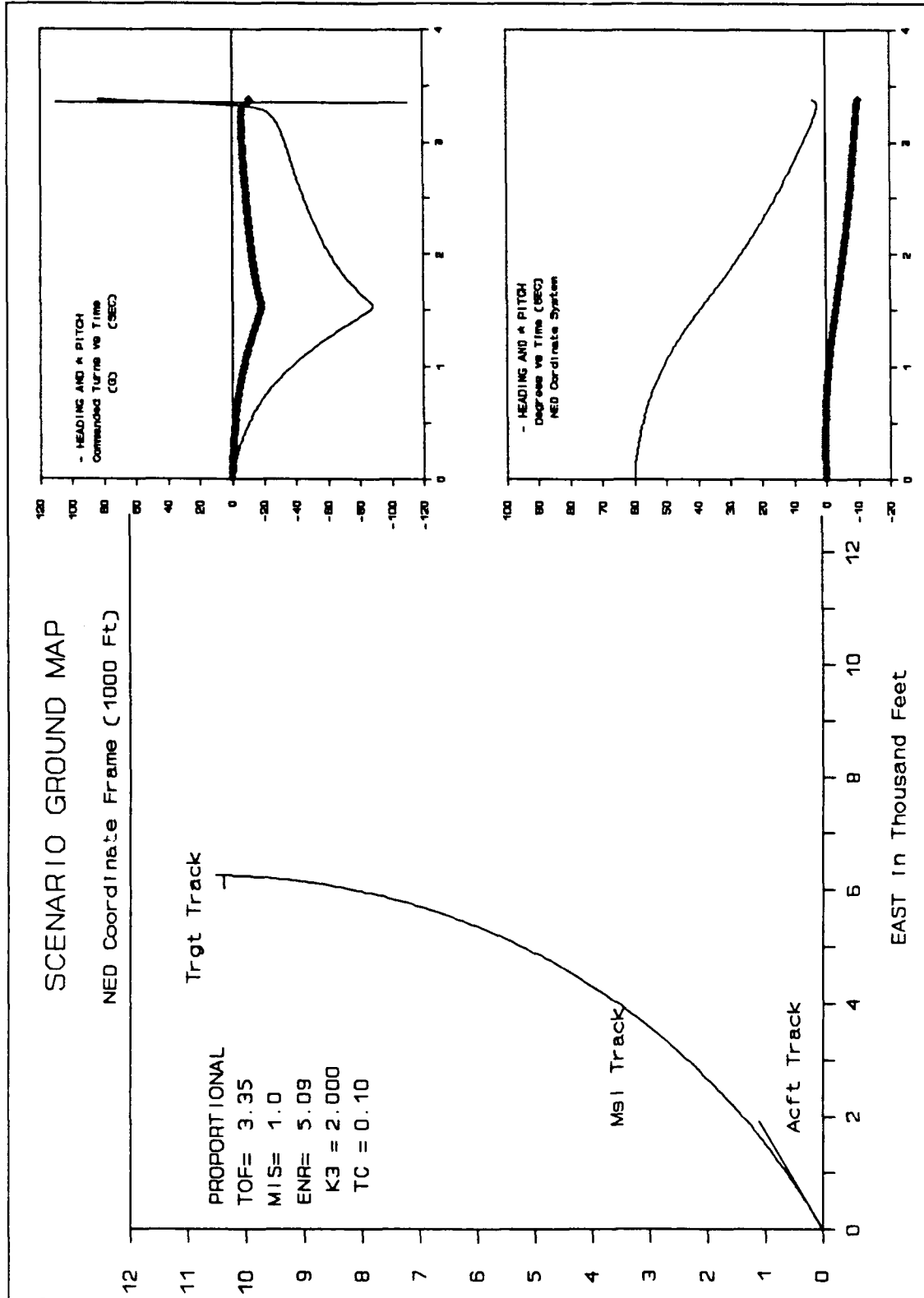
Figure 4-27 Proportional Control Parameter Test #1
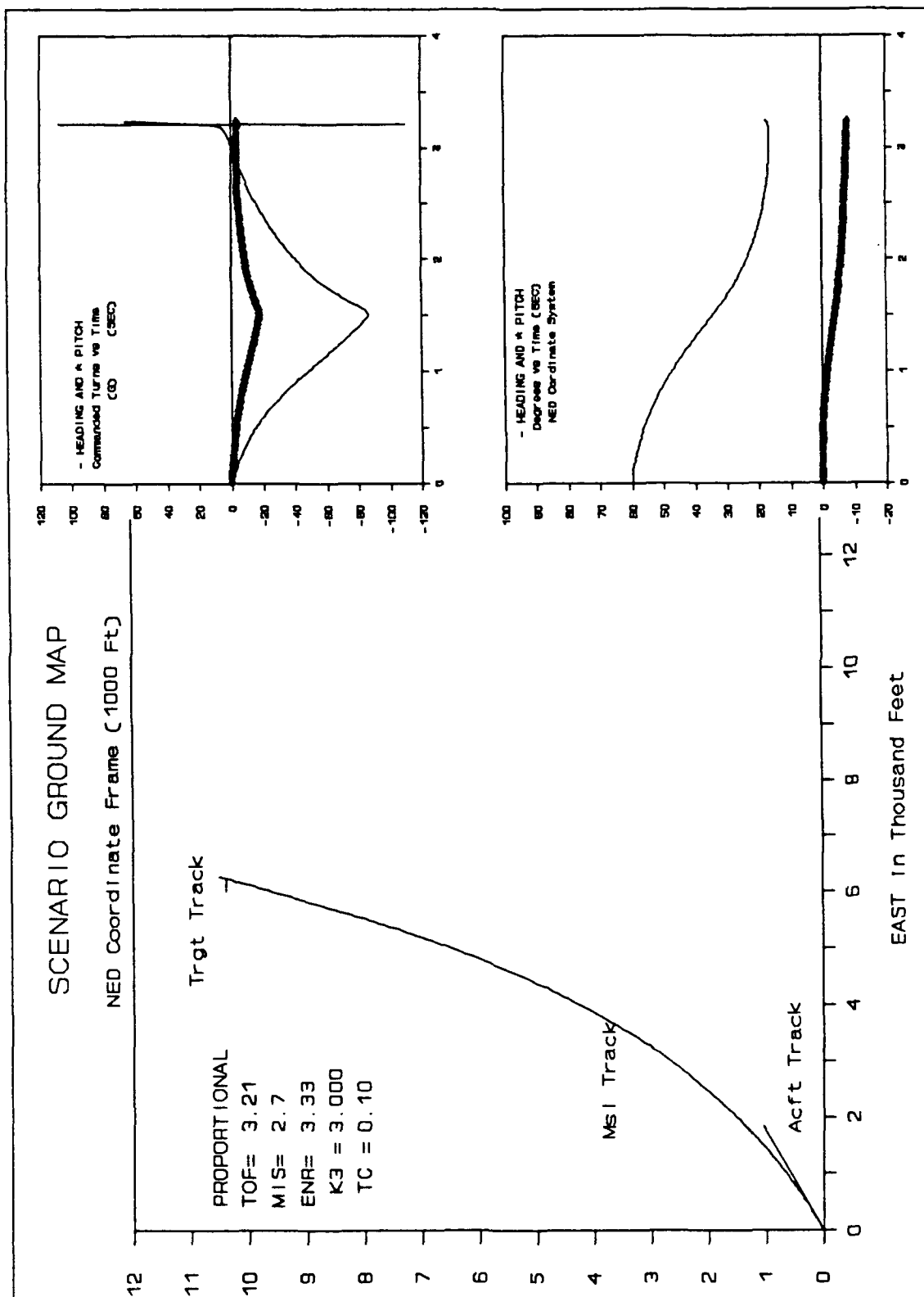
Figure 4-28 Proportional Control Parameter Test #2
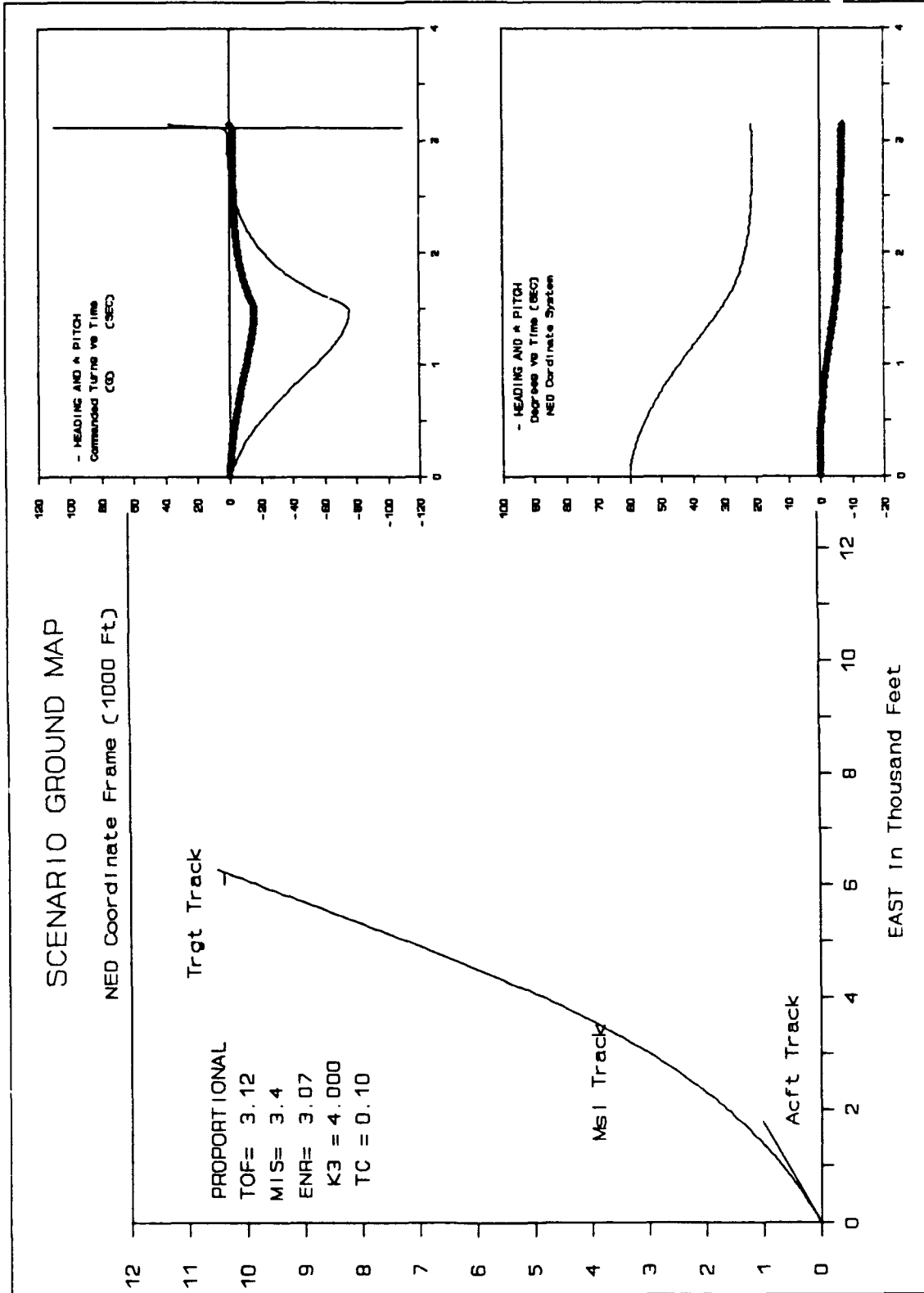
Figure 4-29 Proportional Control Parameter Test #3

SCENARIO GROUND MAP

NED Coordinate Frame (1000 Ft)

PROPORTIONAL
TOF= 3.00
MIS= 2.6
ENR= 2.45
K3 = 6.000
TC = 0.10

Trgt Track

Msl Track

Acft Track

EAST In Thousand Feet
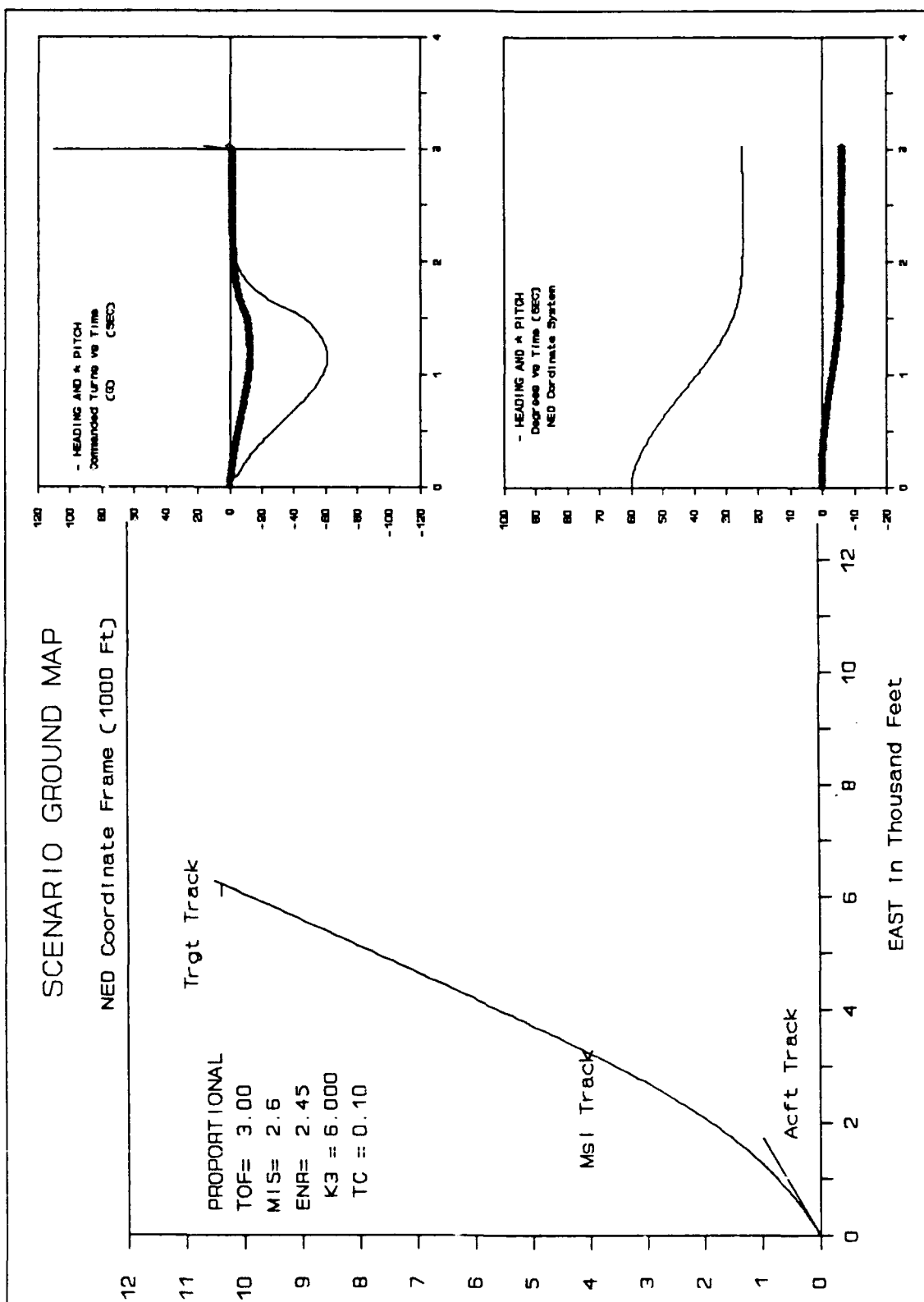
Figure 4-30 Proportional Control Parameter Test #4
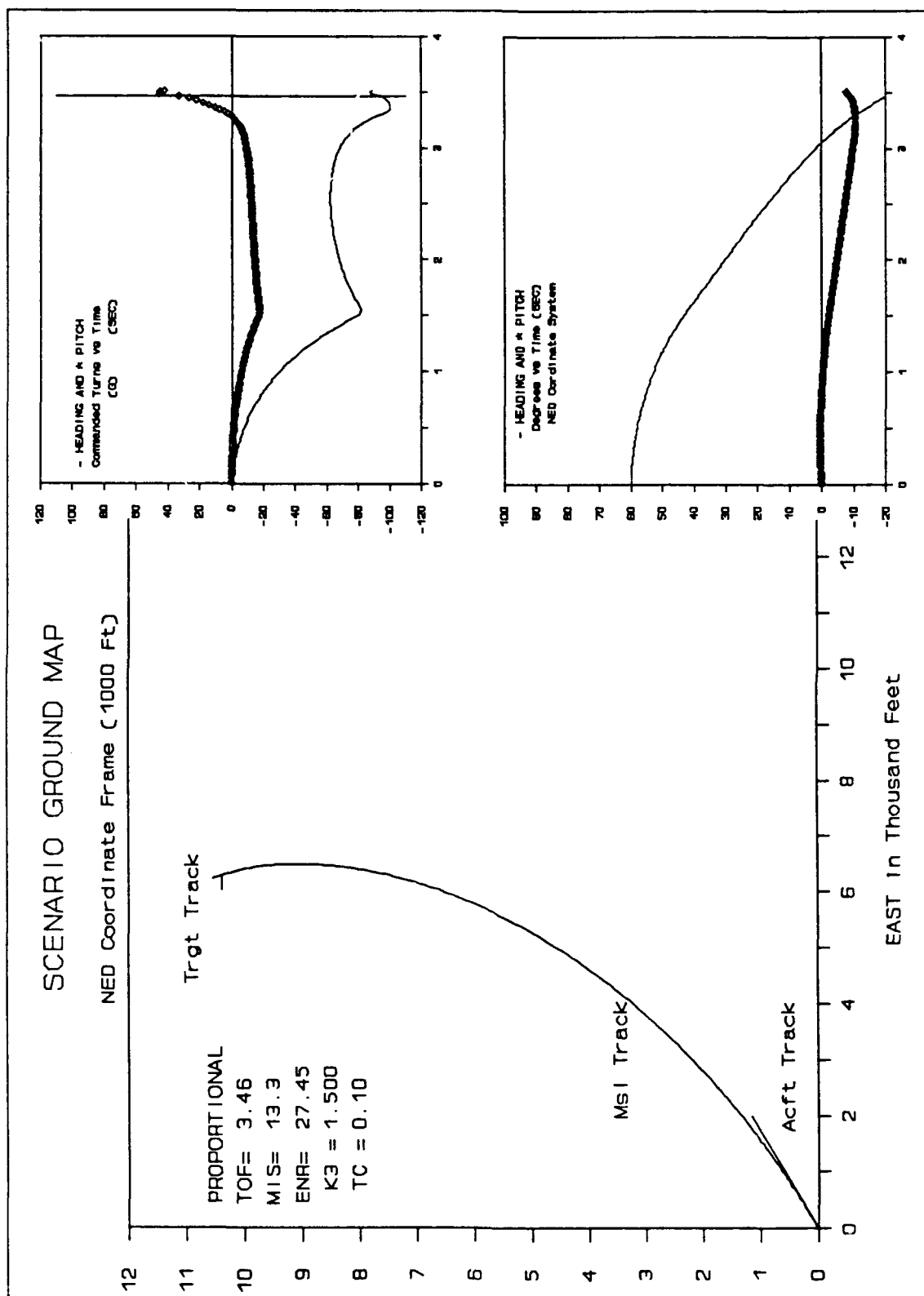
Figure 4-31 Proportional Control Parameter Test #5

Notice here that more of the turn is made before the missile reaches

its maximum velocity.   The higher gain also puts the missile on a good

intercept path faster than the lower gain.   This could be important for

shorter range shots that are not tested.   In a shorter range shot the

lower gain may not provide the correction fast enough to bring the missile

in.   The more rounded flight path of Figure 4-27 is selected as the

nominal control parameter because it is the more conventional navigation

constant.   The higher gain region should be tested in shorter range in

future analysis.

Figure 4-32 shows all the FOM results for the proportional algorithm

runs.   The first five graphs show the tests run on navigation constant

variations.   The navigation constant value of 3 shows a minimum in both
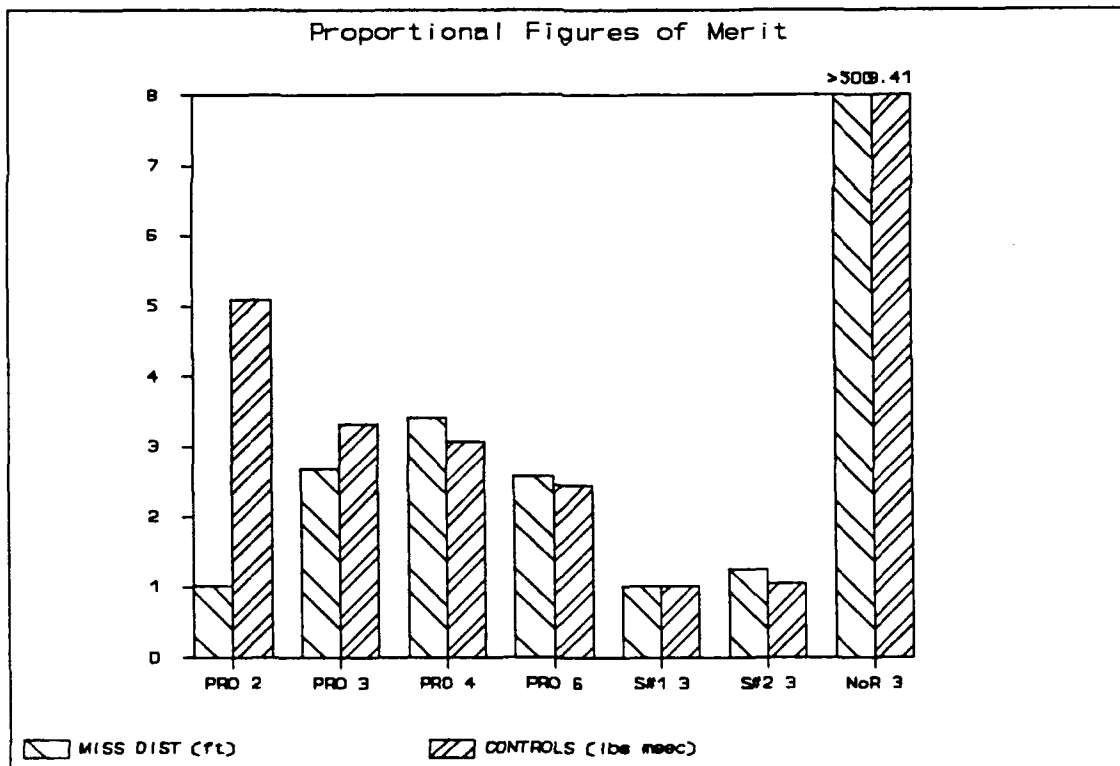
Figure 4-32 FOM For All Proportional Guidance Runs

FOMs and the remainder of the proportional guidance algorithm tests are done with this navigation constant.

4.13 <u>Proportional 5 Degree Off-Angle Tests</u>   The less dynamic 5 degree off-angle shot is run to test the algorithm with less stringent up-front control requirements, and to test the effect of a 5-G aircraft turn on the guidance situation.   The bar graph labeled Sen #1 and Sen #2 in Figure 4-32 represent these two tests. Figure 4-33 and 4-34 give the ground map and control graphs of these two runs.   Comparing these two graphs, the missile to target line of sight rate is relatively independent of accelerations by the sensing aircraft. Recall from the pursuit algorithm that the missile to target line of sight is dependent on aircraft acceleration, where it appeared to the algorithm as target accelerations. Here the aircraft acceleration has minimal effect on the FOMs and the precision of this algorithm rivals the LOS algorithm.

4.14 <u>Radar Off Proportional Tests</u>

When the sensor uses a very simple 3DOF missile model to estimate the range and range rate measurements the algorithm's dependence on accurate range data is examined.   Figure 4-35 shows the no-radar scenario and it should be compared to Figure 4-27 which shows the same shot with accurate range and range-rate data.   It is obvious from examining the figure that the proportional guidance algorithm has a direct dependence on accurate range and range rate measurements.   This dependence is rooted in the calculation of the missile to target line of sight rate.   This rate requires an accurate assessment of the missile velocity vector which cannot be made without accurate range and range rate data.   As in the pursuit algorithm, notice the abrupt change in the commands when the range estimator shows the missile past the target. Notice also that despite the poor range and range rate data the initial portion of the flight shows the smooth and efficient turn into an intercept approach.
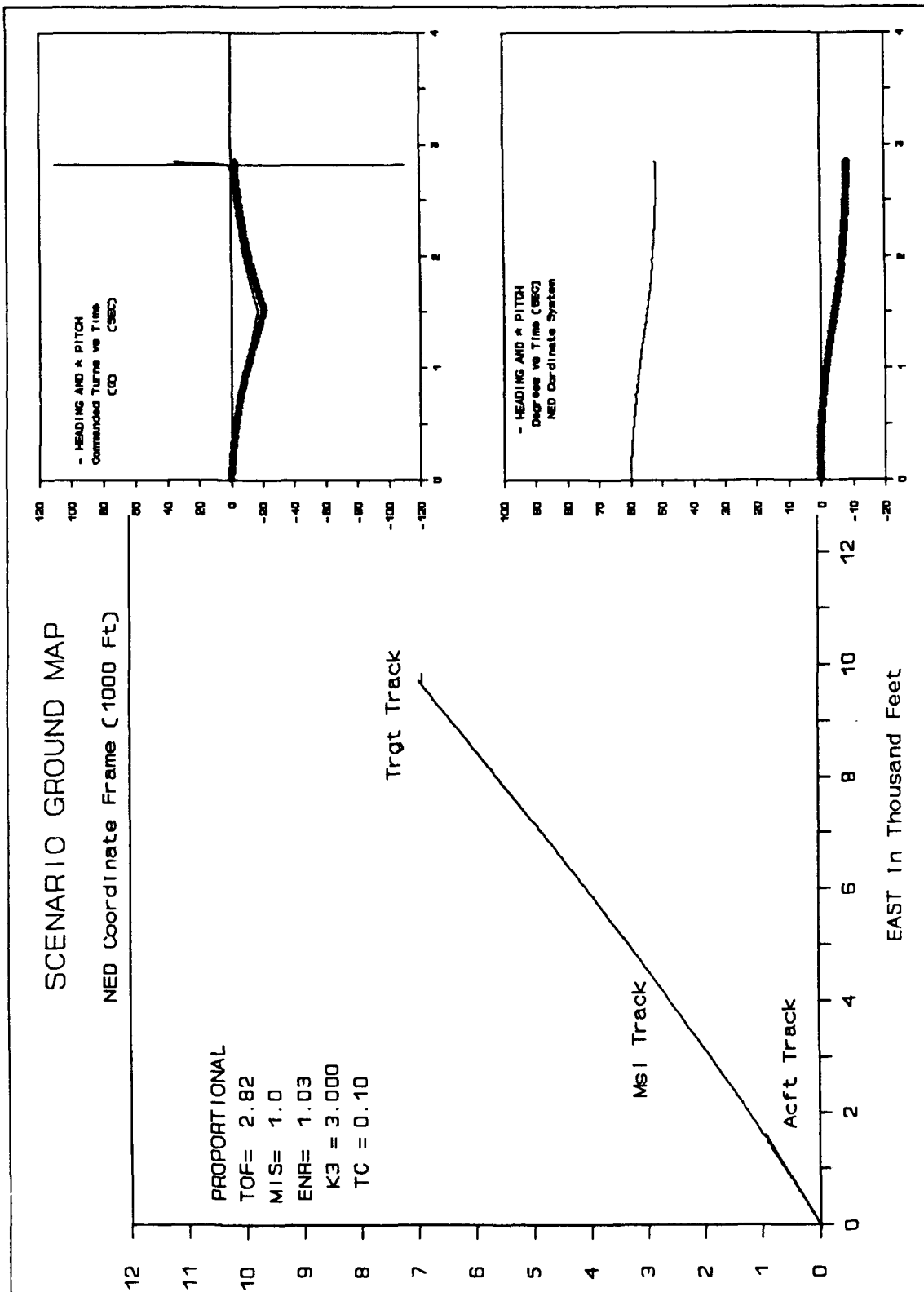
Figure 4-33 Proportional 5 Degree Off Angle Test
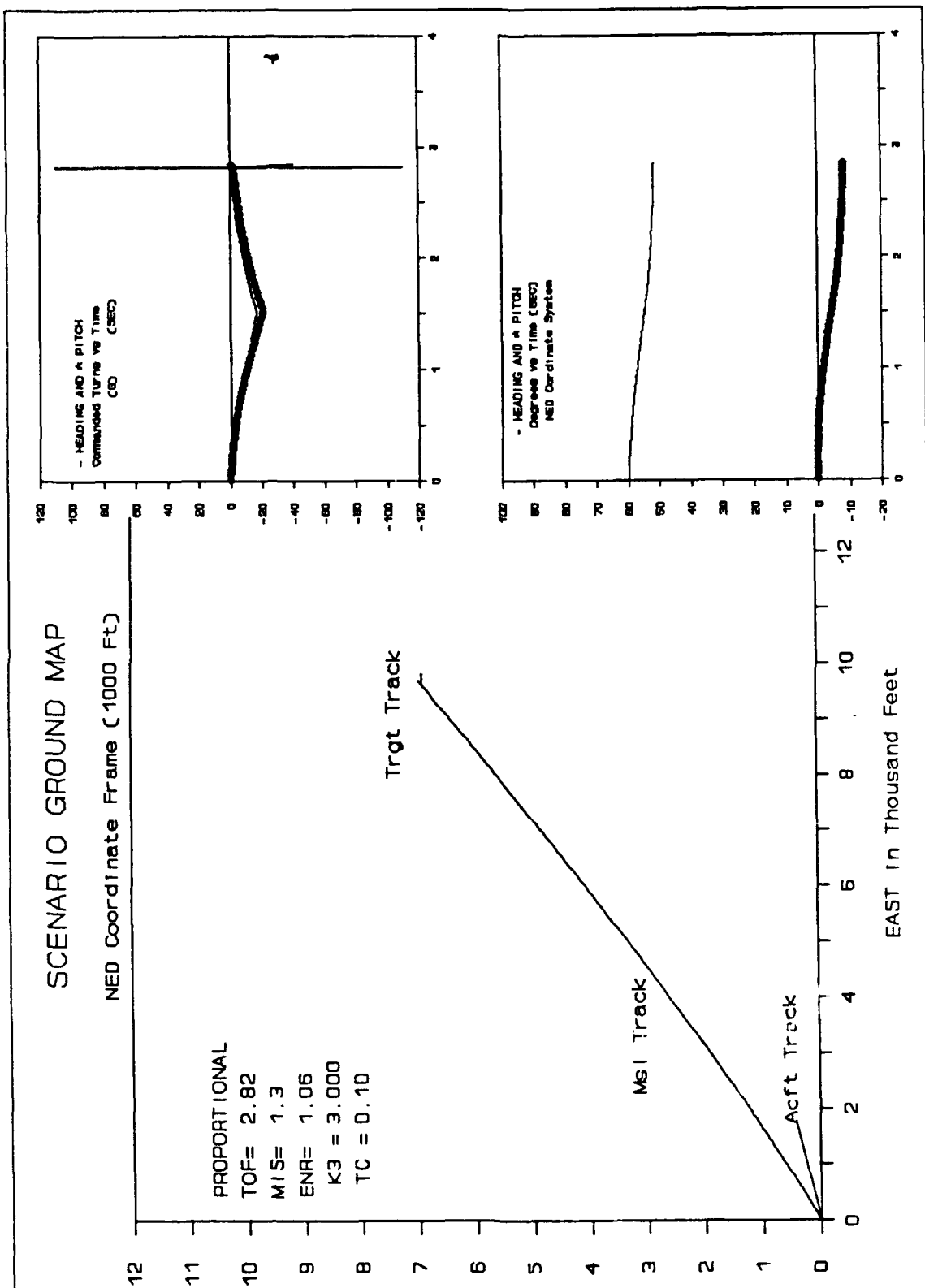
Figure 4-34 Proportional 5 Degree Off Angle Test
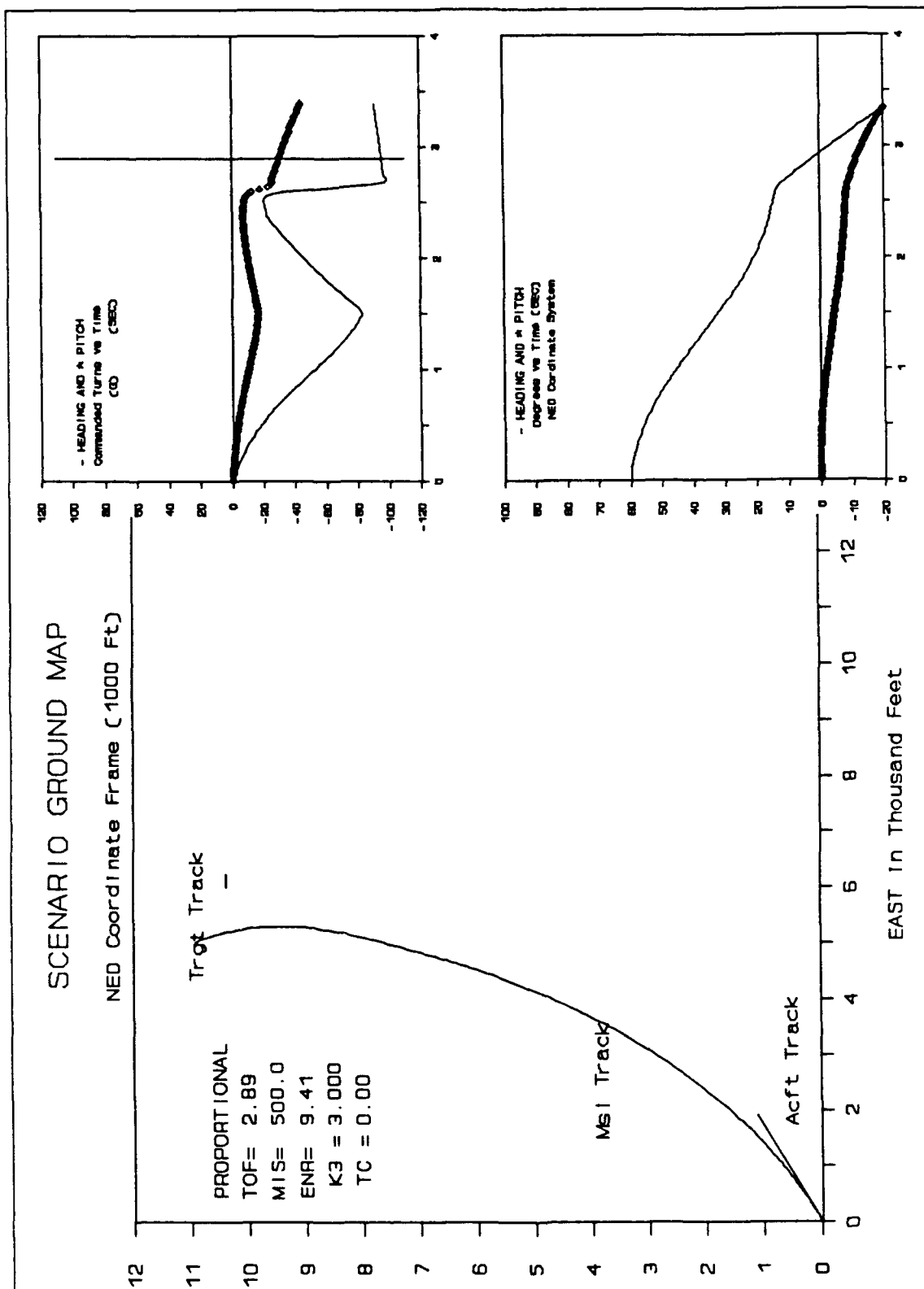
Figure 4-35 Proportional Radar Off Test

The strong dependence on range and range rate accuracy may be the drawback of the algorithm for the HVM. If there is a means of providing this information this algorithm has great potential for the HVM being guided by the launch aircraft.

4.15 Algorithm Comparisons

The performance of each tested algorithm under no-noise conditions is the initial indicator of its worthiness to the task of guiding the HVM missile. The algorithms performance will only degrades under realistic noise conditions. The less robust solutions will degrade more rapidly. Table 4-1 shows the FOMs and some other results of each run described in this chapter. Comparative bar graphs of the FOMs are shown for the best 30 degree off-angle results, in Figure 4-36; the 5 degree off-angle tests, in Figure 4-37; and the radar-off shots, in Figure 4-38.

Figure 4-36 Comparison of All 30 Degree Off Angle Shots

By examining these results it is clear that the LOS guidance algorithm is superior to any of the others in no-noise performance. A close second in overall performance is the proportional algorithm. Its only drawback is the

Table 4-1 Figures of Merit And Parameters For Each Run

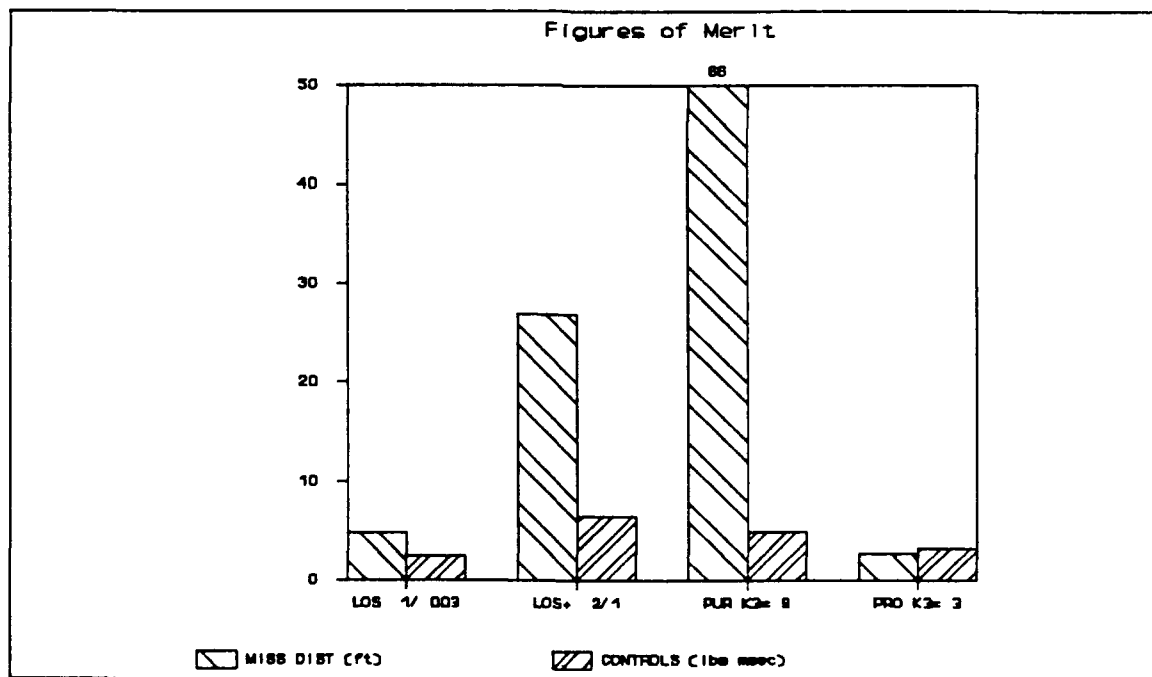| RUN	TIME IMPCT (sec)	MISS DIST (ft)	MISS X (ft)	MISS Y (ft)	MISS Z (ft)	TERM VEL (fps)	ENRGY USED (lb msec)	TC (sec)	K_3 (nu)
LOS 1	2.88	4.83	4.73	0.25	-0.95	4908	2.51	0.100	0.003
LOS 2	2.90	4.18	-2.89	-3.02	-0.05	4842	2.90	0.080	0.003
LOS 3	2.91	5.18	-2.70	-4.41	-0.39	4809	2.92	0.100	0.002
LOS 4	2.87	1.57	1.14	-0.98	-0.45	4940	2.27	0.100	0.004
LOS 5	2.84	3.52	2.89	-1.76	-0.99	5026	1.84	0.200	0.004
LOS S#1	2.76	1.72	-0.15	-1.62	-0.56	5277	0.73	0.100	0.003
LOS S#2	2.78	4.37	4.29	-0.21	-0.82	5076	0.99	0.100	0.003
LOS NoR	2.86	4.60	4.50	0.35	-0.87	4945	2.23	0.100	0.003
LOS+ 1	3.53	26.94	12.01	-22.53	-8.59	2923	6.54	0.200	1.000
LOS+ 2	3.50	53.04	19.56	-48.58	-8.37	3124	9.73	0.200	2.000
LOS+ 3	3.16	106.65	44.95	-95.20	-17.02	3965	5.78	0.400	4.000
LOS+ 4	3.06	107.99	46.16	-96.03	-17.60	4482	4.41	0.400	2.000
LOS+ S#1	2.86	25.98	14.81	-17.28	-12.52	4837	1.43	0.200	1.000
LOS+ S#2	3.1f	98.75	77.25	-60.80	-9.31	3753	4.31	0.200	1.000
LOS+ NoR	3.46	54.71	21.29	-49.46	-9.69	3074	6.14	0.200	1.000
PUR 1	2.89	104.57	31.35	-98.20	-17.63	4596	3.71	**	4.000
PUR 2	2.87	65.62	18.32	-62.20	-10.04	4647	4.95	**	8.000
PUR 3	2.87	44.84	11.69	-42.81	-6.46	4657	8.90	**	16.000
PUR 4	2.87	37.50	14.04	-34.28	-5.84	4640	11.81	**	24.000
PUR 5	2.94	34.34	10.55	-32.29	-5.03	4456	15.01	**	32.000
PUR S#1	2.76	30.02	17.52	-18.85	-15.46	5096	2.60	**	8.000
PUR S#2	2.79	111.53	73.47	-83.16	-11.22	4774	4.98	**	8.000
PUR NoR	2.89	103.73	-27.39	95.78	28.93	4389	36.72	**	8.000
PRO 1	3.35	1.02	-0.14	1.00	-0.14	3526	5.09	**	2.000
PRO 2	3.21	2.68	-2.59	-0.61	0.37	3958	3.33	**	3.000
PRO 3	3.12	3.40	3.16	1.21	-0.41	4251	3.07	**	4.000
PRO 4	3.00	2.58	2.34	1.05	-0.27	4637	2.45	**	6.000
PRO S#1	2.82	1.03	0.61	0.82	-0.14	4972	1.03	**	3.000
PRO S#2	2.82	1.26	0.79	0.97	-0.18	4972	1.06	**	3.000
PRO NoR	2.89	>500.00	**	**	**	4389	9.41	**	3.000

strong dependence on accurate missile range and range-rate measurements. From Figure 4-37 one can see that it is more resilient to aircraft acceleration effects than is the LOS algorithm.

The effort to project an aircraft position in time and fly the missile to a future line of sight is a difficult, dynamic control problem that will require a varying gain control for effective use. The LOS+ algorithm with a constant gain represents a control nightmare that provides neither accuracy nor efficiency.

The pursuit algorithm is unsuitable for any high closing speed missile. Its inefficiency and lacking accuracy for the HVM is prominent in the graphs.
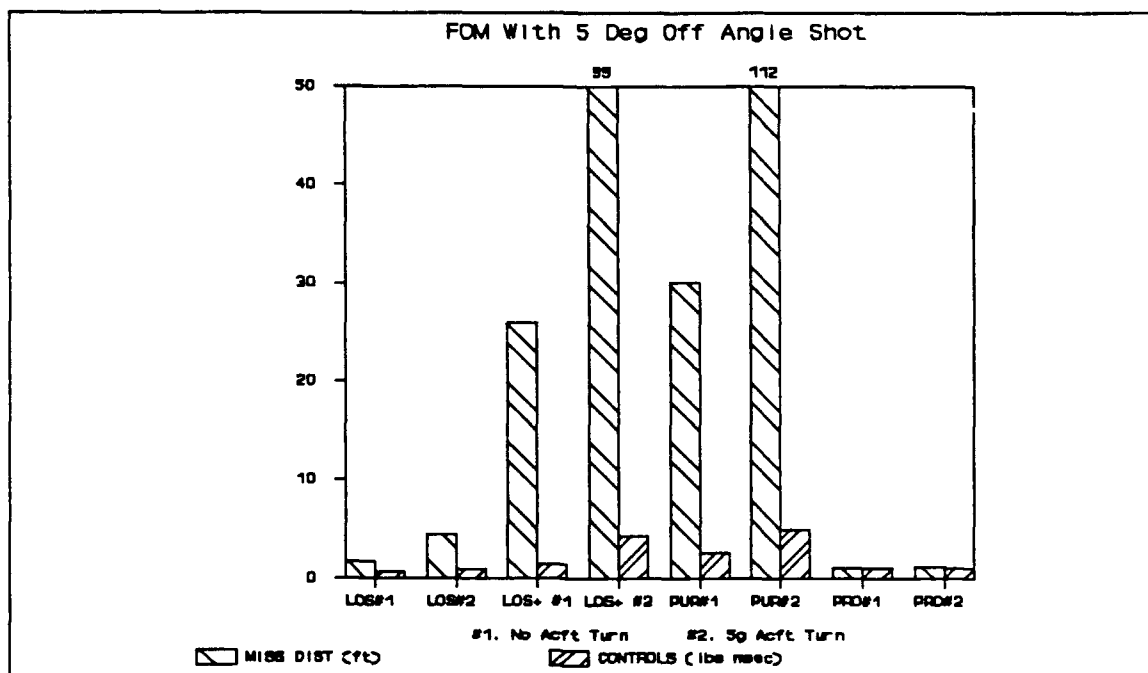
Figure 4-37 Comparison of All 5 Degree Off Angle Shots
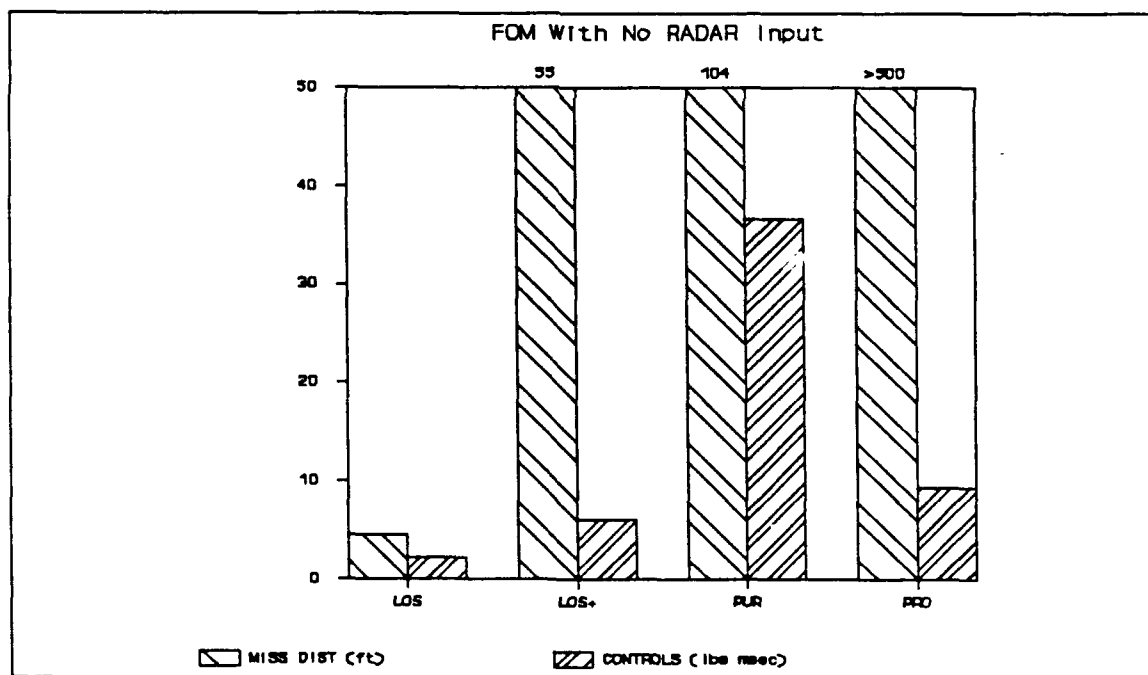
Figure 4-38 Comparison of All Radar Off Shots

V. Conclusions and Recommendations

5.1 Introduction.

After working closely with the proposed HVM weapon system for the initial testing, an insight into the problem and the "personality" of the algorithms is developed. This insight provides the basis for more detailed examination of selected promising algorithms before the HVM can be effectively steered by the launch aircraft. Although this work has been in a no-noise environment a good understanding of the physical limitations of each algorithm can be very useful in selection of the HVM's guidance scheme. The robustness of each algorithm can only be tested with a sensitivity analysis that includes sensor and system noise. This chapter states the conclusions of the completed effort and provides recommendations for future study.

5.2 Conclusions.

Currently used missile guidance-concepts are applicable to the task of guiding a hyper-velocity missile without a target sensor into a direct collision course with a ground target. The following conclusions are drawn from the no-noise tests accomplished on the four algorithms. In each case it must be considered that algorithm robustness and stability is not adequately tested with this effort, only the physical constraints of the algorithms within the HVM weapon system geometry.

5.2.1 LOS Guidance Algorithm.

When the LOS guidance algorithm is developed and controlled with properly tuned control parameters, it can effectively guide the missile into the target under a variety of launch conditions. The LOS algorithm can perform well with only modeled range and range-rate data because it is relatively insensitive to these parameters. Thus a FLIR sensor providing angle data on the missile and target is adequate for this algorithm. Although the LOS algorithm

represents a time dependent, non-linear control system, a constant gain setting can provide stable and accurate results under the no-noise simulation accomplished in this effort. This algorithm preforms the best overall, but it is a dynamic control system that must be tuned in the presence of system noise before a final conclusion can be drawn.

5.2.2 <u>LOS+ Guidance Algorithm</u>. The LOS+ algorithm, devised to increase LOS algorithm efficiency and to move the missile plume away from the aircraft to target line-of-sight, requires time varying gain control to work effectively. Although it does move the missile plume off the target line-of-sight effectively, the non-optimal control and its dependence on predicting the future are insurmountable problems in this effort. A gain balance that optimally moves the missile on to a future, stable line-of-sight and provides the end game gain necessary for accuracy cannot be obtained with a constant gain as attempted with this effort. If this technique will work it will require a time variable gain, preferably a optimal guidance solution.

5.2.3 <u>Pursuit Guidance Algorithm</u>. The pursuit algorithm cannot perform well in a high closing speed environment. The HVM presents an exceptionally high closing speed environment and the pursuit algorithm calls for end game accelerations that cannot be met by the missile. Although this guidance principle is very popular with air-to-air intercepts, and with some missile IR seekers where an up the tail shot is essential, it is not a candidate for the HVM environment.

5.2.4 <u>Proportional Guidance Algorithm</u>. The proportional guidance algorithm performs admirably in the HVM weapon system. It shows excellent independence of launch aircraft maneuvers and with accurate sensor data it can deliver the accuracy required for a direct target hit. The proportional guidance algorithm is more stable than the LOS algorithm and may out perform this algorithm in the presence of system noises. The proportional algorithm has a strong dependence on aircraft to missile

range and range-rate measurement accuracies. The utility of this algorithm will depend on the AFTI/F-16's ability to provide accurate range and range-rate information.

5.2.5 Conclusion Summary. This study effort is the initial examination of guidance concepts for the HVM missile. The no-noise computer simulation runs only establish a baseline performance of the algorithms. Additional work is required to determine the algorithm's performance when sensor inaccuracies and measurement noise are added to the simulation. From the noiseless results the algorithms which provide acceptable performance are the LOS guidance algorithm and the proportional guidance algorithm.

5.3 Recommendations

There are four areas where recommendations are made with confidence. Based on the results of this work and the author's familiarity with the algorithms the best performing algorithms are selected. The effect of the missile plume interference with the FLIR requires further examination, but an approach to solve this potential problem is included. Lastly, some recommendations for the next logical effort, a sensor error analysis, are included. Each of these recommendations is discussed in the following paragraphs.

5.3.1 Algorithm Selection. If the HVM development continues with a missile that can only sense rotation and execute azimuth and pitch turn commands, either the LOS or the proportional guidance algorithm should be developed for it. If studies indicate that a radar can not provide accurate range and range-rate data for the HVM, or if tactical users continue to express a strong desire to launch with out emitting (i.e. radar off), then the LOS algorithm is best suited to guide an HVM to a direct hit on a ground target.

5.3.2 Optimal Guidance Algorithm Development. Several studies indicate that the proportional guidance algorithm preforms as well as an optimal

guidance solution in most situations. [6:237-238] In the tests shown here
with no system noise, the proportional guidance algorithm does not
significantly out perform the LOS algorithm. If an optimal guidance
scheme is pursued for the HVM it should be centered on the final line-of-
sight concept of the LOS+ algorithm. This technique can still provide the
high accuracy and range independence of the LOS algorithm, while moving
the missile off the launch-aircraft to target line-of-sight.

5.3.3 Missile Plume Obstruction Problems. If it is determined that the
missile plume obstructs the target tracking, or that the target FLIR
signature hinders tracking the coasting missile, a hybrid LOS/Proportional
guidance algorithm should be evaluated. The proportional algorithm would
take the missile off the line-of-sight during rocket burn, then the LOS
algorithm can give the final accuracy and range independence necessary for
the direct hit. This can be done by calculating the commands for both
algorithms and time weight them before sending a command set to the
missile. This would represent a simpler solution than a optimal guidance
algorithm development, but would need to be validated in a simulation and
compared to the other algorithms.

This hybrid solution combines two nearly optimal solutions, gives a
controllable time where the missile is off the subject line-of-sight, and
retains the robust accuracy of the LOS algorithm. Examining the 30 degree
off-angle shots for both proportional and LOS guidance shows that the
proportional guidance lines up the missile for a final LOS guidance
scheme. In fact each of the shots tested shows this hybrid to be a
feasible solution.

5.3.4 Suggestions For Further Study. Several areas are suggested for
further study of these algorithms in the no-noise situation in which they
were tested. The proportional algorithm shows a range dependence in this
test but a sensitivity to range and range-rate biases can be further

explored with this simulation capability. Sensitivity to FLIR angle biases can also be explored with this no-noise simulation.

The miss distances used for a FOM in this study are most likely caused by data latency. In the time between each missile update at 50 Hz, the missile moves about 100 feet closer to the target. The resulting phase lag likely causes the terminal oscillations and larger miss distances. The accuracy of range and angle measurements provided to the guidance algorithm is limited in this simulation by the 24 bit mantissa word length. So the miss distances are a function of the guidance algorithms ability to control the hyper-velocity projectile, the latency in the data updates and the missile's second order response to a command. A command rate study can evaluate the missile command update time requirements and the effects of missed updates on the missile accuracy. The performance sensitivity to sensor update times, or filter update times with different missile update times can also be explored with this model. This study can assist the design of the update scheme used on the HVM missile, its robustness, and its timing requirements.

The LOS algorithm was analyzed using small angle assumptions to make a linear control block diagram. A functional analysis of this non-linear algorithm can provide insight to constructing a time varying gain control for this approach. The 3DOF no-noise model constructed for this effort can be used in several of these study areas.

5.3.4 <u>Sensor Error Analysis</u>. As the HVM design matures and emphasis is placed on its development, the results of this effort should be expanded to include a sensor error analysis. The ability of a FLIR to track a HVM missile throughout the course of its flight needs to be analyzed. Capp's Kalman filter development [4:55] and the MSOFE Kalman filter modeling tools should then be used to perform a system simulation with realistic noise. The tests should continue with the LOS algorithm and perhaps the LOS/Proportional hybrid described in paragraph 5.3.3 above. The results

of such a test are expected to continue showing the superiority of the LOS guidance algorithm for the HVM weapon system.

Bibliography

1. Worsley, William H., Major, USAF, Development Engineer, Personal interview and Risk Assessment Memo For Record, WL/TXD WPAFB OH, 9 May 89.

2. Aden, T. C. 'Hyper-Velocity Missile - Based on The Concept of Aircraft/Missile Integration For Maximum Firepower,' _AGARD Conference Proceedings No. 369 Integration of Fire Control, Flight Control, and Propulsion Control Systems, 369_: 2.1-2.14. Langley Field VA: NASA, May 1983.

3. DMS Inc. 'Hyper-Velocity Missile,' _Defence Market Intelligence Report, Missiles_. DMS Inc. 100 Northfield Street. Box 4585, Greenwich Conn. 06830-0585, 1988

4. Capps, Capt David W. and Capt Donald C. Nelson. _A Comparative Analysis of Kalman Filters Using a Hypervelocity Missile Simulation_. MS thesis, AFIT/GE/EE/81D-13. School of Engineering, Air Force Institute of Technology (AU), Wright Patterson AFB OH, December 1981.

5. Michalk, David L. _Implementation of a Target State Estimator for The Air-To-Air Attack Mode of the AFTI/F-16_. MS thesis, AFIT/GE/ENG/87D-44. School of Engineering, Air Force Institute of Technology (AU), Wright Patterson AFB OH, December 1987.

6. Garnell. P. _Guided Weapon Control System_. Pergamon Press Inc. Maxwell House, Fairview Park, Elmsford, New York 10523. 1980

7. Baker. C.D. Winch. J.W. Chandler. D.F. _Guidance, Flight Mechanics and Trajectory Optimization_. George C. Marshall Space Flight Center, Technical Report NAS 8-11495. 1968

APPENDIX A

Various Additional Scenerio Launches

The following additional scenerios were explored to test the conclusions of this effort. The data is presented here for completeness and additional insight into selected guidance algorithms.

Table A-1 Missile Parameters Used

	Description	Default Value	Unit	Coded Variable
1	MSL THRUST TIME	1.5	SEC	TBURN
2	MSL THRUST	5000	LBS	THRUST
3	MSL BODY WEIGHT	25.9	LBS	WTBD
4	MSL FUEL WEIGHT	32.17	LBS	WTFU
5	MSL DIAMETER	3.8	IN	MDIA
6	MSL LENGTH	7.0	FT	MLNGTH
7	MSL Wn	44.0	RPS	WN
8	MSL DAMPING	.7071	NU	ZETA
9	MSL MAX G	102.0	G	GMAX
10	COEFF LIFT DRAG	1.74E-4	NU	KDRAG
11	MAX MSL FLIGHT TIME	4.0	SEC	TMAX

Table A-2 Scenario Parameters Used

	Description	Default Value	Unit	Coded Variable
1	AIRCRAFT VEL	650.00	FPS	VAC
2	ACFT HEADING	60.0	DEG	HDGA
3	ACFT ALTITUDE	1000.0	FT	AALT
4	ACFT LAT ACCEL	000.0	G	AACf
5	ACFT ACCEL PITCH	00.0	DEG	APITCH
6	RANGE TO TARGET	5280.0	FT	RT
7	LOS TO TARGET	30.0	DEG	LOST
8	TARGET VEL	50.0	MPH	VTGT
9	TARGET HEADING	90.0	DEG	HDGT
10	TARGET LAT ACCEL	0.0	FPS^2	ATGT
11	SYSTEM INTEG TIME	.002	SEC	DT
12	MSL UPDATE TIMES	.02	SEC	DTMU
13	SENSOR UPDATE TIMES	.02	SEC	DTSU
14	OUTPUT TIMES	.02	SEC	DTOUT
15	FILTER UPDATE TIME	.02	SEC	DTKU

SCENARIO GROUND MAP

NED Coordinate Frame (1000 Ft)

LOS Guidance
TOF= 1.64
MIS= 8.7
ENR= 2.75
K3 = 0.003
TC = 0.10

1 Mile Shot, Acft Hdg 60 Deg
Tgt Hdg -90 Deg, +5G Turn

Trgt Track

Msl Track

Acft Track

EAST In Thousand Feet

Missile Commanded Turns

Heading and Pitch Rates in G's

LOS
TOF= 1.64
MIS= 8.7
ENR= 2.75
K3 = 0.003
TC = 0.10

Time of Flight in Seconds

— Heading Command   ◆ Pitch Command

Missile Heading and Pitch

NED Coordinate System, Degrees

LOS
TOF= 1.64
MIS= 8.7
ENR= 2.75
K3 = 0.003
TC = 0.10

Time of Flight in Seconds

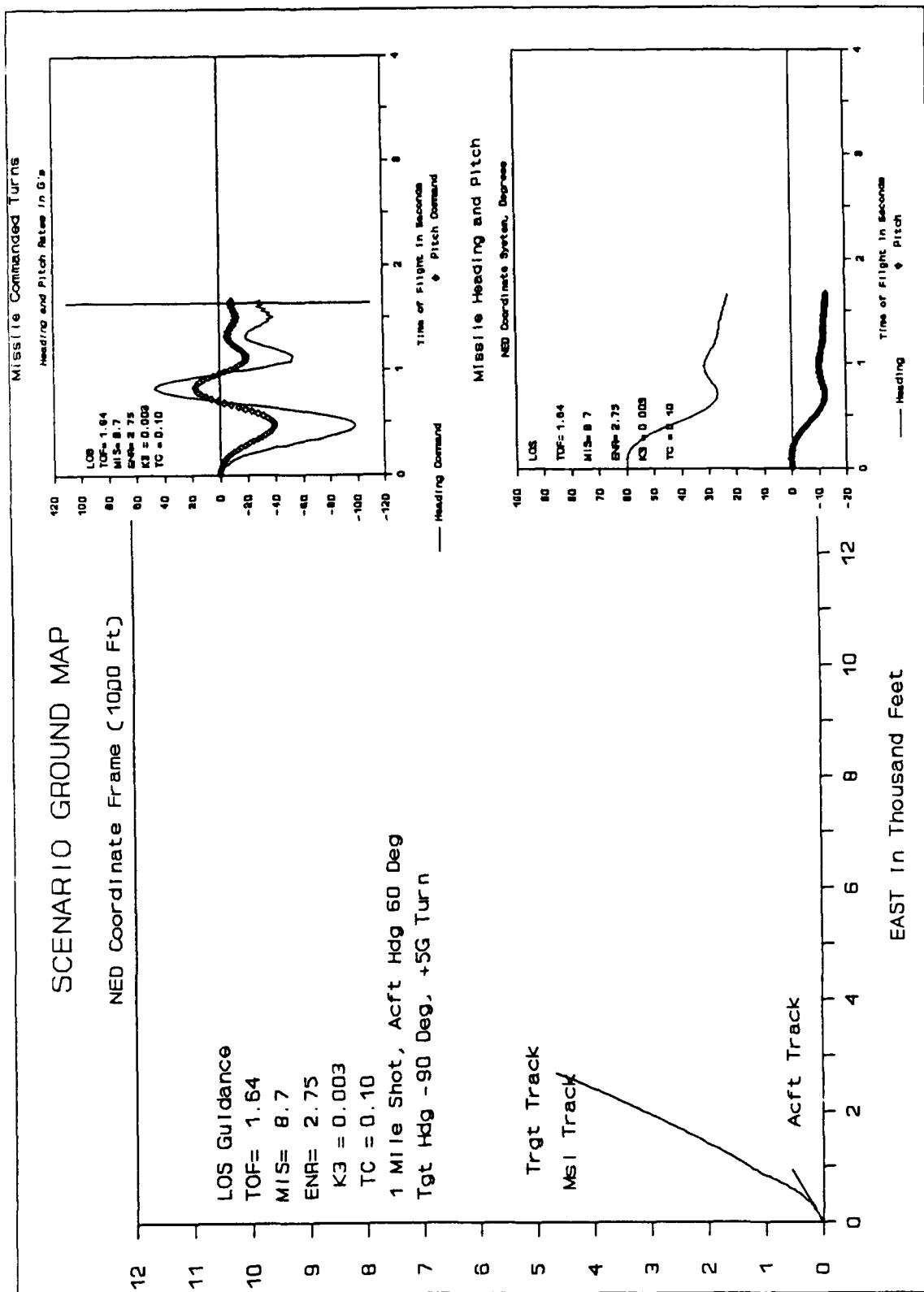— Heading   ◆ Pitch

Figure A-1   One Mile Shot
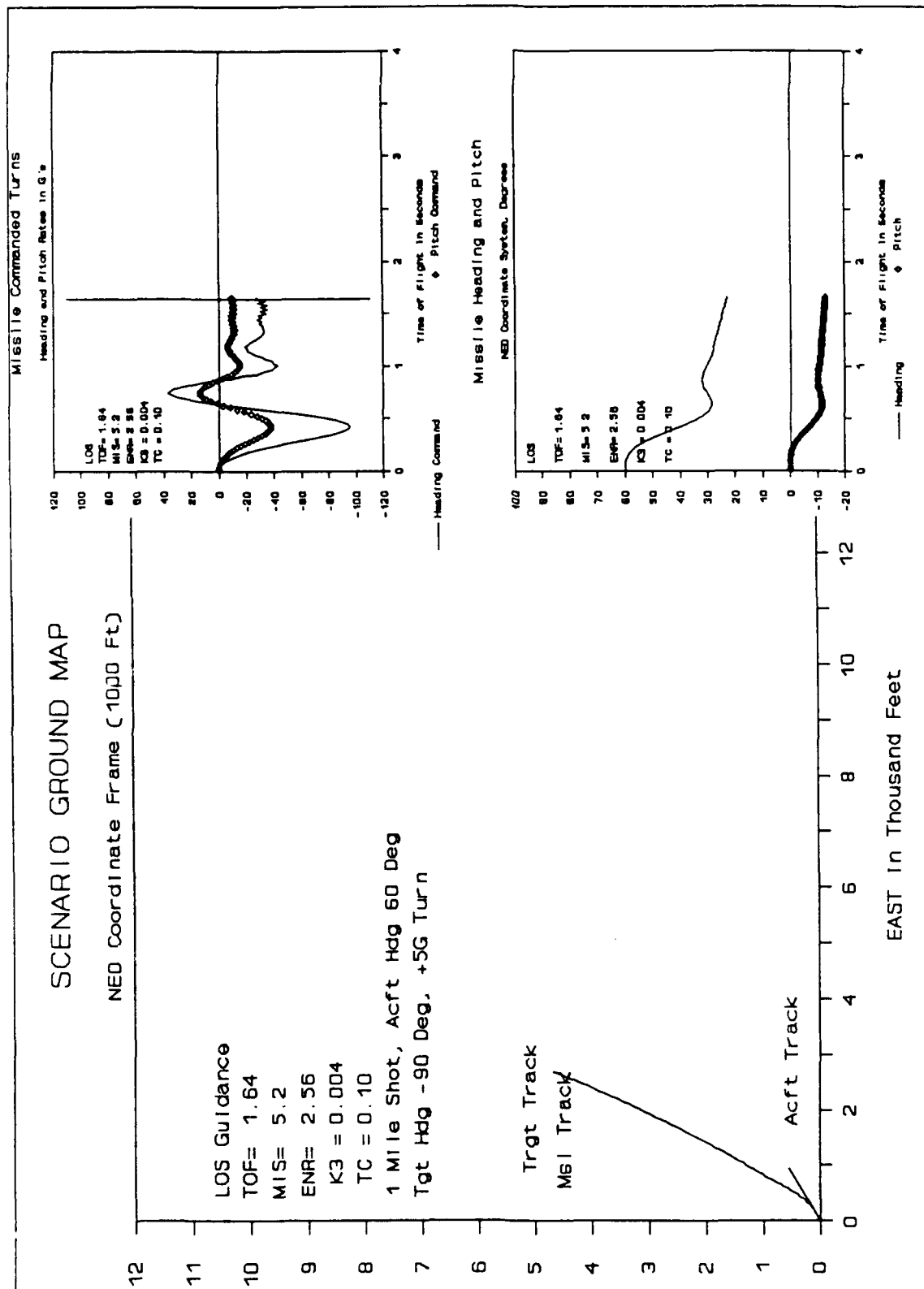
Figure A-2   One Mile Shot
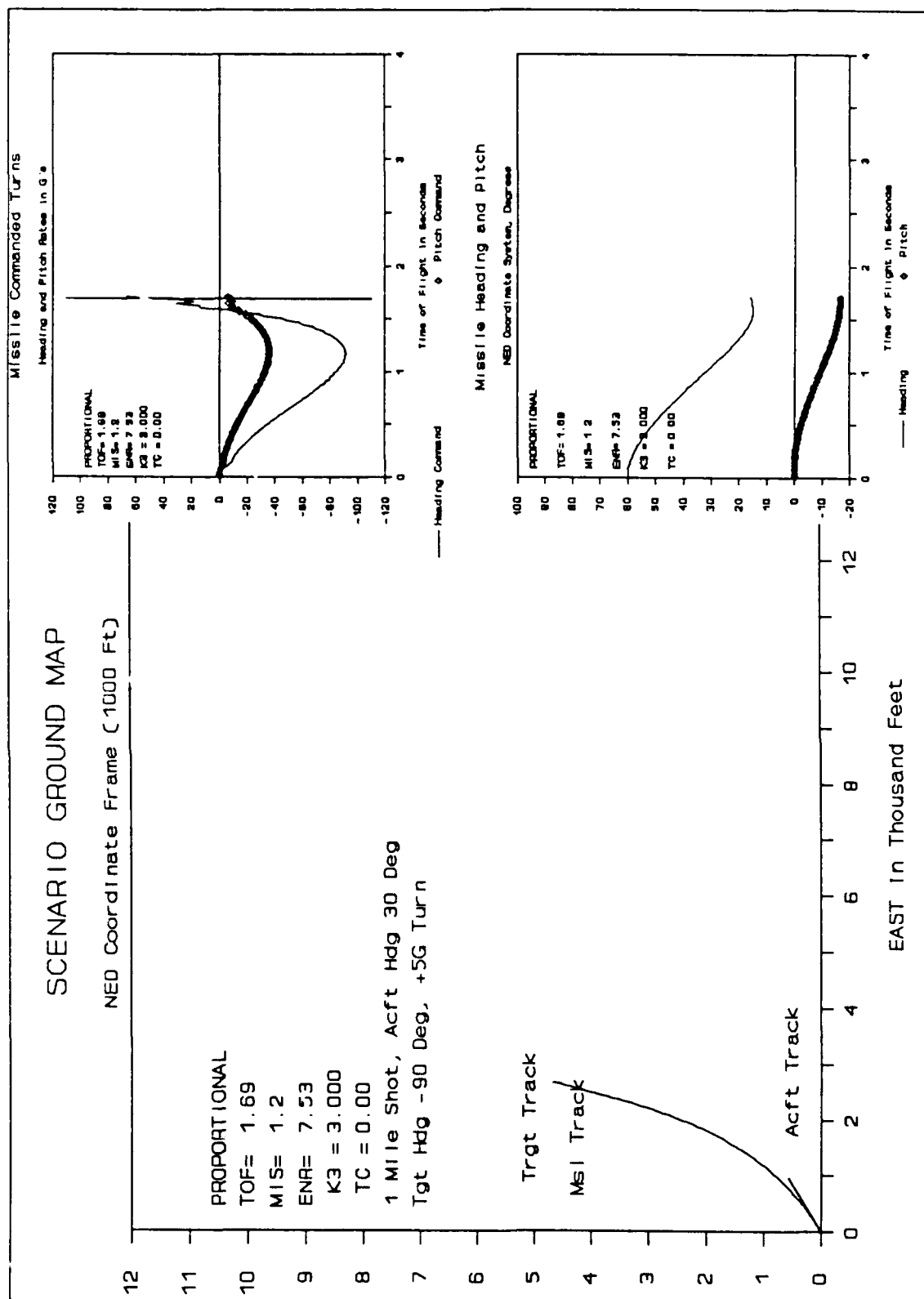
Figure A-3   One Mile Shot
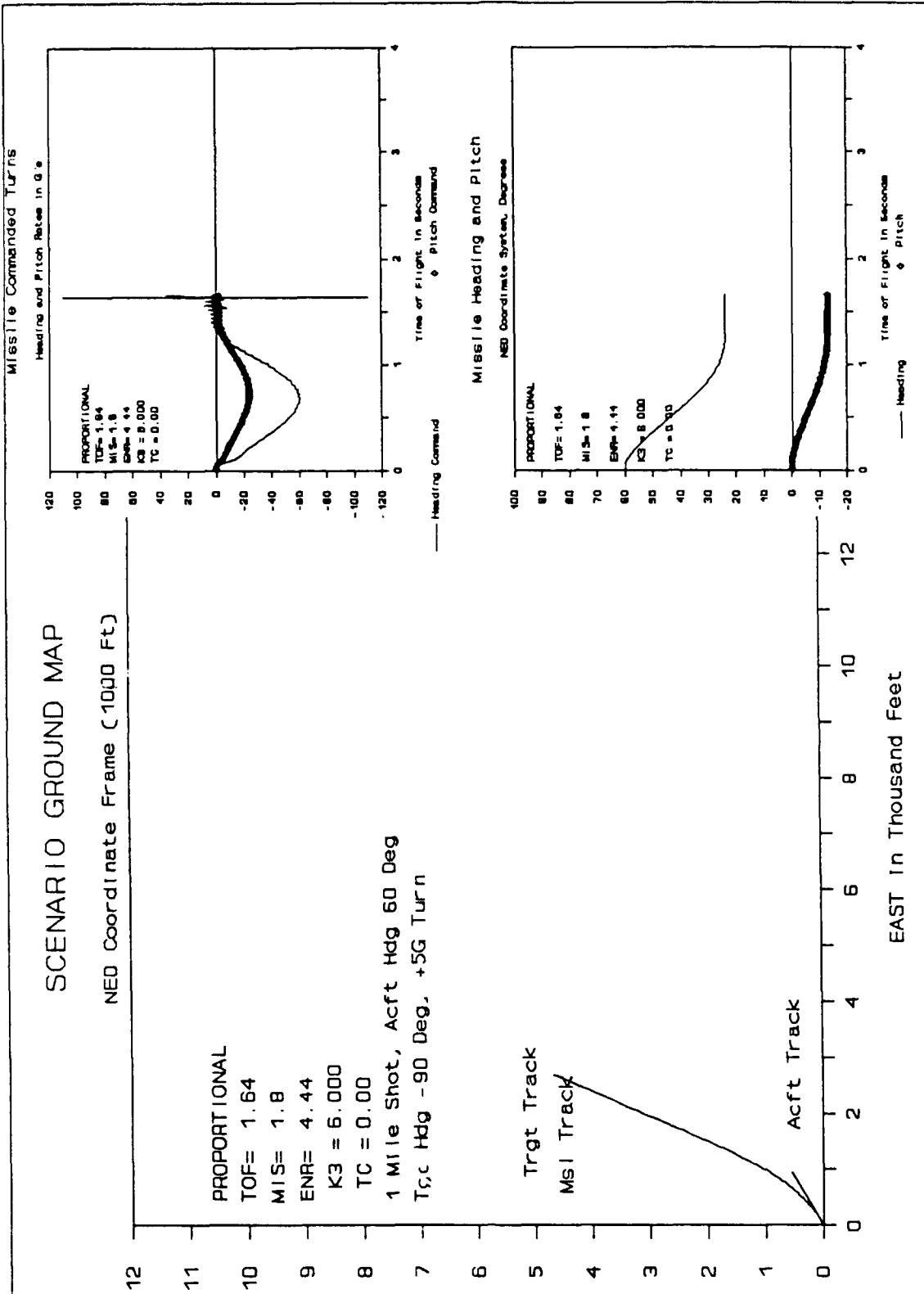
Figure A-4   One Mile Shot

Figure A-5 One Mile Shot

SCENARIO GROUND MAP

NED Coordinate Frame (1000 Ft)

LOS Guidance
TOF= 1.63
MIS= 6.0
ENR= 2.35
K3 = 0.004
TC = 0.10

1 Mile Shot, No Radar, Acft Hdg 30 Deg
Tgt Hdg -90 Deg, +5G Turn

Trgt Track
Msl Track
Acft Track

EAST In Thousand Feet

Missile Commanded Turns

Heading and Pitch Rates in G's

LOS
TOF= 1.63
MIS= 6.0
ENR= 2.35
K3 = 0.004
TC = 0.10

Time of Flight In Seconds

—— Heading Command   ◆ Pitch Command

Missile Heading and Pitch

NED Coordinate System, Degrees

LOS
TOF= 1.63
MIS= 6.0
ENR= 2.35
K3 = 0.004
TC = 0.10

Time of Flight In Seconds

—— Heading   ◆ Pitch

Figure A-6   One Mile Shot

A-8

Figure A-7 One Mile Shot

SCENARIO GROUND MAP

NED Coordinate Frame (1000 Ft)

PROPORTIONAL
TOF= 1.63
MIS= 8.7
ENR= 4.92
K3 = 6.000
TC = 0.00

1 Mile Shot, No Radar, Acft Hdg 30 Deg
Tgt Hdg -90 Deg, +5G Turn

Trgt Track

Msl Track

Acft Track

EAST In Thousand Feet

Missile Commanded Turns

Heading and Pitch Rates in G's

PROPORTIONAL
TOF= 1.63
MIS= 8.7
ENR= 4.92
K3 = 6.000
TC = 0.00

Time of Flight in Seconds

◇ Pitch Command

—— Heading Command

Missile Heading and Pitch

NED Coordinate System, Degrees

PROPORTIONAL
TOF= 1.63
MIS= 8.7
ENR= 4.92
K3 = 6.000
TC = 0.00

Time of Flight in Seconds

◇ Pitch

—— Heading

Figure A-8   One Mile Shot

Table A-3 Missile Parameters Used

	Description	Default Value	Unit	Coded Variable
1	MSL THRUST TIME	1.5	SEC	TBURN
2	MSL THRUST	5000	LBS	THRUST
3	MSL BODY WEIGHT	25.9	LBS	WTBD
4	MSL FUEL WEIGHT	32.17	LBS	WTFU
5	MSL DIAMETER	3.8	IN	MDIA
6	MSL LENGTH	7.0	FT	MLNGTH
7	MSL Wn	44.0	RPS	WN
8	MSL DAMPING	.7071	NU	ZETA
9	MSL MAX G	102.0	G	GMAX
10	COEFF LIFT DRAG	1.74E-4	NU	KDRAG
11	MAX MSL FLIGHT TIME	4.0	SEC	TMAX

Table A-4 Scenario Parameters Used

	Description	Default Value	Unit	Coded Variable
1	AIRCRAFT VEL	650.00	FPS	VAC
2	ACFT HEADING	90.0	DEG	HDGA
3	ACFT ALTITUDE	1000.0	FT	AALT
4	ACFT LAT ACCEL	000.0	G	AACf
5	ACFT ACCEL PITCH	00.0	DEG	APITCH
6	RANGE TO TARGET	5280.0	FT	RT
7	LOS TO TARGET	30.0	DEG	LOST
8	TARGET VEL	50.0	MPH	VTGT
9	TARGET HEADING	-90.0	DEG	HDGT
10	TARGET LAT ACCEL	160.0	FPS^2	ATGT
11	SYSTEM INTEG TIME	.002	SEC	DT
12	MSL UPDATE TIMES	.02	SEC	DTMU
13	SENSOR UPDATE TIMES	.02	SEC	DTSU
14	OUTPUT TIMES	.02	SEC	DTOUT
15	FILTER UPDATE TIME	.02	SEC	DTKU
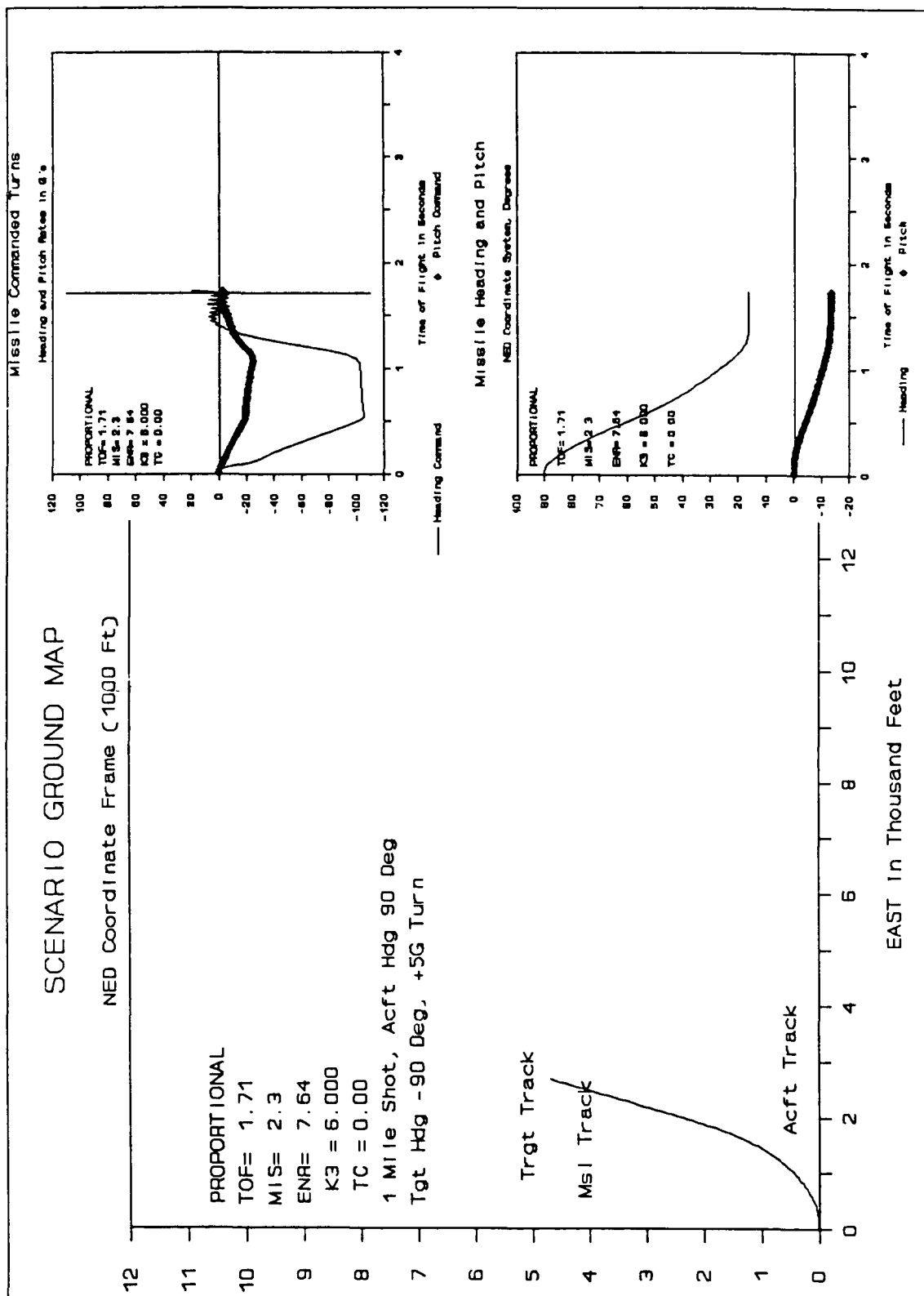
Figure A-10   One Mile Shot
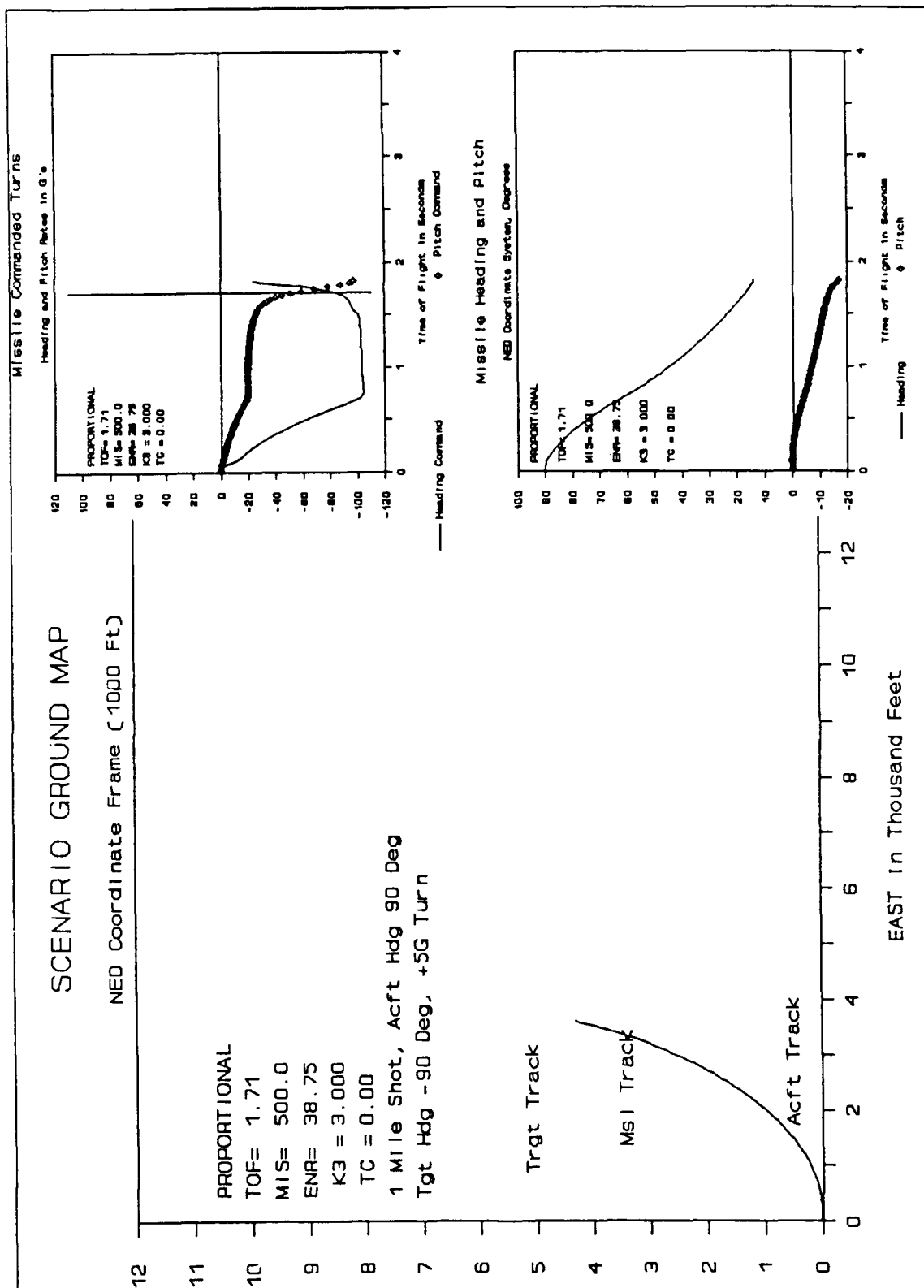
Figure A-11   One Mile Shot

SCENARIO GROUND MAP

NED Coordinate Frame (1000 Ft)

LOS Guidance
TOF= 1.71
MIS= 6.5
ENR= 13.05
K3 = 0.004
TC = 0.10

1 Mile Shot, Acft Hdg 90 Deg
Tgt Hdg -90 Deg, +5G Turn

Trgt Track

Msl Track

Acft Track

EAST In Thousand Feet

Missile Commanded Turns

Heading and Pitch Rates in G's

Time of Flight in Seconds

— Heading Command   ◆ Pitch Command

Missile Heading and Pitch

NED Coordinate System, Degree

Time of Flight in Seconds

— Heading   ◆ Pitch

Figure A-12   One Mile Shot

A-14

Missile Commanded Turns

Heading and Pitch Rates in G's

120
100
80
60
40
20
0
-20
-40
-60
-80
-100
-120

LOS
TOF= 1.72
MIS= 37.4
ENR= 14.88
K3 = 0.003
TC = 0.10

0   1   2   3   4
Time of Flight in Seconds

—— Heading Command   ◆ Pitch Command

Missile Heading and Pitch

NED Coordinate System, Degrees

100
90
80
70
60
50
40
30
20
10
0
-10
-20

LOS
TOF= 1.72
MIS= 37.4
ENR= 14.88
K3 = 0.003
TC = 0.10

0   1   2   3   4
Time of Flight in Seconds

—— Heading   ◆ Pitch

SCENARIO GROUND MAP

NED Coordinate Frame (1000 Ft)

12
11
10
9
8
7
6
5
4
3
2
1
0

LOS Guidance
TOF= 1.72
MIS= 37.4
ENR= 14.88
K3 = 0.003
TC = 0.10

1 Mile Shot, Acft Hdg 90 Deg
Tgt Hdg -90 Deg, +5G Turn

Trgt Track

Msl Track

Acft Track

0   2   4   6   8   10   12
EAST In Thousand Feet

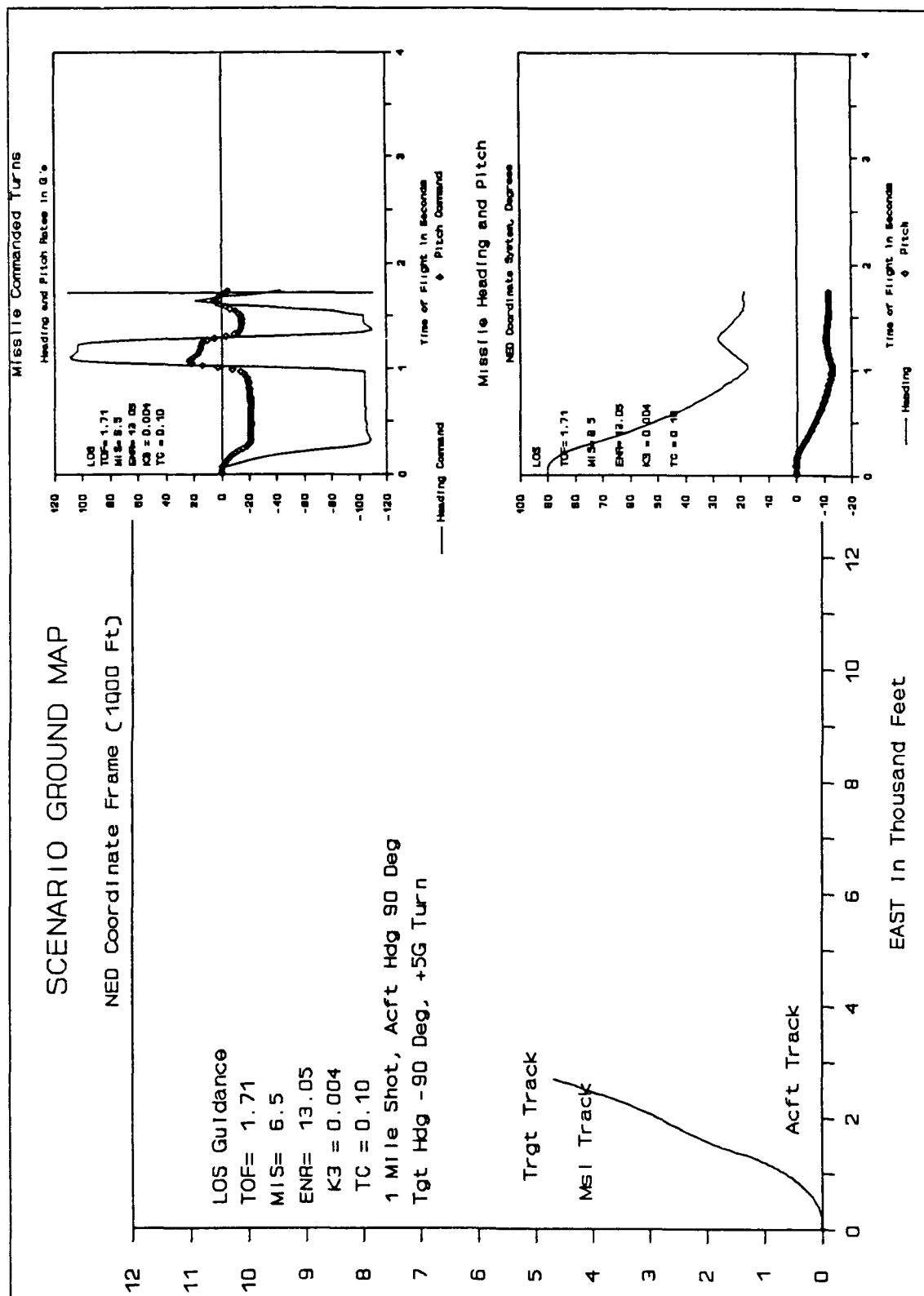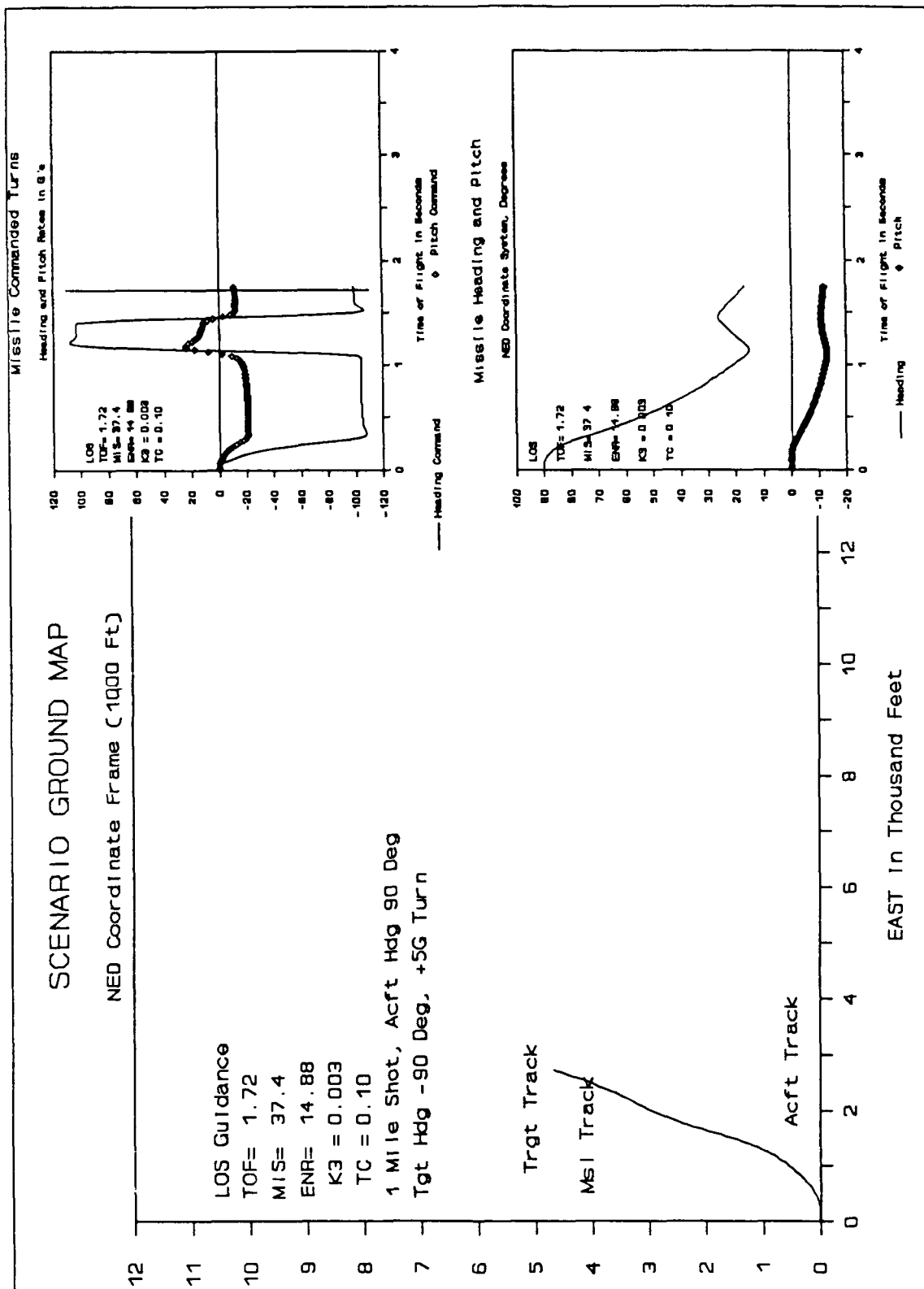Figure A-13   One Mile Shot

A-15

Vita

Captain Edward G. Rice was born on 30 June 1952 in Corning, New York. He graduated from Painted Post West High School in 1970, and entered the Air Force in 1971. While assigned to Griffiss AFB, New York as a Missile System Analyst he completed his Associates Degree in Electronics Technology from part time courses at Mohawk Valley Community College, Utica, New York, and extension courses from Chapman College, Orange California. He was accepted in the Airman Education Commissioning Program in 1979 and received the degree of Bachelor of Science in Electrical Engineering from Ohio State University in 1982. After commissioning from Officer Training School in July of 1982, he was assigned as a Civil Engineer at Cannon AFB, New Mexico. In May of 1984 he was assigned as the Chief of Resources and Requirements at Shemya AFB, Alaska. In May of 1985, after his remote tour, he was assigned to Wright Patterson AFB, Ohio, as a Lead Avionics Integration Engineer. While at Wright Patterson he attended AFIT as a part time student, and matriculated to the School of Engineering in October of 1988.

Permanent address: Box 118, RD#1

Painted Post, New York 14870

REPORT DOCUMENTATION PAGE

1. AGENCY USE ONLY (Leave Blank)	2. REPORT DATE	3. REPORT TYPE AND DATES COVERED
	12 Nov 1991	Final

4. TITLE AND SUBTITLE

Comparative Analysis of Guidance Algorithms
for the Hyper-Velocity Missile and AFTI/F-16

5. FUNDING NUMBERS

6. AUTHOR(S)

Edward G. Rice, B.S., Capt, USAF

7. PERFORMING ORGANIZATION NAME(S) AND ADDRESS(ES)

Air Force Institute Of Technology
Wright Patterson AFB OH 45433-6583

8. PERFORMING ORGANIZATION REPORT NUMBER

AFIT/GE/ENG/92M-02

9. SPONSORING/MONITORING AGENCY NAME(S) AND ADDRESS(ES)

WRDC/FIGX (Attn Mr. Boone)
Wright Patterson AFB OH 45433-5916

10. SPONSORING/MONITORING AGENCY REPORT NUMBER

11. SUPPLEMENTARY NOTES

12a. DISTRIBUTION/AVAILABILITY STATEMENT

Approved for Public Release,
Distribution Unlimited

12b. DISTRIBUTION CODE

13. ABSTRACT (Maximum 200 words)

Thesis Advisor: Col Z. H. Lewantowicz
Adjunct Professor
Department of Electrical and Computer Engineering

14. SUBJECT TERMS

Missile Guidance Proportional Pursuit BeamRider Hyper-Velocity AFTI/F-16 F-16 HVM

15. NUMBER OF PAGES

126

16. PRICE CODE

17. SECURITY CLASSIFICATION OF REPORT	18. SECURITY CLASSIFICATION OF THIS PAGE	19. SECURITY CLASSIFICATION OF ABSTRACT	20. LIMITATION OF ABSTRACT
Unclass	Unclass	Unclass	UL